Analyse der Funktion von Kuzbanian und Uncoordinated 5 während der Herzzelldeterminierung und Herzlumenbildung von *Drosophila melanogaster*

Dissertation
zur Erlangung des Doktorgrades der Naturwissenschaften
(Dr. rer. nat.)

vorgelegt am
Fachbereich Biologie/ Chemie
der Universität Osnabrück

von
Stefanie Albrecht

Osnabrück 2010

Inhaltsverzeichnis

1. Zusammenfassung

Die Kardiogenese kann speziesübergreifend in eine distinkte Abfolge von dynamischen Entwicklungsphasen unterteilt werden. In frühen Stadien der Vertebraten-Herzentwicklung wie auch bei *Drosophila melanogaster* beginnt die Organogenese des Herzens mit der Selektion und Spezifizierung der Herzvorläuferzellen aus bilateral angelegtem, mesodermalem Gewebe. Anschließend resultiert die Differenzierung der determinierten Herzvorläuferzellen in bilateralen Reihen spezifischer Herzzellgruppen. Die Herzzellen migrieren in dorsale Richtung aufeinander zu und assemblieren zu einem Herzrohr. Diese dynamischen Prozesse unterliegen einem komplexen Netzwerk an hoch konservierten Regulationsmechanismen. In der vorliegenden Dissertation konnte gezeigt werden, dass die Metalloprotease Kuzbanian/ADAM10 eine Rolle während der Kardiogenese von *Drosophila* spielt, in dem sie die Selektion der Herzzellvorläufer aus dem kardialen Mesoderm steuert. Durch die unterbleibende Prozessierung des Notch-Rezeptors in *kuzbanian* Mutanten wird eine Überzahl an Herzvorläuferzellen determiniert. Weiterhin ist die Notch-abhängige asymmetrische Zellteilung in *kuzbanian* Mutanten fehlreguliert. Die perikardialen Herzzelllinien verschieben sich zu Gunsten der kardialen Herzzellen und resultieren in einer Hyperplasie der Kardiomyozyten.

Eine weitere Phase der Kardiogenese in *Drosophila* ist die korrekte Ausbildung des Herzrohres und die damit einhergehenden Herzlumenbildung. Durch das Herzlumen kann die Hämolymphe durch das Herzrohr in den Körper des Tieres gepumpt werden. Die Bildung des Lumens bedingt eine stereotype Zellformänderung der Kardiomyozyten. Diese Modulierung der Zellform resultiert in halbmondförmigen Kardiomyozyten, die dorsal und ventral miteinander in Kontakt treten und so einen zentralen, luminalen Bereich umschließen – das Herzlumen. Das Rezeptor/Liganden-Paar Uncoordinated 5 (Unc5) und NetrinB ist für die korrekte Ausbildung der luminalen Kardiomyozytenseite notwendig. Es konnte gezeigt werden, dass ein Fehlen von Unc5 oder NetrinB die Kardiomyozyten in einer runden Zellform verbleiben lässt. Die Kardiomyozyten lagern sich entlang ihrer gesamten Kontaktfläche aneinander ohne dass ein Lumen entsteht. Lebendbeobachtungen an *unc5* Mutanten zeigten, dass das Fehlen des Herzlumens zu einem kompletten Verlust des Hämolymphstroms führt.

2. Einleitung

2.1. Das Dorsalgefäß von *Drosophila melanogaster*

Das embryonale Herz von *Drosophila* ist ein röhrenförmiges Organ, welches entlang der dorsalen Mittellinie des Embryos von anterior nach posterior verläuft (Campos-Ortega and Hartenstein, 1985). Der zelluläre Aufbau des Herzens ist eher einfach. Es besteht aus zwei Zelltypen, den Kardiomyozyten und den Perikardzellen. Exakt 104 Kardiomyozyten bilden eine kontraktile Röhre, die das Herzlumen umschließt. Lateral sind die Kardiomyozyten von Perikardzellen begleitet (Rizki, 1978). Diese akzessorischen, nicht muskulären Zellen werden im Embryo spezifiziert, ihre genaue Funktion ist bisher allerdings nicht vollständig geklärt. Für einige Perikardzellen konnte eine funktionelle Aufgabe ab dem Larvenstadium gezeigt werden. Die zu Nephrozyten differenzierten Perikardzellen agieren als Filtereinheit und entfernen Giftstoffe aus der Hämolymphe (Crossley, 1985; Das et al., 2008). Der anteriore Bereich des Herzrohres wird von der endokrin aktiven Ringdrüse sowie dem hämatopoetischen Lymphdrüsengewebe umgeben. Morphologisch lässt sich das Herz in drei Bereiche einteilen: die anteriore Aorta (Thorakalsegment 3 (T3)), das Vorderherz (Abdominalsegment 1-4 (A1-A4)) und den Ventrikel (Abdominalsegment 5-7 (A5-A7)). Die Bereiche T3-A4 werden häufig zusammengefasst und als Aorta bezeichnet (Rizki, 1978).

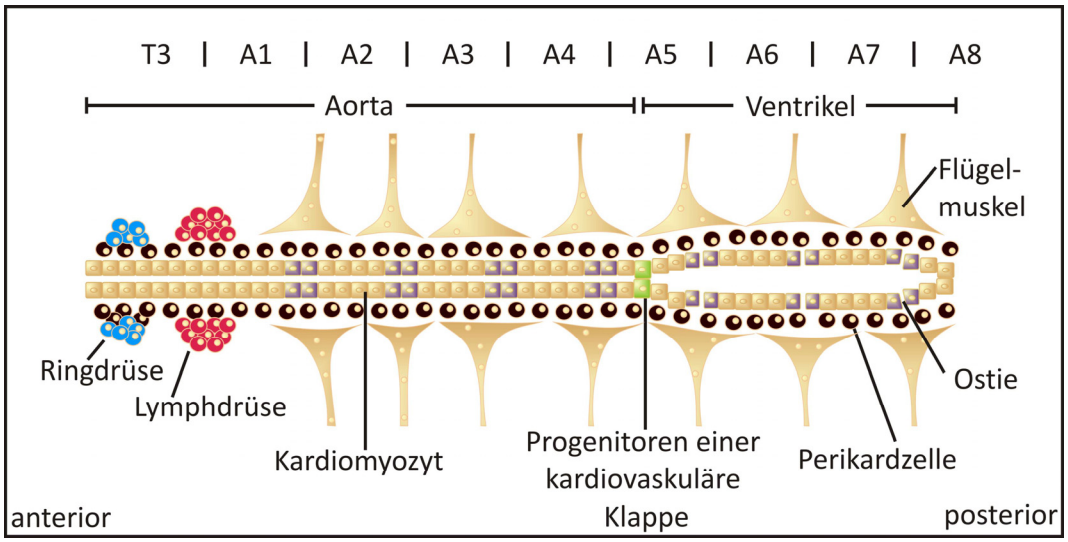

Abb. 1: Das embryonale Herz von *Drosophila melanogaster* erstreckt sich von Thorakalsegment 3 (T3) bis Abdominalsegment 8 (A8). Die Kardiomyozyten bilden die inneren Zellreihen und werden von den Perikardzellen umgeben. Im anterioren Bereich liegen Ring- und Lymphdrüse. In A5 trennen Progenitoren einer kardiovaskuläre Klappe das Herz in Aorta und Ventrikel. Im Ventrikel sind die Einströmöffnungen (Ostien) der Hämolymphe positioniert. Flügelmuskeln bilden den Kontakt vom Herz zur Epidermis.

Im Ventrikel sind sechs Paar Kardiomyozyten zu Ostienzellen differenziert, sie bilden die Einströmöffnungen für die Hämolymphe (Gajewski et al., 2000; Molina and Cripps, 2001). Bereits im Embryo ist das Herz durch sieben Paar synzytiale Flügelmuskeln fixiert und so unterhalb der Epidermis von Abdominalsegment 1-7 aufgespannt (Rizki, 1978) (siehe Abbildung 1).

Zum Ende der Embryogenese beginnen die Kardiomyozyten sich synchron in peristaltischen Wellen zu kontrahieren und somit die Hämolymphe durch das Herz in die Körperhöhle zu pumpen. Kurz nach Einsetzen des Herzschlages schlüpft die erste Larve von *Drosophila melanogaster*. Die Regulation des Herzschlages scheint sowohl myogenem als auch neurogenem Ursprung zu sein. Frühe Studien an larvalen und adulten Herzen haben gezeigt, dass herauspräparierte Herzen eine kontraktile Grundaktivität beibehalten (Miller, 1965; Rizki, 1978). In lavalen und adulten Tieren konnte ein myogener Schrittmacher im posterioren Bereich des Ventrikels lokalisiert werden. Die Herzschlagrate wird in diesem Bereich durch Ionentransport abhängige Modulation des Membranpotentials gesteuert (Lalevee et al., 2006; Ocorr et al., 2007; Senatore et al., 2010). Die genaue Regulation dieser Steuerungsprozesse ist allerdings noch weitgehend unbekannt.

Im Laufe der lavalen Entwicklung, die sich über drei Larvenstadien zieht, gewinnt die Larve an Körperlänge. Mit der Größenzunahme der Larve lässt sich eine Elongation des Herzens beobachten, wobei die Zellzahl der Kardiomyozyten jedoch unverändert bleibt (Molina and Cripps, 2001; Sellin et al., 2006, vorliegende Arbeit). Die Anzahl der Perikardzellen reduziert sich während der larvalen Entwicklung auf ein Viertel der im Embryo determinierten Zellen (Rizki, 1978; Sellin et al., 2006, vorliegende Arbeit). Die als Nephrozyten verbleibenden Perikardzellen weisen einen durch Polytänisierung vergrößerten Zellkern auf und unterscheiden sich somit morphologisch stark von den Kardiomyozyten (Rizki, 1978). Die beiden Hauptabschnitte, Aorta und Ventrikel werden durch eine kardiovaskuläre Klappe getrennt, die durch ein Paar morphologisch distinkte Kardiomyozyten gebildet wird und die Rückströmung der Hämolymphe in den Ventrikel verhindert.

Während der Metamorphose wird die Mehrzahl der larvalen Organe histolysiert und durch Proliferation und Differenzierung embryonal angelegter imaginaler Zellen neu gebildet. Das Herz ist eines der wenigen Organe, welches zumindest zum Teil erhalten bleibt, aber grundlegenden Umbauten unterzogen wird (Curtis et al., 1999; Molina and Cripps, 2001; Rizki, 1978). Dieser Prozess unterliegt zum Teil der Steuerung des Steroidhormons 20-Hydroxyecdyson (Monier et al., 2005). Posterior werden zwei Segmente des Herzens aufgelöst und der verbleibende anteriore Teil in das adulte Herz umgewandelt. Imaginale

Ostienzellen differenzieren während der Metamorphose zu funktionellen Einströmöffnungen und das Herz wird in vier Kammern unterteilt, die durch kardiovaskuläre Klappenzellen von einander getrennt werden (Monier et al., 2005; Zeitouni et al., 2007).

2.2. Molekulare Grundlagen der Kardiogenese bei *Drosophila melanogaster* und Vertebraten

Trotz offensichtlicher Unterschiede teilen sich Wirbeltiere einige grundlegende Charakteristika der Herzentwicklung mit *Drosophila*. Die frühen Stadien der Kardiogenese bei Vertebraten können in folgende sequentiell ablaufende Prozesse unterteilt werden: Spezifizierung des kardialen Mesoderms, Determinierung der bilateralen, symmetrischen Anlagen der herzbildenden Bereiche (*first & second heart field*), Strukturierung des Herzfeldes und schließlich die Differenzierung der Herzvorläuferzellen und Bildung des Herzrohres (Abu-Issa and Kirby, 2007). Die Prozesse während der Kardiogenese bei *Drosophila* lassen sich ebenfalls mit diesen Oberbegriffen beschreiben, wenn auch die Komplexität der einzelnen Schritte bei Vertebraten ungleich höher ist (Zaffran and Frasch, 2002) (siehe Abbildung 2).

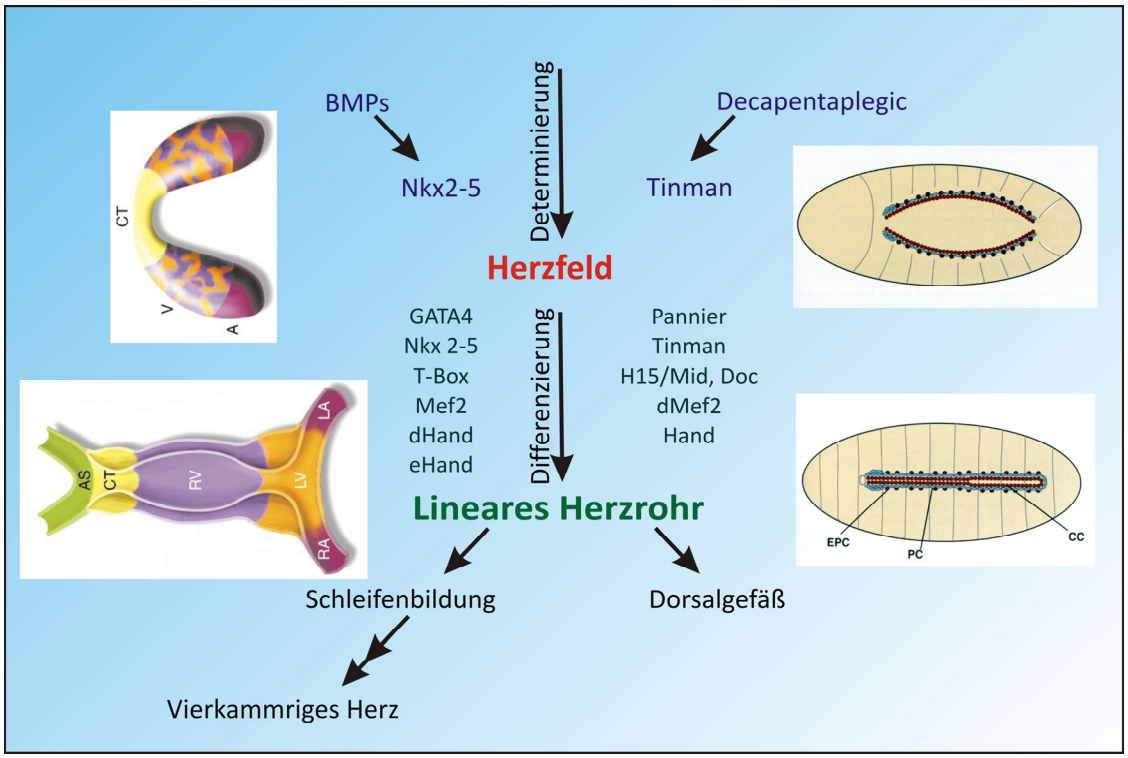

Abb. 2: Schematische Darstellung der Kardiogenese in Vertebraten und *Drosophila*. In Vertebraten zeigen sich in frühen Stadien (Tag 15, Tag 21) konservierte morphologische und molekulare Übereinstimmungen zur Entwicklung des Herzens bei *Drosophila* (Dorsalgefäß). A, Atrium; AS, Aortensack; CT, konotrunkal Region; LA, linkes Atrium; LV, linker Ventrikel; RV, rechter Ventrikel; V, Ventrikel; PC, Perikardzelle; CC, Kardiomyozyte; EPC, Even skipped Perikardzelle
Entnommen aus Richard and Rosenthal (1998); Srivastava and Olson (2000).

Die molekularen Regulationsmechanismen, die diesen distinkten Prozessen zu Grunde liegen, weisen ebenfalls Übereinstimmungen auf: In beiden Systemen induzieren vom Entoderm bzw. Ektoderm sezernierte Morphogene der BMP/Decapentaplegic und Wnt/Wingless Familien spezifische Zellgruppen im Mesoderm, in denen Selektorgene wie *Nkx2-5/tinman* die Herzzellvorläuferzellen determinieren (Evans et al., 1995; Frasch, 1995; Lockwood and Bodmer, 2002; Wu et al., 1995; Yin and Frasch, 1998). Nkx2-5/Tinman kann als Hauptregulator der Herzentwicklung angesehen werden. Ein Fehlen von Nkx2-5 führt zu einer Arretierung der Kardiogenese nach der Bildung des linearen Herzrohres, während in *tinman* defizienten *Drosophila* Embryonen die gesamte Kardiogenese unterbleibt (Azpiazu and Frasch, 1993; Bodmer, 1993; Lyons et al., 1995).
Die weitere Spezifizierung des kardialen Mesoderms unterliegt sowohl in Vertebraten als auch in *Drosophila* weiteren orthologen Faktoren wie GATA4/Pannier; FGFr/Heartless, T-Box Transkriptionsfaktoren und dem bHLH Faktor Hand (zusammengefasst in Reim and Frasch (2010); Tao and Schulz (2006); Zaffran and Frasch (2002)). Weiterhin konnte gezeigt werden, dass homeotische Gene (Hox-Gene) für die Determinierung der anterior-posterior Achse des Wirbeltierherzens als auch des Herzens von *Drosophila* essentiell sind und zur Einteilung der Organe in verschiedene funktionelle Einheiten dienen (Lo et al., 2002; Ponzielli et al., 2002; Searcy and Yutzey, 1998). Durch Analysen von Mutanten und durch Fehlexpressionsversuche von Hox-Genen konnte gezeigt werden, dass homeotische Gene das Potenzial besitzen die Identität der einzelnen Herzbereiche zu bestimmen. Sie definieren die klare Trennung von Aorta und Ventrikel. Eine Beeinflussung der Hox-Gen Expression kann zum Beispiel eine Transformation von Aortazellen zu Zellen des Ventrikels hervorrufen (Lo et al., 2002; Monier et al., 2007).

2.3 Zelldeterminierung im Mesoderm von *Drosophila melanogaster*

Die Spezifizierung des kardialen Mesoderms wird durch die Aktivierung des Homeobox Transkriptionsfaktors Tinman (Tin) eingeleitet. Decapentaplegic (Dpp) wird aus Zellen des Ektoderms in das darunterliegende Mesoderm sezerniert und wirkt als Ligand für die Rezeptortyrosinkinase Thickveins, die die Aktivierung der *tin* Expression im dorsalen Mesoderm gewährleistet (Frasch, 1995; Frasch, 1999). Eine Induzierung der kardialen Zellen benötigt neben Dpp und Tin auch den Wachstumsfaktor Wingless (Wg) (Wu et al., 1995). Durch die segmentale Anordnung der *wg* Expression im Ektoderm ergibt sich auch für die

Anordnung des dorsalen Mesoderms eine Unterteilung in segmentale Felder (Lockwood and Bodmer, 2002).

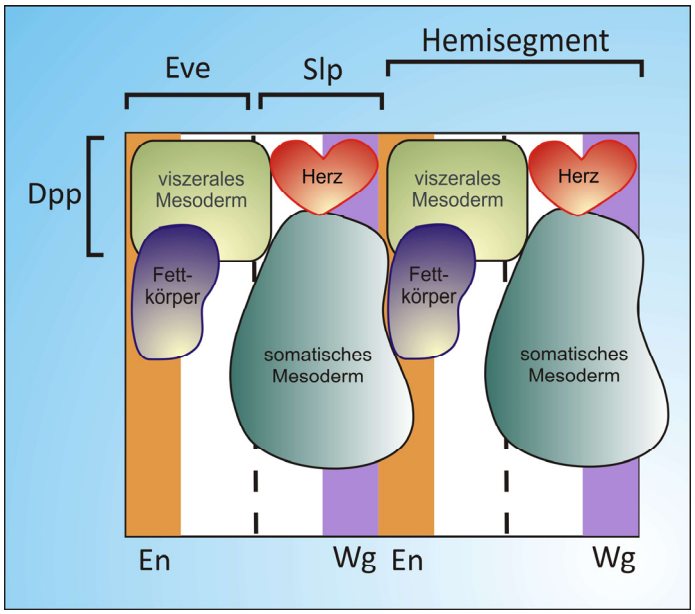

Abb. 3: Schematische Darstellung der mesodermalen Primordien.
Die Selektion der Primordien erfolgt unter dem Einfluss ektodermaler (Decapentaplegic/Dpp, Engrailed /En & Wingless/Wg) und mesodermaler (Even skipped/Eve & Sloppy paired/Slp) Signale. Das Herzprimordium wird im dorsalen Kompartiment durch die kombinatorische Induktion von Dpp, Wg und Slp determiniert. Die Anlage der Primordien erfolgt bilateral, repetitiv pro Segment des Embryos. Hier sind schematisch zwei Hemisegmente (eine Körperseite) gezeigt. Verändert nach (Riechmann et al., 1997).

Diese 13 Felder entlang der Körperseite des Embryos gliedern sich jeweils in die Vorläuferregionen für die somatische und viszerale Muskulatur, die Fettkörperanlagen und die Progenitoren des Herzens. Diese distinkte Kompartimentierung wird durch das regulatorische Zusammenspiel zweier Domänen (anterior – Even skipped (eve) und posterior – Sloppy paired (Slp)) gewährleistet. Unter dem Einfluss der Slp Domäne bilden sich im Zusammenspiel mit Wg im dorsalen Bereich dieses Kompartiments das kardiale Mesoderm (Riechmann et al., 1997). Die Kompetenz zur Bildung der Herzzellprogenitoren wird durch die Aktivierung der *tin* Expression in diesem Bereich verliehen (Lee and Frasch, 2005) (siehe Abbildung 3).

Die Determinierung und Differenzierung der Herzvorläuferzellen aus den so genannten Kompetenzfeldern unterliegt dem Prozess der lateralen Inhibition. Ein einzelner Progenitor wird aus einem Feld von gleichwertigen Zellen ausgesucht und stellt den Vorläufer einer bestimmten Zelllinie dar. Dieser Auswahlprozess unterliegt der Aktivität des Notch/Delta-Signalweges (Carmena et al., 2002; Hartenstein et al., 1992) (siehe Abbildung 4).

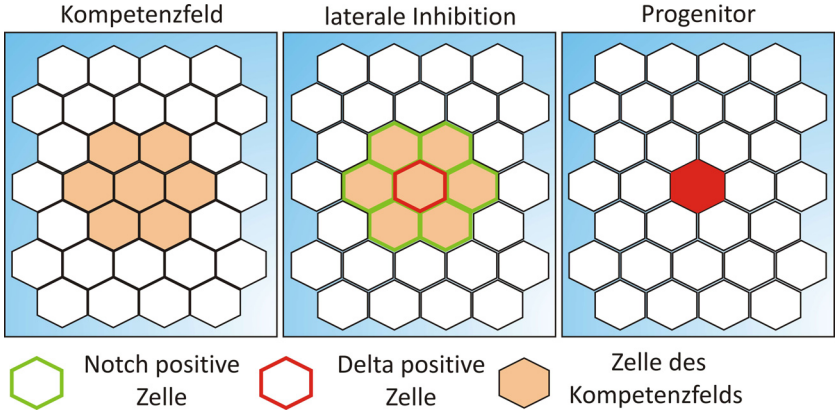

Abb. 4: Die Selektion eines Progenitors unterliegt der lateralen Inhibition. Alle Zellen kompetieren um den höchsten Level an Delta. Das Erreichen der höchsten Delta Expressionsrate in einer Zelle führt zu der Aktivierung des Notch/Delta-Signalweges in den Nachbarzellen. Die einzelne Zelle wird so aus einem Zellpool zum Progenitor ausgewählt.

Die Bindung des membranständigen Liganden Delta der DSL Familie an den Notch Rezeptor führt zur ersten proteolytischen Spaltung innerhalb der extrazellulären Domäne von Notch (N). Diese Spaltung wird durch eine ADAM Metalloprotease (Kuzbanian, ADAM10 in Vertebraten) vermittelt (Kidd et al., 1998; Lieber et al., 2002). Darauffolgend wird Notch durch einen γ-Sekretasekomplex prozessiert und der intrazelluläre Teil des Notch Rezeptors (N_{intra}) transloziert in den Zellkern. Dort assoziiert N_{intra} mit dem DNA Bindeprotein Supressor of Hairless (Su(H)) und dessen Kofaktor Mastermind, um als Transkriptionsregulator zu dienen (Kidd et al., 1998; Lai, 2002; Wu et al., 2000). Mutationen, die Komponenten des Notch-Signalwegs betreffen, führen zu einer deutlichen Vermehrung der determinierten Herzzellprogenitoren, was durch die Fehlregulierung der lateralen Inhibition erklärt werden kann (Albrecht et al., 2006; Hartenstein et al., 1992, vorliegenden Arbeit).

Die Differenzierung der ausgewählten Herzzellvorläufer erfolgt im Weiteren durch symmetrische bzw. asymmetrische Zellteilungen (siehe Abbildung 5) (Zaffran et al., 1995). Der Prozess der asymmetrischen Zellteilung ist ebenfalls Notch abhängig. Die asymmetrische Verteilung des intrazellulären Notch Inhibitors Numb führt zur Determinierung der Zellidentität in eine kardiale (Numb+) oder eine perikardiale (Numb-) Linie (Gajewski et al., 2000; Han and Bodmer, 2003; Su et al., 1999; Ward and Skeath, 2000). Auch hierfür ist die Prozessierung von Notch durch Kuzbanian/ADAM10 essentiell (Albrecht et al., 2006, vorliegende Arbeit).

Diese mehrstufige Determinierung der einzelnen Herzzellen aus dem dorsalen Mesoderm führt zur Ausbildung drei verschiedener Zellgruppen: den Kardioblasten, den Perikardzellen und einem Teil der dorsalen Körpermuskulatur.

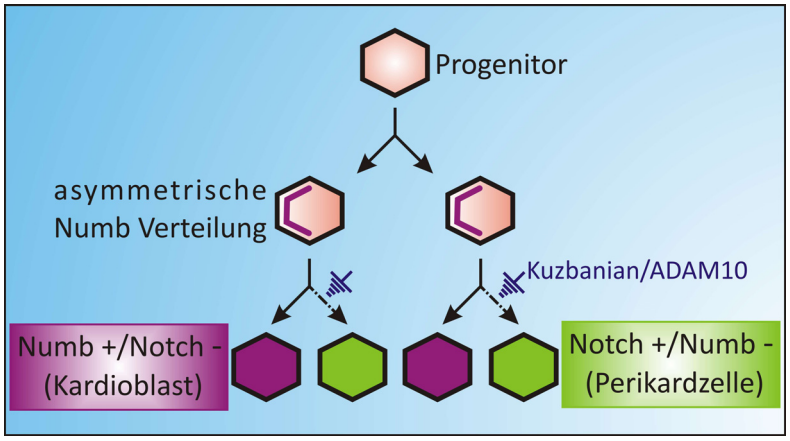

Abb. 5: Schematische Darstellung der asymmetrischen Zellteilung. Die einseitige Lokalisation von Numb bewirkt die Inhibition von Notch in nur einer Tochterzelle. Diese differenziert sich zu einer kardialen Zelle. Die Induktion des Notch/Delta-Signalweges führt über die proteolytische Aktivität von Kuzbanian/ADAM10 zu einem perikardialen Zellschicksal.

2.4. Zellgenealogie der Herzzellen

Das Herz von *Drosophila* besteht am Ende der Embryogenese aus 104 ausdifferenzierten Kardiomyozyten und den assoziierten perikardialen Zellen (Rizki, 1978). Die segmentale Anordnung der Herzzellen ist stereotyp. Pro Hemisegment findet man 6 Kardiomyozyten und 10 Perikardzellen. Die Genealogie der meisten Herzzellen ist bekannt und gut untersucht (siehe Abbildung 6):

Vier der sechs Kardioblasten pro Hemisegment exprimieren Tinman (Tin) und entwickeln sich aus sich symmetrisch teilenden Vorläuferzellen, während die zwei verbleibenden Kardioblasten positiv für den COUP TF Steroid Rezeptor Seven up (Svp) sind und aus einer asymmetrischen Teilung mit einer perikardialen Schwesterzelle stammen (Alvarez et al., 2003; Han and Bodmer, 2003; Ward and Skeath, 2000). Die Perikardzellen können in drei Gruppen unterteilt werden: die Even skipped positiven (EPZs), die Tin positiven (TPZs) und die Odd skipped positiven Perikardzellen (OPZs). Die OPZs entstehen aus drei Progenitoren, wobei zwei Vorläufer *mef2* und *svp* exprimieren und der verbleibende Vorläufer *odd* (P_{OPZ}). Die *mef2/svp* Vorläufer (P_{SOPZ}) teilen sich asymmetrisch und resultieren in Perikardzellen die *odd* und *svp* exprimieren (SOPZs) sowie in Svp positive Kardioblasten (SKBs). Der P_{OPZ} durchläuft eine symmetrischen Teilung aus der zwei Odd positive Perikardzellen hervorgehen (OPZs) (Gajewski et al., 2000; Ward and Skeath, 2000).

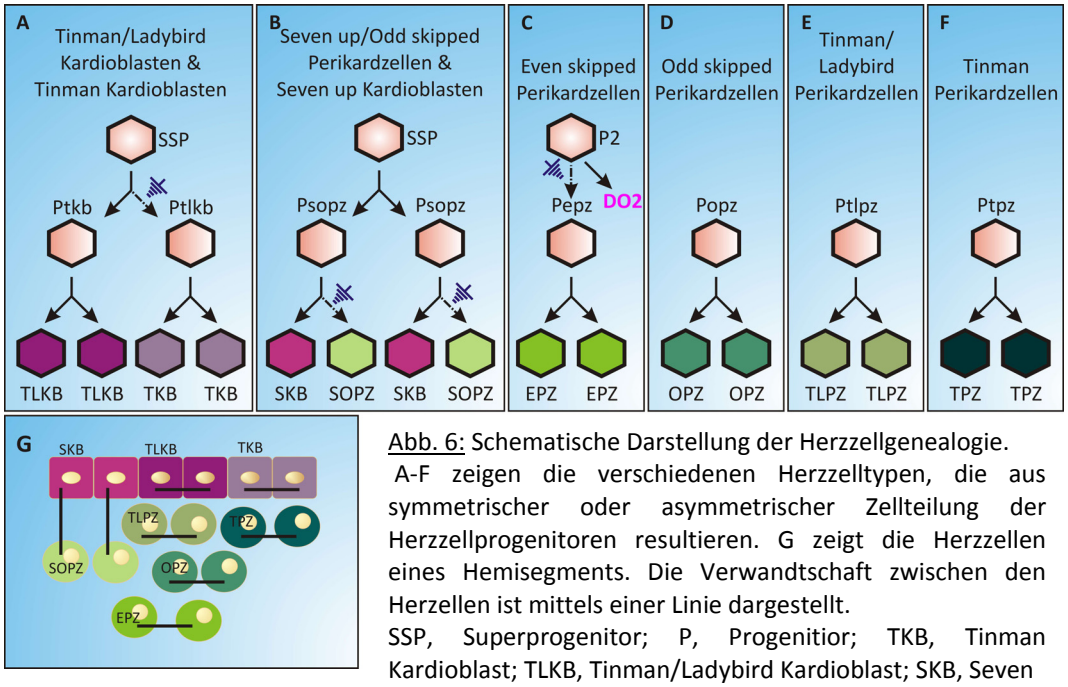

Abb. 6: Schematische Darstellung der Herzzellgenealogie.
A-F zeigen die verschiedenen Herzzelltypen, die aus symmetrischer oder asymmetrischer Zellteilung der Herzzellprogenitoren resultieren. G zeigt die Herzzellen eines Hemisegments. Die Verwandtschaft zwischen den Herzellen ist mittels einer Linie dargestellt.
SSP, Superprogenitor; P, Progenitior; TKB, Tinman Kardioblast; TLKB, Tinman/Ladybird Kardioblast; SKB, Seven up Kardioblast; SOPZ, Seven up/Odd skipped Perikardzelle; DO2, somatische Muskelzellen; EPZ, Even skipped Perikardzelle; OPZ, Odd skipped Perikardzelle; TLPZ, Tinman/Ladybird Perikardzelle; TPZ, Tinman Perikardzelle

Die Perikardzellgruppe der TPCs entstammt einer sich symmetrisch teilenden Vorläuferzelle ab. Die Herkunft der zwei EPCs stellt eine Besonderheit in der Genealogie der Perikardzellen dar, da sie Schwesterzellen eines Vorläufers für somatische Muskelzellen sind. Nach der Selektion der Vorläuferzelle P2 aus dem Kompetenzfeld mittels lateraler Inhibition teilt sich diese asymmetrisch zunächst in zwei Vorläufer (P_{DO2} und P_{EPZ}). Diese teilen sich zum einen in zwei Eve positive Perikardzellen (EPZ) und resultieren zum anderen in die DO2 Muskelzellen (Han and Bodmer, 2003; Su et al., 1999). Diese Differenzierungsprozesse unterliegen dem in 2.3 beschriebenen Mechanismus der Notch/Delta abhängigen asymmetrischen Zellteilung und somit auch der Aktivität von Kuzbanian/ADAM10 (Albrecht et al., 2006, vorliegende Arbeit).

2.5 Epithelbildung, Migration und Lumenbildung

Nach der Anordnung der Kardioblasten in zwei bilateralen Reihen an beiden Seiten des Embryos erlangen diese bislang mesenchymalen Zellen einen epithelialen Charakter (Mesenchym-Epithel Übergang) (Fremion et al., 1999). Die epitheliale Eigenschaft der Kardioblasten resultiert in der Ausbildung einer intrinsischen Zellpolarität, die durch die asymmetrische Verteilung von Zelladhäsionsmolekülen etabliert wird und Grundlage für die Ausbildung von Zell-Zell Kontakten ist. So ist die asymmetrische Lokalisation von E-Cadherin, ß-Catenin und Discs Large (Dlg - eine Membran-assoziierte Guanylkinase) ein deutliches Zeichen für die epithelialen Eigenschaften der Kardioblasten (Haag et al., 1999; Qian et al., 2005; Woods et al., 1996). Weitere Zell-Adhäsionsmoleküle, wie das Immunglobulin-ähnliche Oberflächenmolekül Faint-Sausage oder der Transmembranrezeptor Toll sind während der Kardioblasten Differenzierung von Bedeutung. Mutationen in den korrespondierenden Genen dieser Moleküle führen zu Fehlern in der korrekten Aneinanderreihung der Kardioblasten und zu Lücken in den Herzen (Haag et al., 1999; Wang et al., 2005). Dabei ist die korrekte Ausbildung der die Kardioblasten umgebenden extrazellulären Matrix (*engl. extracellular matrix* (ECM)) von zentraler Bedeutung für die Anordnung der Kardioblasten in bilateralen Reihen. Mutationen in Genen, die für essentielle Komponenten der ECM kodieren, wie LamininA, ßPS Integrin (Mys) oder αPS3 Integrin (Scb) resultieren in einer Beeinträchtigung der Herzrohrbildung (MacMullin and Jacobs, 2006; Yarnitzky and Volk, 1995). Aus ausführlichen Studien ist weiterhin bekannt, dass sogenannte Zielfindungsmoleküle wie die Rezeptor/Liganden-Paare Roundabout (Robo) oder Roundabout2 (Robo2) und Slit an der Regulation des Übergangs von Mesenchym- zu Epithel-

Zustand der Kardioblasten beteiligt sind (Qian et al., 2005). Diese Zielfindungsmoleküle sind auch zum Ende der Kardiogenese für die korrekte Ausbildung des Herzlumens von Bedeutung (Medioni et al., 2008; Santiago-Martinez et al., 2008).

Hat die Anordnung der Kardioblasten zu einem bilateralen, einschichtigen Epithel stattgefunden, migrieren die Zellen in dorsale Richtung aufeinander zu. Im gleichen Zeitraum finden auch im darüber liegenden Ektoderm Reorganisationsprozesse statt. Die ektodermalen Epithelzellen wandern ebenfalls aufeinander zu und verdrängen die restlichen extraembryonalen Amnioserosazellen (Rizki, 1978). Rugendorff und Kollegen konnten zeigen, dass die migrierenden Kardioblasten der Bewegung der dorsalsten Epidermiszellen folgen (Rugendorff et al., 1994). Weitere Analysen geben Hinweise auf eine über ECM-Komponenten vermittelte Verbindung zwischen Kardioblasten und der Epidermis, so dass es sich bei der Wanderung der Kardioblasten zur dorsalen Mittellinie um eine passive Bewegung in dorsale Richtung handeln könnte (Chartier et al., 2002).

Gelangen die Kardioblasten zur dorsalen Mittellinie und treffen dort mit der gegenüberliegenden Kardioblastenreihe zusammen, kommt es zum Zusammenschluss und zur Ausbildung des Herzrohres (Rizki, 1978; Rugendorff et al., 1994) (siehe Abbildung 7). Aus Lebendbeobachtungen und Analysen an fixiertem Gewebe ist bekannt, dass die dorsalen Membranbereiche der Kardioblasten Actin reiche Ausstülpungen ausbilden und mit diesen den Kontakt zu ihren kontralateralen „Partner-Kardioblasten“ aufnehmen. Nach Ausbildung des ersten, dorsalen Kontakts lässt sich eine dynamische Veränderung der Zellform beobachten. Die Kardioblasten nehmen eine Halbmondform ein und treffen anschließend mit ihren ventralen Membranseiten aneinander. Damit entsteht eine von ausdifferenzierten Kardiomyozyten geformte Röhre – das Herzrohr, welches einen luminalen Bereich umschließt – das Herzlumen (Haag et al., 1999; Medioni et al., 2008; Rugendorff et al., 1994). Der Prozess der Lumenbildung in *Drosophila* wird auch als „cell assembly“ bezeichnet (Baer et al., 2009).

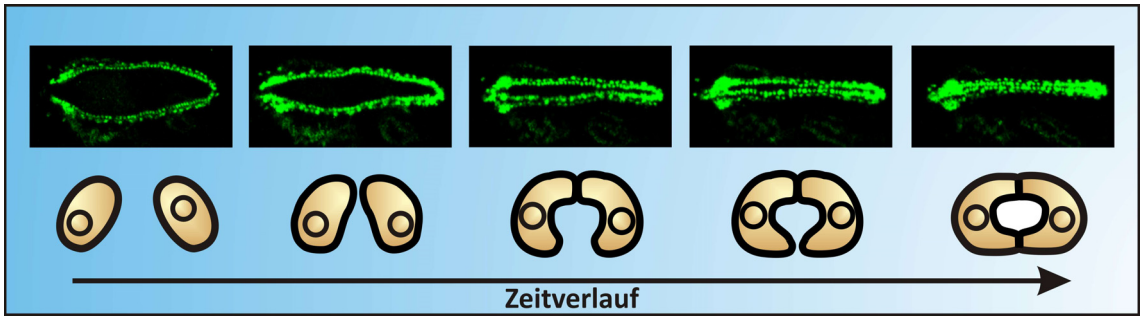

Abb. 7: Obere Reihe: Mit Hilfe einer *hand*CGFP Reporterlinie lassen sich die Phasen der Herzzellmigration zur dorsalen Mittellinie im lebenden Tier verfolgen. Die bilateral angelegten Herzzellen migrieren aufeinander zu, treten in Kontakt und bilden das Herzrohr. Untere Reihe: Schematische Darstellung von Querschnitten durch das Herz. Die gezeigten Positionen und die Zellformänderungen der Kardioblasten korrespondieren mit den oben dargestellten Entwicklungsphasen.

Alle an der Lumenbildung beteiligten Kardiomyozyten weisen eine einheitliche Polarität auf. Die apikale Seite der Zelle weist zum Lumen, während die basale Zellseite abluminal orientiert ist (zusammengefasst in Baer et al. (2009)). Die frühere Hypothese, dass die Herzlumenbildung bei *Drosophila melanogaster* ebenfalls durch Membranen mit einheitlichen, apikalen Membranattributen ausgebildet werden (Haag et al., 1999), konnte nun durch Untersuchungen von Medioni und Kollegen erweitert werden. Die lumenbildende Zellmembran lässt sich nochmals in zwei spezielle Membrandomänen unterteilen, die durch das Vorhandensein verschiedenster Zellpolaritäts-Marker differenziert werden können (Albrecht et al., 2010 in revision; Medioni et al., 2008, vorliegende Arbeit). Die das Lumen umschließende Seite (apikale Zellmembran) wird als L(uminale)-Domäne bezeichnet und weist Charakteristika einer Membran auf, wie sie auf der basalen Seite einer Zelle vorkommt. Der zweite Membranbereich in den sich die dem Lumen zugewandte Membranseite der Kardiomyozyten unterteilen lässt, findet sich, geteilt in zwei Kompartimente, am dorsalen und ventralen Kontaktbereich zwischen den Kardiomyozyten wieder. Diese Adhäsiven-Domänen zeigen eine Lokalisation von Adhäsionsmolekülen wie E-Cadherin und ß-Catenin. Mit Hilfe von elektronenmikroskopischen Aufnahmen lassen sich in diesen Bereichen Adhäsionsverbindungen (adherens junctions) nachweisen, daher werden sie auch als *J(unctional) domains* bezeichnet (Medioni et al., 2008; Santiago-Martinez et al., 2008). Da die J-Domänen keine Expression baso-lateraler Marker (zum Beispiel αSpectrin) zeigen, schließen Medioni und Kollegen auf Membrandomänen mit apikalen Zellattributen (Medioni et al., 2008) (siehe Abbildung 8).

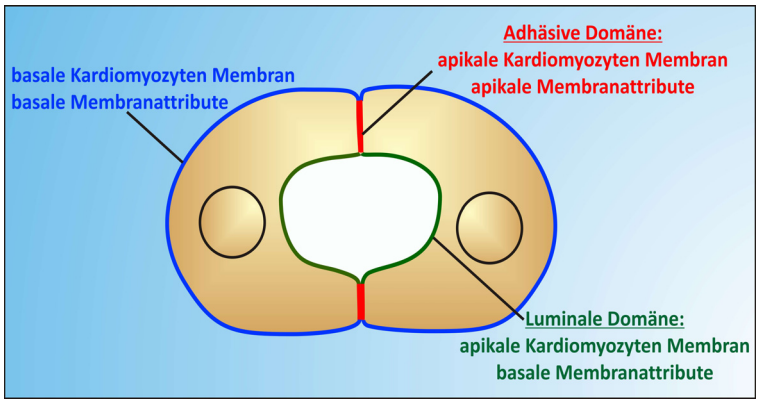

Abb. 8: Schematische Darstellung eines Herzrohr-Querschnittes. Die apikale Membranseite (Lumen zugewandt) der Kardiomyozyten kann in drei Kompartimente aufgeteilt werden. Die beiden adhäsiven Domänen an den Kontaktbereichen der Kardiomyozyten zeigen Charakteristika apikaler Membranen. Die luminale Domäne weist dagegen basale Membran-attribute auf. Die abluminale Seite der Kardiomyozyten repräsentiert eine einheitlich basale Membran.

Die Ausbildung von definierten Membrankompartimenten entlang der lumenzugewandten Kardiomyozytenseite unterliegt der Aktivität von Zielfindungsmolekülen, die auch schon für die Determinierung der Zellpolarität während des Mesenchym-Epithel Übergangs eine Rolle spielen (Medioni et al., 2008; Santiago-Martinez et al., 2008). Der Ligand Slit und sein Transmembranrezeptor Robo sind an der L-Domäne der Kardiomyozyten lokalisiert und

wirken dort als Repellanten der kontralateralen Membranbereiche, um einen Kontakt während des Prozesses der Lumenbildung zu verhindern. In *Drosophila* ist die Aktivität beider Proteine als Repellanten und/oder Attraktanten bereits in ausführlichen Studien während der Entwicklung des Nervensystems (Steuerung der Motoraxon Zielfindung), des Tracheensystems oder der Migrationssteuerung des frühen Mesoderms gezeigt worden (Bashaw and Goodman, 1999; Kramer et al., 2001; Lundstrom et al., 2004; Simpson et al., 2000). Neueste Studien belegen, dass Slit3 und Robo1 & Robo2 eine spezifische Expression im embryonalen Mausherz aufweisen. Die durch Nkx2-5 und T-Box Faktoren restringierte Expression von Slit3 weist auf eine Funktion des Robo/Slit-Signalsweges während der Entwicklung des Kammermyokards hin (Medioni et al., 2010). Es ist ebenfalls bekannt, dass Slit und Robo in Vertebraten unter anderem während der Angiogenese und der Bildung von tubulären Drüsen im Brustgewebe agieren (Klagsbrun and Eichmann, 2005; Strickland et al., 2006; Weinstein, 2005). In *Drosophila melanogaster* Mutanten für *slit* und *robo* unterbleibt die Lumenbildung im Herzen völlig. Die Kardiomyozyten adhärieren entlang der kompletten Kontaktseite. Die J-Domänen sind nicht mehr auf die dorsalen und ventralen Bereiche der Kardiomyozyten reduziert, sondern verlängern sich entlang der gesamten Kontaktseite (Medioni et al., 2008; Santiago-Martinez et al., 2008). Durch den fehlenden repulsiven Effekt von Slit und Robo auf die L-Domäne könnte die Regulation des Actin-Zytoskeletts betroffen sein, so dass eine Zellformänderung der Kardiomyozyten nicht gewährleistet werden kann (Medioni et al., 2008; Santiago-Martinez et al., 2008). Die Verteilung des Zytoskelettregulators Enabled/VASP (Ena), der an der Polymerisation der Actinfilamente beteiligt ist, ist in *robo* Mutanten beeinträchtigt (Santiago-Martinez et al., 2008). Im Nervensystem von *Drosophila* konnte bereits gezeigt werden, dass Ena mit der zytoplasmatischen Domäne von Robo interagiert und somit als Downstream-Effektor im Robo/Slit-Signalweg eine Rolle spielt (Bashaw et al., 2000).

Die vorliegende Arbeit beschäftig sich mit zwei weiteren Zielfindungsmolekülen, die als repulsiv wirkendes Rezeptor/Liganden-Paar interagieren (Keleman and Dickson, 2001). Es konnte gezeigt werden, dass im Herz von *Drosophila* Uncoordinated 5 (Unc5) und sein korrespondierender Ligand NetrinB (NetB) ebenso wie Robo und Slit die Repulsion der luminalen Membranseite der Kardiomyozyten vermitteln. Die Zellformänderung der Kardiomyozyten unterbleibt durch das Fehlen von Unc5 oder NetB völlig, die Kardiomyozyten lagern sich entlang ihrer apikalen Seite aneinander ohne ein Lumen zu umschließen. Die Determinierung der klar abgegrenzten Membrankompartimente (J- und L-Domäne) zeigt allerdings keine Beeinträchtigung in *unc5* mutanten Embryonen. Dies lässt auf

einen Robo/Slit unabhängigen Regulationsprozess schließen, in dem Unc5 und NetB eine zusätzliche, putative Rolle während der Steuerung der Zellformänderung übernehmen könnten (Albrecht et al., 2010 in revision, vorliegende Arbeit).

Zusammenfassend lässt sich sagen, dass das Herz sowohl bei Vertebraten als auch bei *Drosophila melanogaster* als ein Organ betrachtet werden kann, welches sich in distinkte morphologische Teilbereiche gliedert. Der korrekte Ablauf der Kardiogenese bedingt eine präzise Abfolge an dynamischen Steuerungsprozessen, die durch komplexe Interaktionen konservierter Moleküle realisiert werden müssen.

Referenzen

Abu-Issa, R., and Kirby, M. L. (2007). Heart field: from mesoderm to heart tube. *Annu Rev Cell Dev Biol* **23,** 45-68.

Albrecht, S., Altenhein, B., and Paululat, A. (2010 in revision). The transmembrane receptor Uncoordinated 5 (Unc5) is essential for heart lumen formation in *Drosophila melanogaster*. *Dev Biol*

Albrecht, S., Wang, S., Holz, A., Bergter, A., and Paululat, A. (2006). The ADAM metalloprotease Kuzbanian is crucial for proper heart formation in *Drosophila melanogaster*. *Mech Dev* **123,** 372-87.

Alvarez, A. D., Shi, W., Wilson, B. A., and Skeath, J. B. (2003). *pannier* and *pointedP2* act sequentially to regulate *Drosophila* heart development. *Development* **130,** 3015-26.

Azpiazu, N., and Frasch, M. (1993). *tinman* and *bagpipe*: two homeo box genes that determine cell fates in the dorsal mesoderm of *Drosophila*. *Genes Dev* **7,** 1325-40.

Baer, M. M., Chanut-Delalande, H., and Affolter, M. (2009). Cellular and molecular mechanisms underlying the formation of biological tubes. *Curr Top Dev Biol* **89,** 137-62.

Bashaw, G. J., and Goodman, C. S. (1999). Chimeric axon guidance receptors: the cytoplasmic domains of slit and netrin receptors specify attraction versus repulsion. *Cell* **97,** 917-26.

Bashaw, G. J., Kidd, T., Murray, D., Pawson, T., and Goodman, C. S. (2000). Repulsive axon guidance: Abelson and Enabled play opposing roles downstream of the roundabout receptor. *Cell* **101,** 703-15.

Bodmer, R. (1993). The gene tinman is required for specification of the heart and visceral muscles in *Drosophila*. *Development* **118,** 719-29.

Campos-Ortega, J. A., and Hartenstein, V. (1985). "The embryonic development of *Drosophila melanogaster*." Springer, Berlin , Heidelberg, New York.

Carmena, A., Buff, E., Halfon, M. S., Gisselbrecht, S., Jimenez, F., Baylies, M. K., and Michelson, A. M. (2002). Reciprocal regulatory interactions between the Notch and Ras signaling pathways in the *Drosophila* embryonic mesoderm. *Dev Biol* **244,** 226-42.

Chartier, A., Zaffran, S., Astier, M., Semeriva, M., and Gratecos, D. (2002). Pericardin, a *Drosophila* type IV collagen-like protein is involved in the morphogenesis and maintenance of the heart epithelium during dorsal ectoderm closure. *Development* **129,** 3241-53.

Crossley, A. C. (1985). Nephrocytes and pericardial cells. *In* "Comprehensive insect physiology, biochemistry, and pharmacology" (G. A. Kerkut and L. I. Gilbert, Eds.), Vol. 3. Pergamon Press, Oxford.

Curtis, N. J., Ringo, J. M., and Dowse, H. B. (1999). Morphology of the pupal heart, adult heart, and associated tissues in the fruit fly, *Drosophila melanogaster*. *J Morphol* **240,** 225-35.

Das, D., Aradhya, R., Ashoka, D., and Inamdar, M. (2008). Post-embryonic pericardial cells of *Drosophila* are required for overcoming toxic stress but not for cardiac function or adult development. *Cell Tissue Res* **331,** 565-70.

Evans, S. M., Yan, W., Murillo, M. P., Ponce, J., and Papalopulu, N. (1995). *tinman*, a *Drosophila* homeobox gene required for heart and visceral mesoderm specification, may be represented by a family of genes in vertebrates: XNkx-2.3, a second vertebrate homologue of *tinman*. *Development* **121,** 3889-99.

Frasch, M. (1995). Induction of visceral and cardiac mesoderm by ectodermal Dpp in the early *Drosophila* embryo. *Nature* **374,** 464-7.

Frasch, M. (1999). Intersecting signalling and transcriptional pathways in *Drosophila* heart specification. *Semin Cell Dev Biol* **10,** 61-71.

Fremion, F., Astier, M., Zaffran, S., Guillen, A., Homburger, V., and Semeriva, M. (1999). The heterotrimeric protein Go is required for the formation of heart epithelium in *Drosophila*. *J Cell Biol* **145,** 1063-76.

Gajewski, K., Choi, C. Y., Kim, Y., and Schulz, R. A. (2000). Genetically distinct cardial cells within the *Drosophila* heart. *Genesis* **28,** 36-43.

Haag, T. A., Haag, N. P., Lekven, A. C., and Hartenstein, V. (1999). The role of cell adhesion molecules in *Drosophila* heart morphogenesis: *faint sausage, shotgun/DE-cadherin,* and *laminin A* are required for discrete stages in heart development. *Dev Biol* **208,** 56-69.

Han, Z., and Bodmer, R. (2003). Myogenic cells fates are antagonized by Notch only in asymmetric lineages of the *Drosophila* heart, with or without cell division. *Development* **130,** 3039-51.

Hartenstein, A. Y., Rugendorff, A., Tepass, U., and Hartenstein, V. (1992). The function of the neurogenic genes during epithelial development in the *Drosophila* embryo. *Development* **116,** 1203-20.

Keleman, K., and Dickson, B. J. (2001). Short- and long-range repulsion by the *Drosophila* Unc5 netrin receptor. *Neuron* **32,** 605-17.

Kidd, S., Lieber, T., and Young, M. W. (1998). Ligand-induced cleavage and regulation of nuclear entry of Notch in *Drosophila melanogaster* embryos. *Genes Dev* **12,** 3728-40.

Klagsbrun, M., and Eichmann, A. (2005). A role for axon guidance receptors and ligands in blood vessel development and tumor angiogenesis. *Cytokine Growth Factor Rev* **16,** 535-48.

Kramer, S. G., Kidd, T., Simpson, J. H., and Goodman, C. S. (2001). Switching repulsion to attraction: changing responses to slit during transition in mesoderm migration. *Science* **292,** 737-40.

Lai, E. C. (2002). Notch cleavage: Nicastrin helps Presenilin make the final cut. *Curr Biol* **12,** R200-2.

Lalevee, N., Monier, B., Senatore, S., Perrin, L., and Semeriva, M. (2006). Control of Cardiac Rhythm by ORK1, a *Drosophila* Two-Pore Domain Potassium Channel. *Curr Biol* **16,** 1502-8.

Lee, H. H., and Frasch, M. (2005). Nuclear integration of positive Dpp signals, antagonistic Wg inputs and mesodermal competence factors during *Drosophila* visceral mesoderm induction. *Development* **132,** 1429-42.

Rugendorff, A., Hartenstein, A. Y., and Hartenstein, V. (1994). Embryonic origin and differentiation of the Drosophila heart. *Roux`s Archives Develomental Biology* **203,** 266-280.

Santiago-Martinez, E., Soplop, N. H., Patel, R., and Kramer, S. G. (2008). Repulsion by Slit and Roundabout prevents Shotgun/E-cadherin-mediated cell adhesion during Drosophila heart tube lumen formation. *J Cell Biol* **182,** 241-8.

Searcy, R. D., and Yutzey, K. E. (1998). Analysis of Hox gene expression during early avian heart development. *Dev Dyn* **213,** 82-91.

Sellin, J., Albrecht, S., Kolsch, V., and Paululat, A. (2006). Dynamics of heart differentiation, visualized utilizing heart enhancer elements of the Drosophila melanogaster bHLH transcription factor Hand. *Gene Expr Patterns* **6,** 360-75.

Senatore, S., Rami Reddy, V., Semeriva, M., Perrin, L., and Lalevee, N. (2010). Response to mechanical stress is mediated by the TRPA channel painless in the Drosophila heart. *PLoS Genet* **6**.

Simpson, J. H., Kidd, T., Bland, K. S., and Goodman, C. S. (2000). Short-range and long-range guidance by slit and its Robo receptors. Robo and Robo2 play distinct roles in midline guidance. *Neuron* **28,** 753-66.

Srivastava, D., Olson, E. N. (2000) A genetic blueprint for cardiac development. *Nature*, **407**, 221-6

Strickland, P., Shin, G. C., Plump, A., Tessier-Lavigne, M., and Hinck, L. (2006). Slit2 and netrin 1 act synergistically as adhesive cues to generate tubular bi-layers during ductal morphogenesis. *Development* **133,** 823-32.

Su, M. T., Fujioka, M., Goto, T., and Bodmer, R. (1999). The Drosophila homeobox genes zfh-1 and even-skipped are required for cardiac-specific differentiation of a numb-dependent lineage decision. *Development* **126,** 3241-51.

Tao, Y., and Schulz, R. A. (2006). Heart development in Drosophila. *Semin Cell Dev Biol* **18,** 3-15.

Wang, J., Tao, Y., Reim, I., Gajewski, K., Frasch, M., and Schulz, R. A. (2005). Expression, regulation, and requirement of the toll transmembrane protein during dorsal vessel formation in Drosophila melanogaster. *Mol Cell Biol* **25,** 4200-10.

Ward, E. J., and Skeath, J. B. (2000). Characterization of a novel subset of cardiac cells and their progenitors in the Drosophila embryo. *Development* **127,** 4959-69.

Weinstein, B. M. (2005). Vessels and nerves: marching to the same tune. *Cell* **120,** 299-302.

Woods, D. F., Hough, C., Peel, D., Callaini, G., and Bryant, P. J. (1996). Dlg protein is required for junction structure, cell polarity, and proliferation control in Drosophila epithelia. *J Cell Biol* **134,** 1469-82.

Wu, L., Aster, J. C., Blacklow, S. C., Lake, R., Artavanis-Tsakonas, S., and Griffin, J. D. (2000). MAML1, a human homologue of Drosophila mastermind, is a transcriptional co-activator for NOTCH receptors. *Nat Genet* **26,** 484-9.

Wu, X., Golden, K., and Bodmer, R. (1995). Heart development in Drosophila requires the segment polarity gene wingless. *Dev Biol* **169,** 619-28.

Yarnitzky, T., and Volk, T. (1995). Laminin is required for heart, somatic muscles, and gut development in the Drosophila embryo. *Dev Biol* **169,** 609-18.

Yin, Z., and Frasch, M. (1998). Regulation and function of tinman during dorsal mesoderm induction and heart specification in Drosophila. *Dev Genet* **22,** 187-200.

Zaffran, S., Astier, M., Gratecos, D., Guillen, A., and Semeriva, M. (1995). Cellular interactions during heart morphogenesis in the Drosophila embryo. *Biol Cell* **84,** 13-24.

Zaffran, S., and Frasch, M. (2002). Early signals in cardiac development. *Circ Res* **91,** 457-69.

Lieber, T., Kidd, S., and Young, M. W. (2002). kuzbanian-mediated cleavage of Drosophila Notch. *Genes Dev* **16,** 209-21.

Lo, P. C., Skeath, J. B., Gajewski, K., Schulz, R. A., and Frasch, M. (2002). Homeotic genes autonomously specify the anteroposterior subdivision of the Drosophila dorsal vessel into aorta and heart. *Dev Biol* **251,** 307-19.

Lockwood, W. K., and Bodmer, R. (2002). The patterns of wingless, decapentaplegic, and tinman position the Drosophila heart. *Mech Dev* **114,** 13-26.

Lundstrom, A., Gallio, M., Englund, C., Steneberg, P., Hemphala, J., Aspenstrom, P., Keleman, K., Falileeva, L., Dickson, B. J., and Samakovlis, C. (2004). Vilse, a conserved Rac/Cdc42 GAP mediating Robo repulsion in tracheal cells and axons. *Genes Dev* **18,** 2161-71.

Lyons, I., Parsons, L. M., Hartley, L., Li, R., Andrews, J. E., Robb, L., and Harvey, R. P. (1995). Myogenic and morphogenetic defects in the heart tubes of murine embryos lacking the homeo box gene Nkx2-5. *Genes Dev* **9,** 1654-66.

MacMullin, A., and Jacobs, J. R. (2006). Slit coordinates cardiac morphogenesis in *Drosophila*. *Dev Biol* **293,** 154-64.

Medioni, C., Astier, M., Zmojdzian, M., Jagla, K., and Semeriva, M. (2008). Genetic control of cell morphogenesis during Drosophila melanogaster cardiac tube formation. *J Cell Biol* **182,** 249-61.

Medioni, C., Bertrand, N., Mesbah, K., Hudry, B., Dupays, L., Wolstein, O., Washkowitz, A. J., Papaioannou, V. E., Mohun, T. J., Harvey, R. P., and Zaffran, S. (2010). Expression of Slit and Robo genes in the developing mouse heart. *Dev Dyn*.

Miller, A. (1965). The internal anatomy and histology of the imago. *In* "Biology of *Drosophila*" (M. Demerec, Ed.), pp. 420-534. Hafner Pub. Co., New York.

Molina, M. R., and Cripps, R. M. (2001). Ostia, the inflow tracts of the Drosophila heart, develop from a genetically distinct subset of cardial cells. *Mech Dev* **109,** 51-9.

Monier, B., Astier, M., Semeriva, M., and Perrin, L. (2005). Steroid-dependent modification of Hox function drives myocyte reprogramming in the Drosophila heart. *Development* **132,** 5283-93.

Monier, B., Tevy, M. F., Perrin, L., Capovilla, M., and Semeriva, M. (2007). Downstream of homeotic genes: in the heart of Hox function. *Fly (Austin)* **1,** 59-67.

Ocorr, K., Reeves, N. L., Wessells, R. J., Fink, M., Chen, H. S., Akasaka, T., Yasuda, S., Metzger, J. M., Giles, W., Posakony, J. W., and Bodmer, R. (2007). KCNQ potassium channel mutations cause cardiac arrhythmias in Drosophila that mimic the effects of aging. *Proc Natl Acad Sci U S A* **104,** 3943-8.

Ponzielli, R., Astier, M., Chartier, A., Gallet, A., Therond, P., and Semeriva, M. (2002). Heart tube patterning in Drosophila requires integration of axial and segmental information provided by the Bithorax Complex genes and hedgehog signaling. *Development* **129,** 4509-21.

Qian, L., Liu, J., and Bodmer, R. (2005). Slit and robo control cardiac cell polarity and morphogenesis. *Curr Biol* **15,** 2271-8.

Reim, I., and Frasch, M. (2010). Genetic and Genomic Dissection of Cardiogenesis in the Drosophila Model. *Pediatr Cardiol* **31,** 325-34.

Richard, P. H., Rosenthal, N. (1998) Heart Development. *Academic Press*, New York

Riechmann, V., Irion, U., Wilson, R., Grosskortenhaus, R., and Leptin, M. (1997). Control of cell fates and segmentation in the Drosophila mesoderm. *Development* **124,** 2915-22.

Rizki, T. M. (1978). The circulatory system and associated cells and tissues. *In* "The Genetics and Biology of *Drosophila*" (M. Ashburner and T. R. F. Wright, Eds.), Vol. 2b, pp. 397-452. Academic Press, New York, NY.

Zeitouni, B., Senatore, S., Severac, D., Aknin, C., Semeriva, M., and Perrin, L. (2007). Signalling Pathways Involved in Adult Heart Formation Revealed by Gene Expression Profiling in Drosophila. *PLoS Genet* **3,** e174.

3. Ergebnisse – Publikationen

- **Sellin, J., Albrecht, S., Kölsch, V. and Paululat, A.** (2006).
  Dynamics of heart differentiation, visualized utilizing heart enhancer elements of the *Drosophila melanogaster* bHLH transcription factor Hand.
  Gene Expression Patterns 6, 360-75.

- **Albrecht, S., Wang, S., Holz, A., Bergter, A. and Paululat, A.** (2006).
  The ADAM metalloprotease Kuzbanian is crucial for proper heart formation in *Drosophila melanogaster*.
  Mechanisms of Development 123, 372-87.

- **Albrecht, S., Altenhein, B. and Paululat, A.** (2011).
  The transmembrane receptor Uncoordinated 5 (Unc5) is essential for heart lumen formation in *Drosophila melanogaster*.
  Developmental Biology 350, 89-100.

ELSEVIER

Gene Expression Patterns 6 (2006) 360–375

GEP

www.elsevier.com/locate/modgep

Dynamics of heart differentiation, visualized utilizing heart enhancer elements of the *Drosophila melanogaster* bHLH transcription factor Hand

Julia Sellin [a], Stefanie Albrecht [a], Verena Kölsch [b], Achim Paululat [a,*]

[a] *Universität Osnabrück, Fachbereich Biologie/Chemie - Zoologie, Barbarastraße 11, 49069 Osnabrück, Germany*
[b] *Universität Köln, Fachbereich Biologie, Institut für Genetik, Zülpicher Strasse 47, 50674 Köln, Germany*

Received 20 September 2005; accepted 25 September 2005
Available online 7 February 2006

Abstract

Drosophila melanogaster has become one of the important model systems to investigate the development and differentiation of the heart. After 24 h after egg deposition (h AED), a simple tube-like organ is formed, consisting of essentially only two cell types, the contractile cardioblasts and non-myogenic pericardial cells. In contrast to the detailed knowledge of heart formation during embryogenesis, only a few studies deal with later changes in heart morphology and/or function. This is mainly due to the difficulties to carry out whole mount stainings in later stages without complicated dissections or treatments of the cuticle and puparium. In this paper we describe the identification of a *hand* genomic region, which is fully sufficient to drive GFP expression in heart cells of embryos, larvae, and adults. This serves as an initial step to understand the position of *hand* in the early regulatory network in heart development. Furthermore, we demonstrate that our newly created GFP reporter line is extremely useful to study postembryonic heart differentiation. For the first time we document heart differentiation in living animals throughout all developmental stages of *Drosophila melanogaster*, including embryogenesis, all three larval stages, metamorphosis, and the adult life with respect to pericardial cells and cardiomyocytes.

1. Results and discussion

The *Drosophila* dorsal vessel is an excellent model for studying cell determination and differentiation due to its simple, tube-like organization consisting essentially of only two major cell types: the contractile cardiomyoblasts, that form the lumen of the heart, and the associated non-myogenic pericardial cells (reviewed e.g. in Zaffran and Frasch, 2002). Nevertheless, as simple as the fly heart appears, functional differences between specific subsets of cardiomyoblasts and pericardial cells are necessary to develop the fully functional circulatory organ. For example, the cardioblasts in the posterior part of the dorsal vessel (the ventricle) form a wider lumen than cardioblasts in the anterior part (the aorta) and are thought to bear pacemaker activity (Rizki, 1978). Another example is the population of *seven-up (svp)* expressing cardioblasts which specifically participate in ostia or ostia precursor formation (Lo and Frasch, 2001; Molina and Cripps, 2001).

The early events in *Drosophila* heart development are quite well understood. Genetic and molecular studies have revealed numerous components of the regulatory network involved in the early determination and differentiation of the cardiac primordium. Many of the identified factors, like Twist or Tinman, are transcriptional regulators showing a remarkable evolutionary conservation between numerous animals on the level of protein structure and their functional roles in determination of mesodermal primordia (reviewed e.g. in Zaffran and Frasch, 2002). The subsequent cellular processes that allow a primordial heart cell to develop into a fully differentiated and functional cardiomyocyte are less understood so far since there is a lack of information about genes that are regulated by the early mesodermal transcriptional activators and repressors. One route to understand gene regulation and consequently cell differentiation of heart cells is to identify and analyze genes specifically expressed in the developing heart. In previous studies we and others have characterized the *Drosophila melanogaster hand* gene that encodes a highly conserved bHLH transcription factor expressed in heart cells (Kölsch and Paululat, 2002; Moore et al., 2000). *hand* genes were found in a variety of vertebrate species including humans. Higher vertebrates have two *hand* genes, eHand and dHand, also known as Hand1, Hxt, Thing1 and Hand2, Hed, Thing2 (Angelo, et al., 2000; Charité et al.,

* Corresponding author. Tel.: +49 541 969 2285; fax: +49 541 969 2587.
E-mail address: paululat@biologie.uni-osnabrueck.de (A. Paululat).

1567-133X/$ - see front matter © 2005 Elsevier B.V. All rights reserved.
doi:10.1016/j.modgep.2005.09.012

2000; Cross et al., 1995; Fernandez-Teran et al., 2000; Firulli et al., 1998; Hollenberg et al., 1995; Howard et al., 1999; Knöfler et al., 1998; Riley et al., 1998; Russell et al., 1997; Russell et al., 1998; Sparrow et al., 1998; Srivastava et al., 1995; Srivastava et al., 1997; Tanaka et al., 2002; Thomas et al., 1998; Yamagishi et al., 2000; Yelon et al., 2000). A common feature of all *hand* genes investigated so far is their expression in cardiac tissues during embryogenesis (recently reviewed in Firulli, 2003). We have shown that *Drosophila melanogaster hand* has a specific expression profile including expression in all cells of the embryonic heart - cardioblasts and pericardial cells as well (Kölsch and Paululat, 2002). Additional expression of *hand* was observed in the visceral mesoderm, the lymph gland cells, the garland cells, and a few cells of the developing CNS.

As an initial step to understand the regulatory network of cardiac factors considering *hand* as an example, we have conducted a functional dissection of the regulatory regions of the *hand* gene. We found the third intron fully capable to drive reporter gene activity in embryos in a wildtype like manner. Separating the spatial and temporal regulation events of *hand* activity during cardiogenesis may provide an entry point for studying the principles of cardiac regulatory networks, especially since *hand* is the only known transcription factor expressed in all cell types of the heart.

Morphologically, the dipterian larval dorsal vessel consists of clearly distinguishable regions along the anterio-posterior axis, described by e.g. Jensen (1973) and Rizki (1978). Recently, the identification of molecular markers and the analysis of mutants affecting the regionalization of the dorsal vessel shed light on the cellular mechanisms underlying the formation of a coordinated anterio-posterior morphology (Alvarez et al., 2003; Lo et al., 2002; Lovato et al., 2002; Perrin et al., 2004; Ponzielli et al., 2002). The anterior region of the dorsal vessel, the aorta (Jensen, 1973) or anterior aorta (Perrin et al., 2004), is the outflow tract with a narrow lumen, projecting slightly inwards to release the hemolymph into the body cavity (Zikova et al., 2003). The cardioblasts of the anterior aorta are of a different origin than the ones situated more posteriorly as shown by lineage tracing and clonal analyses (Alvarez et al., 2003; Han & Bodmer, 2003), and they specifically express the homeobox gene *homothorax* (*hth*) (Perrin et al., 2004). The next region of the larval dorsal vessel, the front-heart (Jensen, 1973) or posterior aorta (Perrin et al., 2004), has four pairs of non-functional ostia and does not express *homothorax* but *ultrabithorax* (*ubx*) (Ponzielli et al., 2002). In the absence of *hox* gene function, the posterior aorta is converted into an anterior aorta fate. The most posterior part of the *Drosophila* dorsal vessel, the ventricle or heart proper, has a wider lumen, is separated from the anterior region by a valve-like structure, and contains three pairs of functional ostia. Furthermore it is characterized by the expression of unique markers like Abd-A and Abd-B (Lo et al., 2002; Ponzielli et al., 2002). In the absence of Abd-A this part develops posterior aorta like (Lo et al., 2002). The cardioblasts of the ventricle are of the same origin than the cardioblasts in the posterior aorta (Alvarez et al., 2003; Han and Bodmer, 2003). Interestingly, in other dipterian species the posterior aorta is supplied with functional ostia (Jensen, 1973). Together with the fact that the posterior part of the aorta contributes completely to the adult heart, this is an argument to consider it as being part of the heart instead of the aorta as suggested by Jensen (1973).

Our knowledge of postembryonic cardiac development, like growth and elongation of heart cells or differentiation of functional ostia from precursor cells, is widely limited, mainly because immunohistological techniques are not applicable on postembryonic stages without preparation or further treatment, since cuticle and puparium are not permeated easily. A transgenic *Drosophila* line, carrying a living cell marker such as GFP, continuously expressed on high levels specifically in all heart cells throughout the whole life cycle, is an ideal tool to investigate important aspects of postembryonic heart differentiation. In addition, such a fly line will be of great benefit for studying physiological aspects of heart function, e.g. the influence of drugs on the heart beat, since it allows observation of heart function in the living animal. A few enhancer trap or Gal 4 driver lines mediating GFP expression in the heart exist, but to our knowledge all of those harbor specific disadvantages, e.g. the expression is restricted to a subset of heart cells, or they are not active in later developmental stages (Ponzielli et al., 2002; Wang et al., 2005). Taking advantage of our functional dissection approach to find the embryonic cardiac enhancers of *hand*, we therefore tested if the identified elements are sufficient to drive postembryonic reporter gene activity as well, thus reflecting larval or adult *hand* expression in order to use it for monitoring heart cell differentiation in living animals.

In this paper we show that the third intron of the *hand* gene harbors all elements sufficient to drive GFP expression in larvae, pupae and adults continuously and on high levels, therefore allowing us to conduct a detailed study of the dynamics of postembryonic heart differentiation in living animals. In addition we have analyzed the expression of *hand* or *hand* C-mediated GFP in various mutant backgrounds in order to identify potential regulators and to verify the usefulness of the *hand* C-GFP reporter line.

1.1. Embryonic expression of hand in cardiac tissues is driven by cis-regulatory elements located within the third intron

As a first step to identify cis-acting regulatory sequences in the *hand* gene, 1 kb of 5′ flanking sequence, intronic sequences and about 1 kb 3′ flanking sequence were tested in vivo by using P-element-mediated germline transformation. In this initial series of experiments five different constructs were tested: U (upstream region), A (first intron), B (second intron), C (third intron), and D (downstream region). All constructs were made using a P-element vector carrying a lacZ (pCaSpeR-hs43-ßGal, Thummel and Pirrotta, 1992) or an eGFP reporter gene (Barolo et al., 2000). These constructs, which are schematically illustrated in Fig. 1, were tested for embryonic reporter gene activity by immunohistochemical staining using antibodies against LacZ or GFP (see experimental procedures) and compared to the endogenous *hand* expression (Kölsch and Paululat, 2002). None of the tested genomic regions, with one

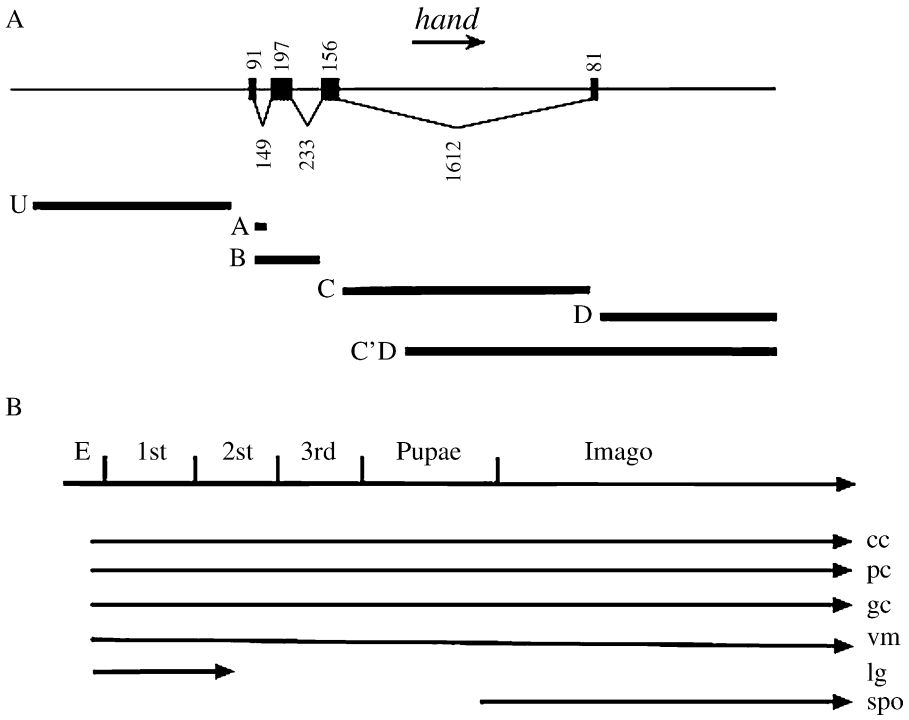

Fig. 1. (A) Schematic diagram of the genomic *hand* region, showing the relative position of *hand*-lacZ and *hand*-GFP P-element constructs used in this study. Numbers indicate the size in bps of the exons (above black squares) and the introns (below the triangles). Constructs are defined relative to the ATG of the coding region (ATG = +1). All fragments were amplified by PCR and cloned into pCRII-TOPO. Using restriction sites present in this vector, the fragments were removed and cloned into P-element vectors as described in the material and methods section. The constructs harbor the following genomic fragments: U (−1095/−35), A (+92/+240), B (+92/+670), C (+827/2438), D (+2520/+2873). For the exact sequences of the used constructs we refer to the published sequence of the genomic *hand* region (Genbank Acc. Nr. AE003628). (B) The scheme summarizes the results of the observed reporter gene activity of the *hand* C-construct with respect to embryonic, larval, pupal and adult stages. Abbreviations: E, embryos; 1st, first larvae; 2nd, second larvae; 3rd, third larvae; cc, cardioblasts; pc, pericardial cells; gc, garland cells; vm, visceral circular muscles; lg, lymph gland; spo, scutellar pulsatile organ.

exception, revealed staining in embryos. For each construct, at least four independent transgenic lines were established to exclude position effects. The only part of the *hand* gene capable of driving reporter gene activity during development is the third intron (C-construct, Fig. 1). Consistently, this part of the hand locus contains the HCH (hand cardiac and hematopoeitic) enhancer described by Han and Olson (2005). The expression of the reporter gene mimics the endogenous *hand* expression and starts at about stage 11 in a segmentally arranged group of cells within the trunk mesoderm (Fig. 2A,B). These cells give rise to the circular visceral muscles of the gut (Kölsch and Paululat, 2002). Slightly later, the bilaterally located rows of the differentiating heart cells become visible (Fig. 2C,D). The high expression level in the heart is maintained throughout embryogenesis in cardioblasts as well as in pericardial cells (Fig. 2E–H). We observed additional reporter gene expression in lymph gland cells, garland cells, and circular visceral muscles (Fig. 2E,G,I), which are *hand* positive in wildtype embryos as well. Only the endogenous expression of *hand* in so far unidentified cells within the CNS (Kölsch and Paululat, 2002) is not resembled by any of the described constructs. The expression in those cells is covered by an additional construct we made, harboring part of the third intron, the fourth exon and the 3′ downstream region of *hand* (construct C/D, Fig. 1). Its expression pattern in the embryo is similar to *hand* C-GFP, but includes the cells of the nervous system (data not shown), which indicates a combinatorial activity of intronic and downstream enhancer elements required for neuronal expression of *hand*.

The expression of *hand* C-GFP in cells of the cardiogenic cell lineage was additionally verified by coexpression studies with selected markers including Mef2, Tinman, Zfh-1, Odd-skipped and Even-skipped (Fig. 2J–X). *hand*-GFP expression overlaps with this markers in all cardioblasts, all pericardial cells, and the lymph glands.

The initial aim of this work was to identify regulatory regions of the *hand* gene responsible for expression in the embryonic heart. Our results, summarized in Fig. 1B, indicate that all regulatory modules needed for *hand* expression in the embryonic dorsal vessel are located within the third intron (construct C). Our second aim was to verify whether the *hand* heart enhancer, once successfully identified, could serve as an appropriate tool for visualizing the *Drosophila* dorsal vessel in living individuals at different developmental stages. Indeed, GFP expression in specimens bearing the *hand* C-GFP construct is very strong in all heart cells and can easily be observed directly in dechorionated embryos from stage 14 onwards (due to delayed maturing of GFP, fluorescence can not be detected earlier) (see Fig. 3A) and furthermore persists in older stages and throughout the whole life cycle of *Drosophila* (see next section).

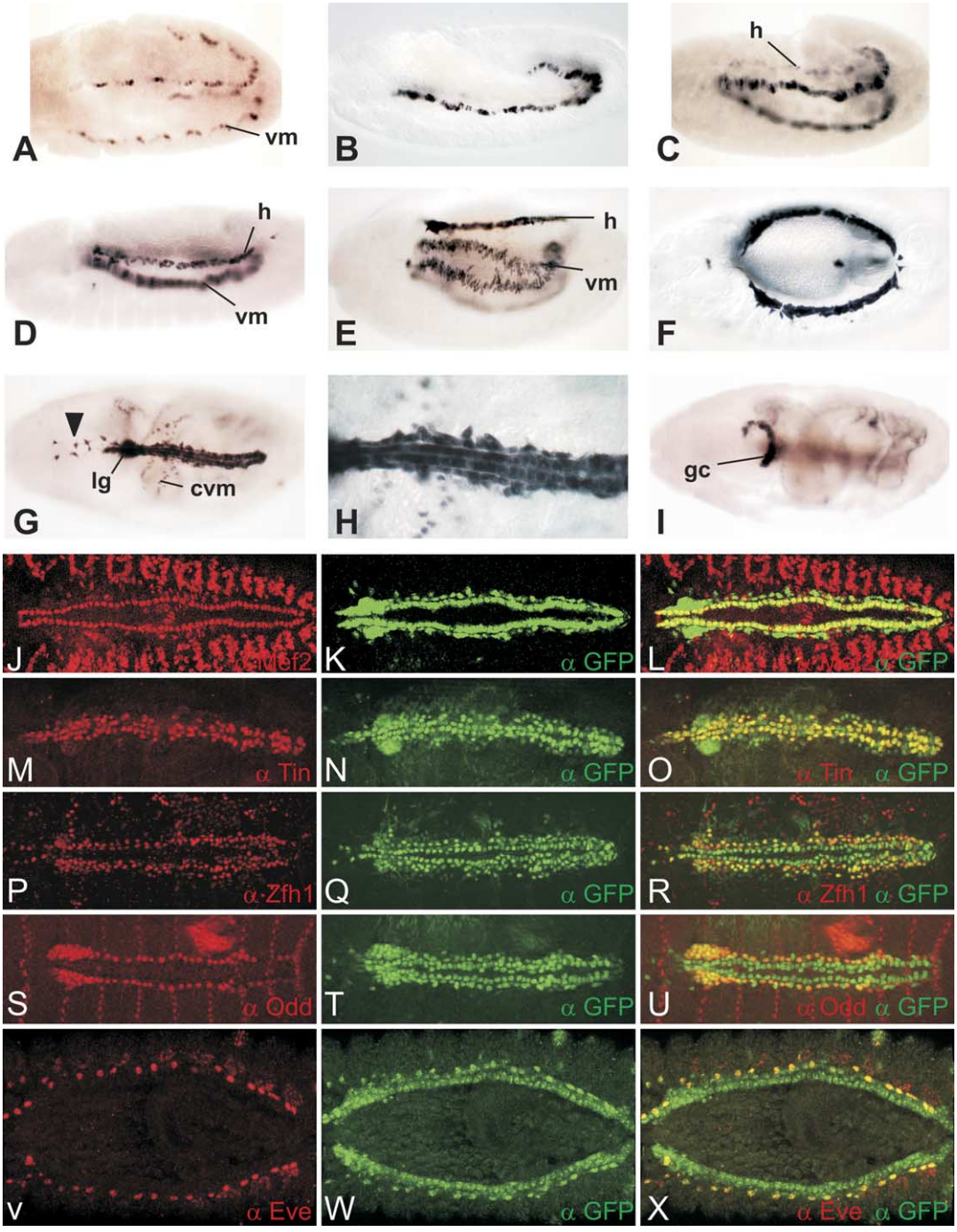

Fig. 2. The third intron of the *hand* gene harbors all cis-regulatory sequences necessary to control reporter gene expression in embryonic cardiac tissues. All embryos shown here are transgenic specimens carrying a construct of the third intron of the *hand* gene cloned into a GFP reporter P-element. (A–I) Staining was performed using an anti-GFP antibody. (A) Reporter protein is first detectable at stage 11 in the visceral mesoderm in segmentally arranged patches of cells. As we have shown previously, these cells are the progenitors of the circular visceral muscles (Kölsch & Paululat, 2002). (B) Slightly later, these cells form a continuous row. (C) At stage 12, heart precursor cells expressing the GFP reporter become visible (h). (D) Strong reporter gene activity is observed in the heart precursors (h) and the differentiating visceral mesoderm (vm) at stage 12/13. (E) At stage 14, fusion of visceral mesodermal cells is finished and the binucleated circular muscles elongate in their dorsal-ventral extension, visible by their anti-GFP labeled nuclei (vm) (F) A dorsal view of a stage 14/15 embryo with strong reporter activity in the heart cells. (G) A dorsal view of a stage 16/17 embryo with a labeled heart after closure. Heart lumen formation is already finished at this stage. A few cells (nuclei) in the visceral mesoderm are in plane as well (cvm). Reporter activity is also observed in the lymph gland cells (lg) and in some unidentified cells in the anterior region (arrowhead). (H) Same embryo as shown in G at higher magnification reveals reporter gene activity in cardioblasts and pericardial cells. Note that although the GFP reporter protein contains a nuclear localization signal (see experimental procedures), a significant portion of the GFP is also detectable within the cytoplasm. (I) Same embryo as in G but focused on the garland cells (gc) that show strong GFP expression. (J–X) Colocalization of *hand* C driven GFP and selected markers. (J–L) All cardioblasts marked by the expression of Mef2 coexpress *hand*-GFP. (M–O) Cardioblasts and pericardial cells show coexpression of *hand*-GFP (green) and Tinman (red). (P–R) Pericardial cells that express Zfh-1 (red) are also labeled by *hand*-GFP (green). (S—U) *hand*-GFP (green) colocalizes with Odd-skipped expressing pericardial cells (red). (V-X) The two pericardial cells per hemisegment that express Even-skipped (red) also express *hand*-GFP (green).

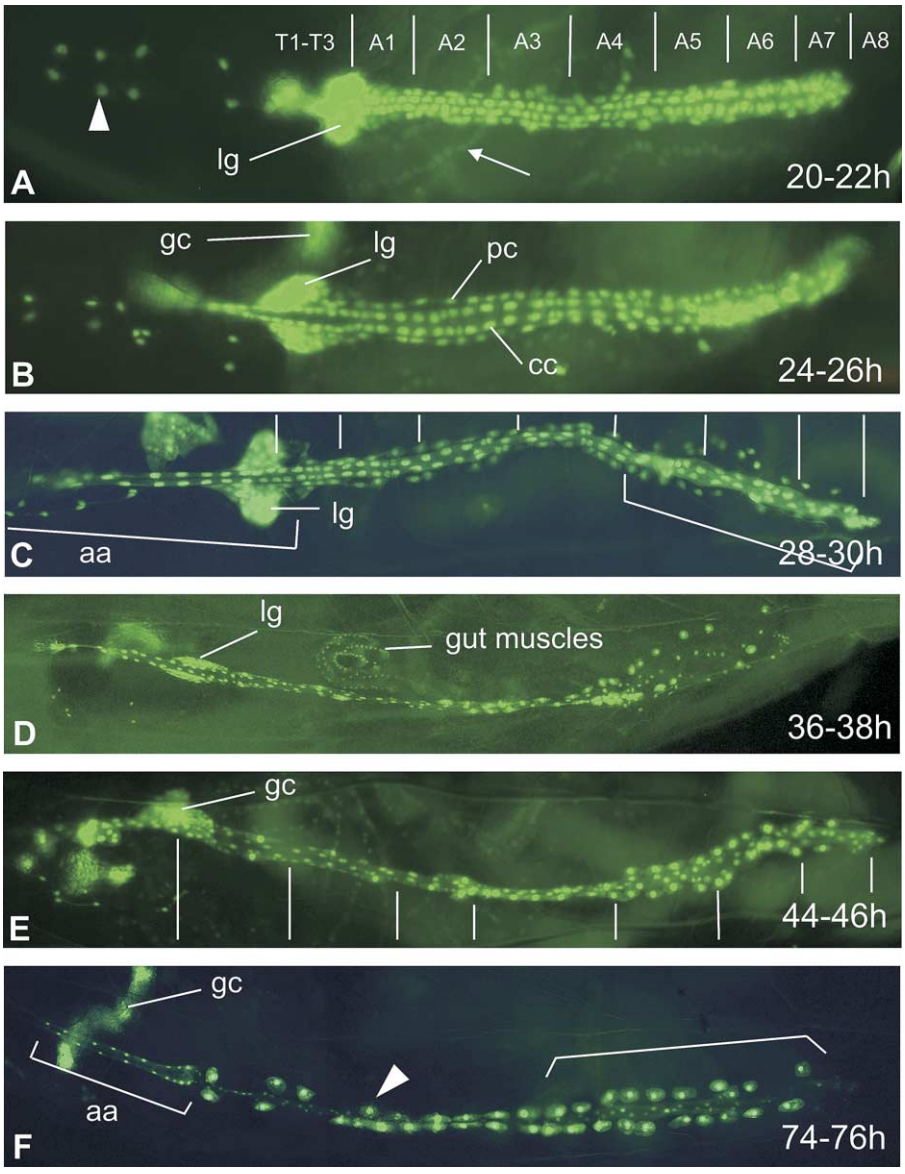

Fig. 3. Larval expression of GFP driven by the *hand* third intron regulatory element *hand* C. Image capturing was done under an UV-lamp equipped stereomicroscope (except of A, which was captured under a Zeiss Axioskop2 microscope). Because of the huge size differences between the larval stages (280 μm to 1.7 mm at 74–76 h APF), we adjusted the dorsal vessel to about the same size for presentation using Photoshop. (A) For comparison we show a living stage 16/17 embryo. The chorion was removed in 50% DanKlorix in water before inspection. GFP expression is clearly visible in all cardioblasts, pericardial cells, lymph gland cells (lg), visceral circular muscles (arrow) and some unknown cells in the anterior region (arrowhead), as already shown in Fig. 2. The segment borders (T1–A8) are indicated. (B) The picture shows a crawling, newly hatched first instar larva. GFP expression is identical compared to old embryos. The garland cells can be seen out of focus (gc). Cardiomyocytes (cc) and pericardial cells (pc) are indicated. (C) In first larvae, 28–30 h after egg deposition (h AED), the dorsal vessel has elongated in its anterio-posterior extension. Anterior to the labeled lymph glands (lg), pericardial cells are absent (anterior aorta, aa). The bracket indicates the ventricle or heart proper. (D) After 36–38 h AED, the lymph glands (lg) adopt a spindle-like shape. The cell morphology of cardioblasts has changed from a compact shape into an anterio-posterior stretched appearance, clearly indicated by the increased distance between the labeled nuclei. Nuclei of the visceral circular muscles (gut muscles) are visible as well. (E) After 44–46 h, lymph gland cells are no longer labeled, indicating that *hand* expression in this tissue decreases during late first larval stage. The posterior part of the dorsal vessel, the heart proper, has a broader appearance with obviously enlarged associated pericardial cells. (F) Early third instar larvae exhibit an extremely stretched dorsal vessel with three distinguishable regions. Anterior of the lymph glands (which are not labeled by GFP but visible in light microscope under nomarski optics), a region encompassing 9 pairs of cardioblasts is free of associated pericardial cells (bracket, anterior aorta). Within the mid-part region (front heart), the first section harbors the splitted parts of the lymph glands intersected by pericardial cells. The second section of the front heart exhibits the typical bilateral pearl-necklace-like arrangement of pericardial cells (arrowhead). The third region of the dorsal vessel (bracket) shows a broader appearance with a wider heart-lumen (the ventricle).

1.2. Postembryonic expression of hand: larval stages

A variety of transcription factors responsible for determination and differentiation of the embryonic cardiac cells are also active in the dorsal vessel postembryonically. For example, the MADS/Mef-box factor Mef2, which is expressed in all cardioblasts in the embryo, is also expressed in cardioblasts of third instar larvae (Molina and Cripps, 2001). Tinman, a homeobox-containing transcription factor, which is essential for the formation of the early embryonic cardiac

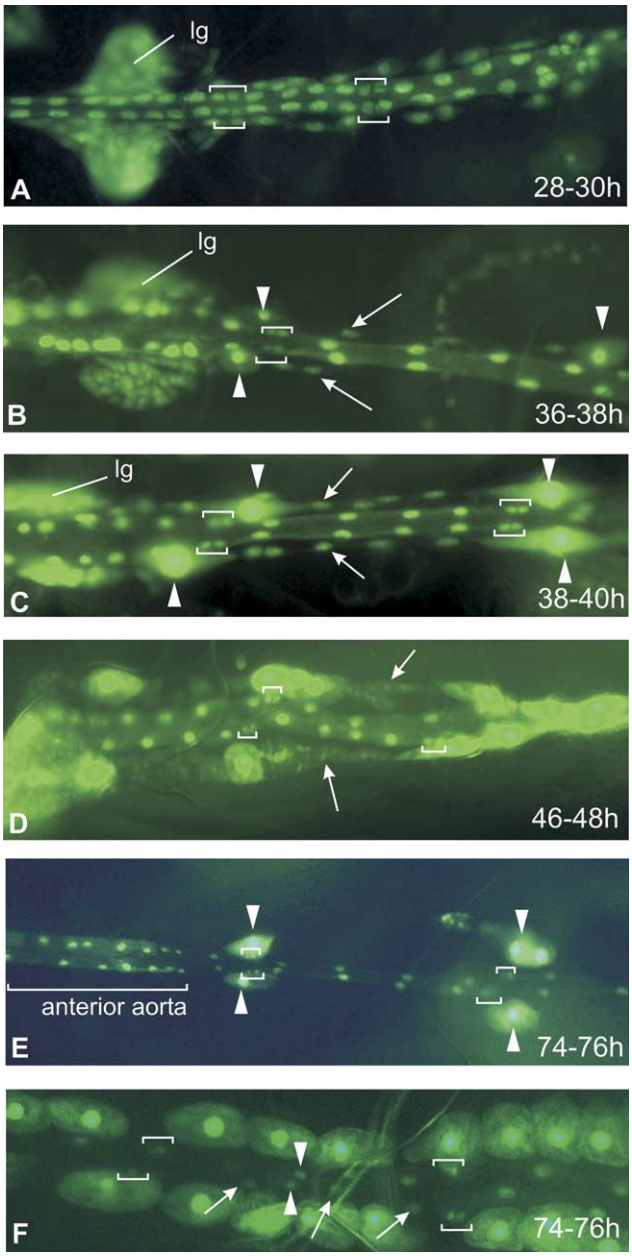

Fig. 4. Higher magnifications of larval *hand*-GFP expression in the region of segments T3 to A3 (A–E) and A4–A6 (F). (A) shows the dorsal vessel of a first instar larva. *hand*-GFP is visible in lymph gland cells (lg) and all cardioblasts and pericardial cells. Note the smaller cardioblast nuclei, two of six in each hemisegment (brackets), that correspond with the ostia building cardioblasts. (B) At 36–38 h AED, the nuclei of pericardial cells (arrowheads) and cardioblasts are about the same size, indicating that polytenization of pericardial nuclei is not complete at this stage. Some of the pericardial cells (arrows) show a decreased GFP expression. The lymph glands (lg) begin to stretch, finally adopting a spindle-like appearance. (C) Slightly later, the lymph glands appear stretched, and the nuclei of some, but not all, pericardial cells show a strong GFP fluorescence and increased size (arrowheads) due to polytenization. These cells are in close association to the ostia forming cardioblasts that are recognizable by their small nuclei (brackets). Interestingly, the majority of pericardial cells in this region (segments A1–A3) exhibit small nuclei (arrows). (D) At 46–48 h AED we observe disappearance of a subset of pericardial cells, namely those that do not increase in size as depicted in C. Spotted GFP fluorescence (arrows) in this area indicates that these pericardial cells might undergo cell death. (E) High magnification of a third instar larval dorsal vessel. Notably, the single pericardial cells in this region (arrowheads) are situated always in close proximity to the ostia forming cardioblasts with small nuclei (brackets). This presumably indicates a functional requirement of this localization, e.g. to prevent the entry of particles into the heart lumen through the neighboring ostia. (F) Transition from larval front heart to ventricle (segments A4–A6). The cell pair building the valve can be recognized due to the close proximity of their nuclei (arrowhead). Ostium precursor in segment A4 and ostium in segment A5 are indicated by brackets, the remaining cardioblasts of one side by arrows. An additional movie showing the heart beat and the valve motion is available online.

mesoderm, is expressed in four of six cardioblasts per hemisegment in the late embryonic heart as well as in third instar larvae (Molina and Cripps, 2001). We thought it likely that the very strong expression of *hand-GFP* in heart cells at the end of embryogenesis is presumably extended into larval stages. The fact that the *hand* expression pattern in cardiac tissue is conserved between flies and vertebrates further supported this hypothesis, since recent publications provide evidence that the vertebrate *hand* genes are expressed postembryonically in the adult heart of e.g. mouse, rat and humans (Thattaliyath et al., 2002). Therefore we analyzed whether the assessed *Drosophila hand* enhancer confers postembryonic activity of the reporter gene.

Similar to our findings for embryonic stages, solely the third intron of *hand* (construct C) is sufficient to drive the reporter gene postembryonically. No other element mediates reporter activity distinguishable from background staining. *hand*-GFP is found in newly hatched first instar larvae in all cardioblasts, pericardial cells, the lymph glands, garland cells and the visceral mesoderm, resembling the corresponding pattern in stage 16/17 embryos precisely (Fig. 3B). Within the next hours of development, cardiac cells start to grow and elongate anterio-posteriorly (an overview of larval heart development is given in Fig. 3). The pericardial cells lose their close contact to the heart tube. Between 36 and 40 h AED (hours after egg deposition), a subset of pericardial cells shows a dramatic enlargement of nuclei size in correlation with polytenization (Kambysellis and Wheeler, 1972; Rizki, 1978), whereas the nuclei of another subset of pericardial cells remain small (Fig. 4B,C). At the end of the first larval stage, we observe a decrease of *hand*-GFP expression in those pericardial cells that harbor small nuclei, predominantly located in the anterior part of the dorsal vessel. Closer inspection showed that these cells start to disappear; the GFP fluorescence in the nuclei becomes spot-like and the nuclei adopt a deformed overall appearance (Fig. 4D). Whether these cells undergo apoptosis, or if they simply loose *hand*-GFP expression while further differentiation events take place, is unclear. The deformed structure of the nuclei and the residual clouds of GFP fluorescence seem to indicate a degeneration of these cells, however, this hypothesis has to be proven in additional studies. Compared to newly hatched first instar larvae, after 50 h AED, the dorsal vessel shows a stretched morphology, a maintained number of cardioblasts and a reduced number of pericardial cells. The remaining pericardial cells have large nuclei, a characteristic oval shape, and they are associated only loosely with the heart tube (see Figs. 3F and 4E). Furthermore, they exhibit a characteristic positioning along the anterio-posterior axis. The

pearl necklace-like arrangement, seen in young first larvae, is broken up with gaps in the anterior part of the dorsal vessel, where GFP positive pericardial cells have disappeared and the secondary lymph gland lobes will form (see below).

Expression of *hand*-GFP in the lymph gland cells, which starts during embryogenesis, is maintained throughout the first larval stage. In embryos and early to mid-stage first larvae, the lymph gland cells are arranged in two groups, which are located bilaterally to the anterior dorsal vessel. At the end of the first larval stage, the ball-like arranged group of lymph gland cells on each side of the embryo adopts a spindle-like appearance (Fig. 3D) and starts at about 44 h AED to lose GFP expression, shortly before splitting up into several lobes arranged along the dorsal vessel. Additional *hand*-GFP activity is observed in the circular visceral muscles and the garland cells (see Fig. 3E,F).

From the second up to the end of the third larval stage, a robust expression of *hand*-GFP in all heart cells is maintained (Figs. 3,4, additional movies available online). A dramatic enlargement of the larval heart in its anterio-posterior extension characterizes this period of development. Molina, Cripps and others pointed out that this extension is caused by cell growth and not by an increased number of cardiac cells (Molina & Cripps, 2001). This observation is consistent with our results when counting *hand*-GFP expressing cardioblasts at different developmental stages. Besides the cardiac expression we furthermore observe continuous *hand*-mediated GFP fluorescence in garland cells and circular visceral muscles. In contrast, the expression in lymph gland cells, as mentioned above, is no longer present in third larvae.

During larval development, the size of a subset of cardioblast nuclei changes significantly, to our knowledge first mentioned by Jensen who studied heart differentiation in the dipterian fly *Calliphora erythrocephala,* whose heart morphology resembles the situation in *Drosophila melanogaster* (Jensen, 1973, compared to our findings). Molecularly, the cardioblasts with smaller nuclei, two out of six per hemisegment, were shown to express *seven-up* but not *tinman (tin)*, which marks the remaining set of cardioblasts (Gajewski et al., 2000; Ward and Skeath, 2000). The two cell types can be distinguished easily in the *hand*-GFP larvae (Fig. 4). Jensen for *Calliphora*, Rizki, Molina and Cripps for *Drosophila* observed that the last three posterior pairs of *seven-up* expressing cardioblasts form the larval ostia (Jensen, 1973; Molina and Cripps, 2001; Rizki, 1978). Additional pairs of *seven-up* expressing cardioblasts, recognizable by their smaller nuclei, differentiate into imaginal ostia during metamorphosis (see below and Jensen, 1973; Molina and Cripps, 2001).

During second and third instar larval development, ostia are always accompanied by an associated pair of pericardial cells (Fig. 4C–E). At about 70–80 h AED, the dorsal vessel is clearly regionalized along its anterio-posterior extension (see Fig. 3F). Following the nomenclature introduced by Jensen, the three regions are the anterior aorta, the front heart and the ventricle. The anterior aorta contains no ostia, has a small lumen and projects with its opening into the head region. The front heart harbors four pairs of *svp* positive cells and is separated from the ventricle by a valve-like structure. The ventricle (usually termed heart in the *Drosophila* literature) harbors three pairs of functional ostia and has a wider lumen (Rizki, 1978). This region is predominantly responsible for heart contraction and, because of the functional ostia, is the inflow tract of the dorsal vessel in larvae. We found that the anterior aorta is completely free of associated pericardial cells at any time of larval development. This region ends posteriorly with a bulge-like structure (Fig. 3F) and forms the adult aorta exclusively. The following mid part (the front heart) starts with an anterior region where only a few pericardial cells associate with the heart, always in close proximity to the ostia forming cells. In its posterior half, pericardial cells are arranged bilaterally of the heart lumen in a more or less pearl necklace-like fashion. The ventricle of the late larval dorsal vessel is characterized by a wider lumen and a broader over all appearance and is accompanied by large pericardial cells at any stage of larval development. It is comprised of the last 18 cell pairs, including three pairs of ostia building cells. Cell pair number 34 builds the valve at the anterior border of the ventricle, as concluded from the close proximity of their nuclei and their movement during the beating of the heart (Fig. 4F, arrowhead and Supplementary materials).

The number of cells and their characteristic individual features in *Drosophila* correspond to the description of the larval heart of *Calliphora erythrocephala*, given by Jensen (1973): 9 cell pairs form the aorta, followed by two cell pairs with small nuclei. Jensen described those to build the valve between adult aorta and heart after metamorphosis. Together with the following ordinary cardiac cell pair, those twelve cells on either side of the larva are documented to be of a different lineage than the remaining 40 pairs (Alvarez et al., 2003). Three repeated units of two ostia forming cells (recognized by their smaller nuclei) and four intermediate cells (recognized by their larger nuclei) plus two more ostia forming cells and two cells with larger nuclei (cells number 13–34 on either side) form the front heart (Figs. 3C and 4F), while the remaining 18 cell pairs build the ventricle (see above).

1.3. Pupation and metamorphosis

Studies of *Drosophila* metamorphosis have been hampered by the difficulties to apply e.g. immunohistochemical methods on pupae, since puparium and cuticle cannot be penetrated easily by the necessary chemical components. On the other hand, dissections of larvae and pupae did not always allow the analysis of a complete organ. For instance, the dorsal vessel cannot be prepared easily in total, thus only a limited number of studies address questions related to dynamic changes of heart morphology occurring in the puparium. The few existing publications have shown that a significant part of the dipterian larval heart persists through the pupal stage to form the imaginal heart (Curtis et al., 1999; Jensen, 1973; Molina and Cripps, 2001; Rizki, 1978). The postembryonic expression of GFP under the control of the *hand* cardiac regulatory region circumvents the inability to visualize the dynamics of remodeling processes of the heart because it allows us to

follow heart differentiation in living animals directly. GFP expression also facilitates the preparation and dissection under a stereo microscope equipped with UV-illumination. Indeed, we were able to observe strong and specific GFP expression in cardioblasts as well as in pericardial cells in white prepupae and during all further pupal stages until hatching, as depicted in Fig. 5 at different pupal stages, starting with white prepupae and continuing with different time points up to 80 h after puparium formation (h APF). We found that within 24 h APF, the retraction of the dorsal vessel becomes clearly visible (compare Fig. 5A,C). The most anterior located pair of pericardial cells is associated with the first pair of ostia and marks the transition of the anterior to the posterior aorta (Perrin et al., 2004), or aorta to front heart respectively (Jensen, 1973), and serves as a useful landmark (Fig. 3F). Between 48 and 80 h APF, the dorsal vessel curves internally at the border between the thoracic aorta and abdominal front heart, best seen in lateral views (Fig. 6D). From 48 h APF onwards the formation of four heart chambers can be observed (Fig. 5E–H), including the formation of a conical chamber in the first and second abdominal segment (Fig. 5H) as described by e.g. Curtis et al. (1999). The other three chambers are smaller and span the segments A3, A4, and A5, respectively.

During metamorphosis, *hand*-driven GFP expression is furthermore clearly detectable in two diaphragm-like structures located bilaterally in the last thoracic segment close to the dorsal cuticle. GFP analysis in living animals revealed them to be contractile (movie available online), and closer inspection specified them to be the paired scutellar pulsatile organs (SPOs), also known as accessory wing circulatory organs

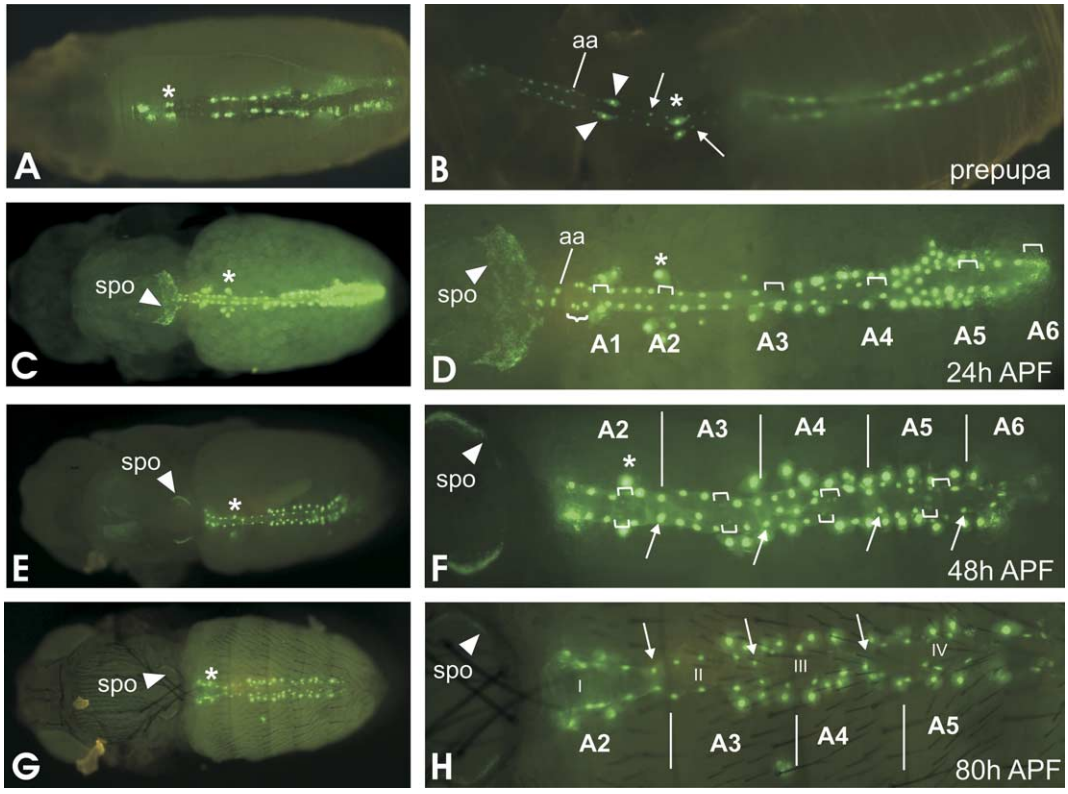

Fig. 5. Dynamics of heart morphogenesis during metamorphosis. Time scale is relative to puparium formation (white prepupae) set to zero. h APF = hours after puparium formation. GFP was captured directly from undissected, living animals freed from puparium (with exception of A and B). Asterisk marks the position of the ostia in segment A2. (A,C,E,G) show overviews of whole animals at the same magnification. (B,D,F,H) show higher magnifications that were stitched together from several images from anterior to posterior to increase resolution. (A) Prepupa in its puparium. (B) Prepupa dissected in the anterior region (anterior aorta and front heart) to remove the puparium in this area to show cardioblasts (arrows) and pericardial cells (arrowheads). No changes compared to third larvae can be observed (aa = anterior aorta). (C) 24 h old pupa overview. Head, thorax and abdomen are clearly distinguishable. The heart is shortened due to retraction of the abdomen caused by evagination of the head (compare to A). In the thorax, a group of bilaterally located cells show GFP expression that give rise to the scutellar pulsatile organ (spo, arrowhead). (D) Abdomen of the same animal as in C in higher magnification. The posterior end of the anterior aorta is visible (aa). The following two cells correspond to the valve building cells described by Jensen (curly brace). The ostia forming cardioblast pairs can not be seen at this magnification due to their small size and fainter GFP expression than the other cardiomyocytes, but their position corresponds to the gaps in the cardiomyocyte row (brackets). The posterior tip of the heart is out of focus due to the curvature of the dorsal vessel. (E) 48 h old pupa overview. The paired scutellar pulsatile organ that appears boomerang shaped in dorsal views is visible (spo). The heart is even shorter than at 24 h APF (compare to C) due to histolysis (compare Fig. 7B). (F) Abdomen of another specimen of the same age as in E at higher magnification. The dorsal vessel extends now only until segment A6. The forming ostia of segments A2–A5 can be recognized (brackets; higher magnification of this specimen shown in Fig. 6E). Heart chamber formation has already started. Arrows indicate the cells forming the valves between the chambers. (G) 80 h APF old pupa overview. Bristles and eyes have developed. (H) The abdomen of the same specimen than in G in higher magnification. The four adult heart chambers (I–IV) can be distinguished. The cells building the valves between them are indicated by arrows. Ostia building cells are not recognized at this magnification; higher magnification of about this age shown in Fig. 7C.

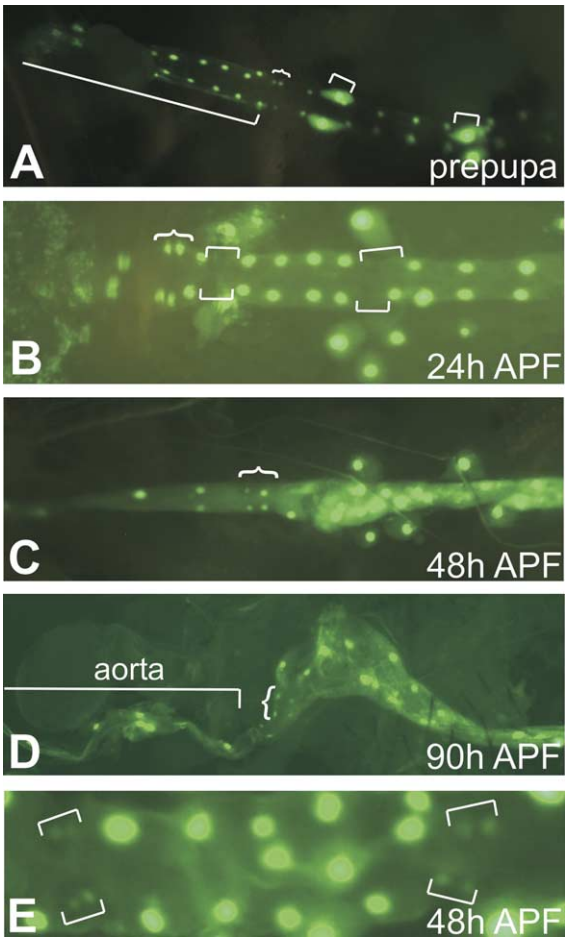

Fig. 6. Details of heart differentiation during metamorphosis: transition from the aorta (located in the thorax) to the front heart (abdomen). All pictures show dissected specimens of the indicated age (except of B, which shows an intact pupa). (A) In prepupae, the transition region is identical to the situation in third larvae (compare Fig. 4E). The two valve building cells at the posterior end of the aorta are indicated by a curly brace. Brackets mark the ostia building cells accompanied by large pericardial cells. (B) Same specimen as in 5D at higher magnification. At 24 h APF, there are still no significant changes in overall morphology. The two cells at the very end of the anterior aorta (curly brace) correspond to the valve building cells described by Jensen (compare Fig. 5D). The positions of ostia precursors in A1 and A2 are indicated by brackets. Their cell nuclei cannot be recognized in this picture, but at higher magnification of a different animal shown in E. (C) Preparation of a pupal heart at 48 h APF (dorsal view). The border of heart to aorta has changed significantly: the aorta opens to the ventral side of the fourth heart chamber (as visible in the lateral view at 90 h APF, D). The heart has been stretched in its anterio-posterior extension by pulling at the most anterior end with fine forceps to show all cells from different levels. The two cells marked by a curly brace are the same valve-building ones as in A and B. (D) Lateral view of a heart preparation from a 90 h APF old pupa. Aorta and heart can be distinguished easily by their width. Note the rectangular bending of the aorta. The curly brace marks the small-nucleated cells building the valve between aorta and heart. (E) Higher magnification of segments A3–A4 of the same specimen as in Fig. 5F. The nuclei of the ostia forming cells are indicated (brackets).

(Krenn and Pass, 1994a,b; Perttunen, 1955). Formation of the SPOs starts at about 18 h APF by the appearance of a group of small-nucleated cells situated medially at a dorsal position in segment T3 (Fig. 7D). The cells then split up into two groups that migrate laterally during the next hours, finally adopting a boomerang like shape in dorsal views. At about 40 h APF, the SPOs start to contract rhythmically (see Figs. 5,6,7, and Supplemental material). Whether the SPO forming cells derive from proliferating dorsal vessel cells or from a different source is still unknown. An overview about SPOs and additional associated pulsatile organs is given by Pass (1998, 2000).

1.4. Formation of the adult heart

At the end of embryogenesis, a linear dorsal vessel is differentiated. At this time, 104 cardioblasts form the tube-like heart spanning from segments T3–A8 (Zaffran et al., 1995). During larval development, the number of cardioblasts is constant as shown by analyzing Mef2 expression in third instar larvae (Molina and Cripps, 2001), which is consistent with our results. As mentioned above, the dramatic enlargement of the larval heart tube (from about 280 μm in the embryo to 1.7 mm in third larvae after 74–76 h AED, Fig. 3) is exclusively due to cell growth of cardioblasts, originally postulated by Rizki (1978).

In pupae, the length of the heart is reduced. This shortening of the heart during metamorphosis seems to be partly due to the retraction of the abdomen while the head evaginates, but it has been suggested that, in addition, heart cells are lost through histolysis (Jensen, 1973; Molina and Cripps, 2001). Molina and Cripps discuss that the posterior part of the larval dorsal vessel undergoes histolysis during metamorphosis, based on the observation that the transcription factor Tinman is down-regulated in the last two posterior segments of the vessel and the observation of large cells, presumably macrophages, engulfing the posterior tip of the heart. Jensen showed in a classical histological study that the posterior part of the heart of *Calliphora erythrocephala*, including the last two pairs of ostia, is histolyzed (Jensen, 1973). The front heart, harboring the four pairs of non-functional larval ostia, forms the heart of the imago. It is complemented by a remaining portion of the larval ventricle, which harbors the fifth pair of imaginal ostia. Indeed, it has been shown that the heart of the imago spans fewer segments than the larval heart (Curtis et al., 1999; Miller, 1965; Rizki, 1978). Our studies on living pupae carrying *hand*-GFP, which provides a reliable source of strong GFP fluorescence, visualize the dynamics of this process. We observe that the dorsal vessel (without the anterior aorta) shortens from 2.8 mm in fully-grown third larvae to 2.4 mm continuously during metamorphosis, becoming compacted and relocated more anteriorly. The total number of cardioblasts that form the inner heart tube, 104 in embryos (52 on either side), remains constant until pupation. Afterwards, histolysis results in a reduced number of cardioblasts. Estimating the cell numbers in the GFP expressing pupae by using the ostia as landmarks revealed that after 24 h APF, still all of the 104 cardiomyocytes are present, while from 48 h APF onwards up to adult stage, only about 84 cardiomyocytes are visible (Figs. 7A,B and 8). In 48 h old pupae, preparations of the posterior tip of the ventricle revealed the presence of cell accumulations probably constituting histolytic tissue (Fig. 7B). Nevertheless, apoptotic stainings with propidium iodid and acridine orange gave no reproducible results so far.

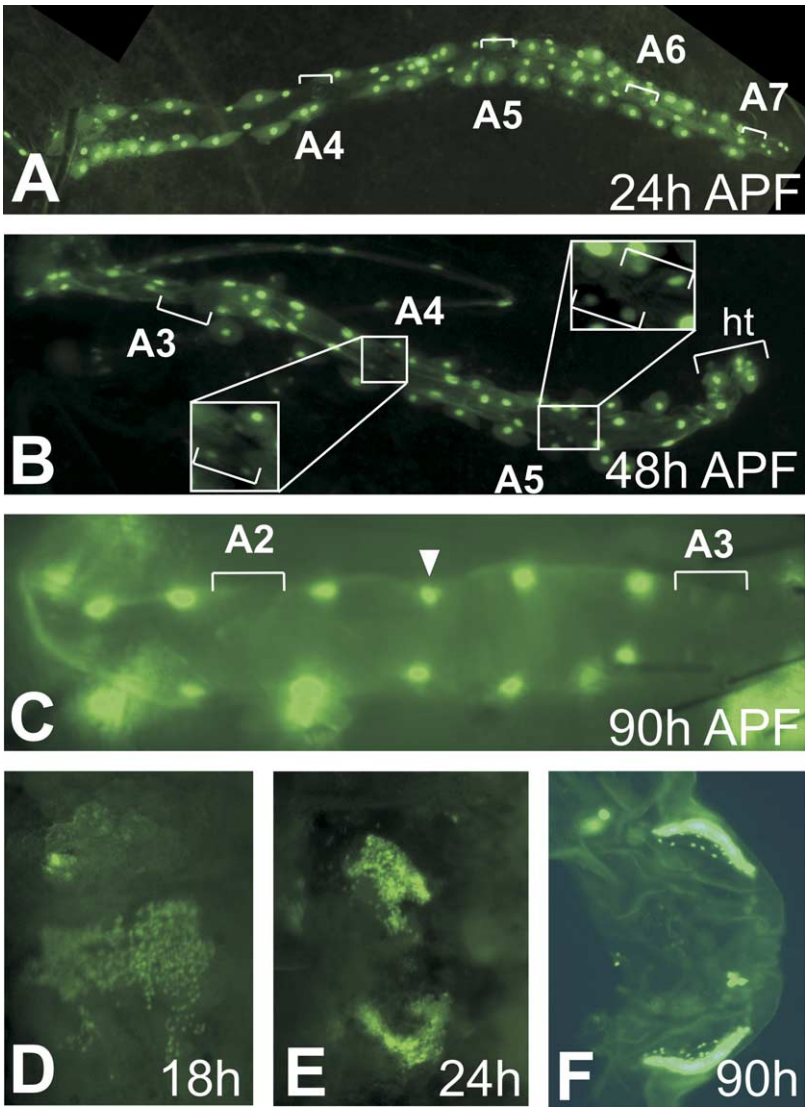

Fig. 7. Details of heart differentiation during metamorphosis. (A,B) show the posterior part of whole heart preparations. (C) shows segments A2 and A3 at high magnification in a living pupa (additional movie available online). (D–F) show the development of the scutellar pulsatile organ during metamorphosis. (A) Whole heart preparation of a 24 h APF old pupa showing only the posterior half. The position of ostia pairs in segments A4–A7 are indicated by brackets. No histolysis of the posterior tip cells has occurred yet. (B) Whole heart preparation of a 48 h APF old pupa. Only the ostia pairs of A3–A5 are present (insets show ostia at higher magnification in segments A4 and A5, respectively), indicating that the most posterior cardiomyocytes are lost through histolysis at this stage. The uncoordinated accumulation of cells at the most posterior tip of the heart probably constitutes histolytic tissue (bracket, ht). The degeneration of cardiomyocytes therefore happens early in metamorphosis. (C) The second and third pair of ostia in a living 90 h APF old pupa. Movies of this specimen showing the beating heart and the functioning of the ostia are available online. The arrowhead indicates the valve building cell pair between first and second heart chamber. (D) First appearance of the GFP positive cells building the scutellar pulsatile organ after 18 h APF in a living pupa (dorsal view). (E) After 24 h APF, the group of cells forming the scutellar pulsatile organ has splitted up into two boomerang shaped clusters. (F) Dissection of the scutellum of a 90 h APF old pupa (ventral view). The GFP positive myogenic cells forming the contractile diaphragms of the paired scutellar pulsatile organ are clearly visible. They function by flattening through contraction, thereby pumping the hemolymph from the wings into the body cavity (additional movie available online).

The total number of pericardial cells that finally contribute to the embryonic heart is still undetermined. A rough estimation of Mab3-positive pericardial cells (Yarnitzky and Volk, 1995) indicates a total number of about 110–130 cells (own observation). Alvarez et al., (2003) have estimated a total number of about 120 Zfh-1-expressing pericardial cells. It is known from earlier histological work that the heart of the third instar larva is accompanied by about 40–50 pericardial cells, easily recognized by their specific appearance and size (Rizki, 1978). Thus, the number of pericardial cells is dramatically reduced during larval development. As described above, we assume degeneration of pericardial cells in the first larva, predominantly in the anterior portion of the dorsal vessel. At the end of the third larval stage we could detect a total number of 40–42 *hand*-GFP positive pericardial cells, confirming Rizkis observation. The disparity between the numbers of pericardial cells in larvae compared to late embryos is likely due to the degeneration of a specific subset of the pericardial cell population during larval stages. Which subset of pericardial cells degenerates remains to be answered, for

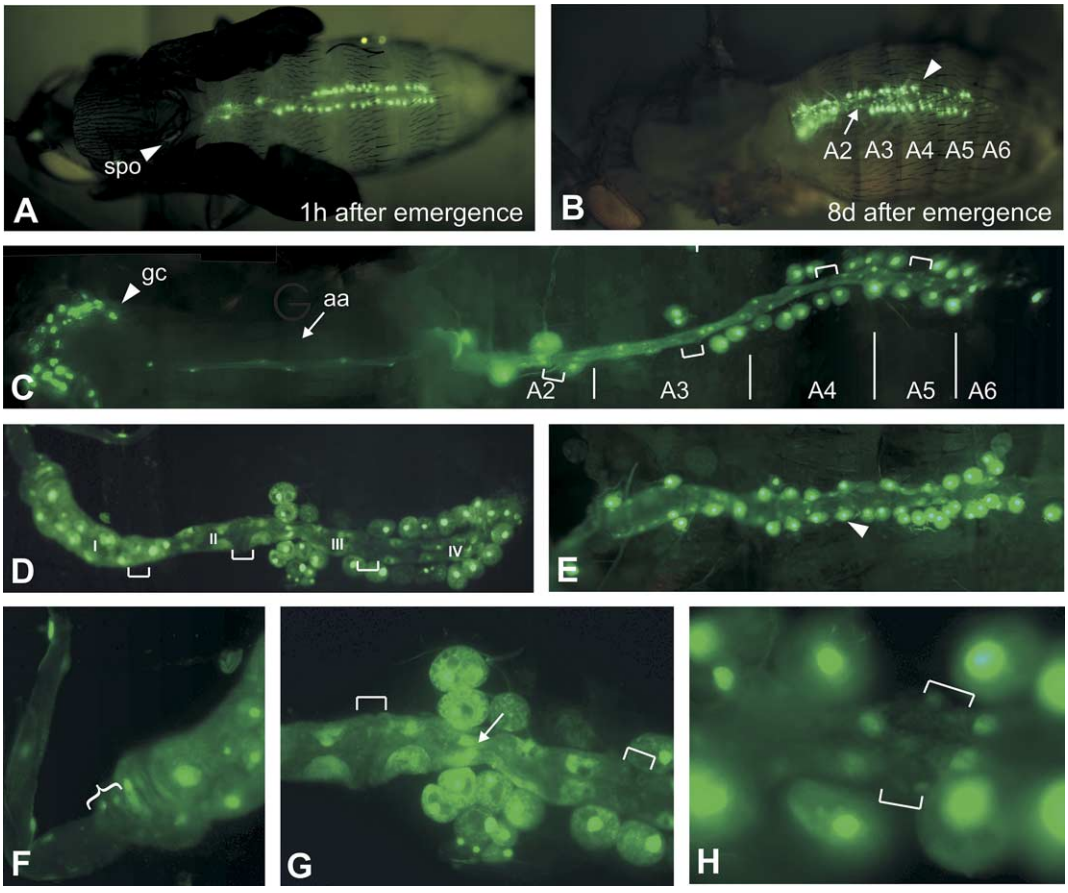

Fig. 8. *hand* GFP expression in adult flies. (A,B) show whole live specimens after 1 h and 8 days after emergence, respectively. (C) depicts a whole, GFP fluorescent heart of a dissected adult, 3 days after emergence. (D,E) show heart preparations of animals 3–5 days old. (F–H) show details from C and D at higher magnification. (A,B) The overall appearance of the adult heart resembles the situation in pupae 80 h APF (compare Fig. 5G) and does not change during the aging of flies (data not shown). The abdominal segments can be recognized. Pericardial cells (arrowhead) and cardiomyocytes (arrow) are GFP positive. (C) At closer inspection, the resemblance to the earlier stages is confirmed: higher magnification of a complete heart preparation shows the aorta, the heart, and the garland cells to be GFP positive. (D) The four heart chambers (I–IV) can be recognized. The brackets indicate the positions of the ostia. (E) A heart preparation carefully conserving all pericardial cells (arrowhead) showing their total number to be 34 in this individual adult. (F) Same animal as in D at higher magnification. The transition between aorta and heart exhibits the same features as seen in pupae 80–90 h APF (compare Fig. 6C,D). The two small nucleated cells, described to build the valve between the two compartments, can be recognized (curly brace). (G) Same specimen as in D at higher magnification. The ostia (brackets) in segments A3 and A4 and the bordering cells between chamber II and III (arrow) are depicted. (H) Detail from panel C (segment A5) at higher magnification. The nuclei of the ostia building cells can be recognized (brackets).

example by analyzing GFP enhancer lines that mark specific subsets of pericardial cells in the larva. Interestingly, we discovered an even further reduction of pericardial cells during metamorphosis. Counting their number in pupae after 48 h APF revealed that about eight cells at the posterior tip vanish, probably histolyzed together with the lost cardiomyocytes in this region, thus resulting in a number of about 32–36 pericardial cells in the adult heart (about 16–18 on either side, Fig. 8).

Curtis et al., pointed out that the transition from the larval to the adult heart is accompanied by specific features: (a) a conical chamber is formed de novo in the first and second abdominal segments, (b) the heart curves to follow the contour of the abdomen, (c) a layer of longitudinal muscles appears on the ventral side of the heart, (d) a fourth pair of ostia is added to the three already existing ones in the early pupa, (e) the ostia are valve-like in the adult (Curtis et al., 1999). Indeed, the analysis of GFP allows for the first time the visualization of some of the dynamic changes in heart morphogenesis during metamorphosis and the formation of the imaginal heart in living pupae. The finally formed heart of the imago extends from the sixth abdominal segment to the brain in the dorsal anterior region and is divided in four chambers separated by valve-like structures. The formation of the chambers, as visualized by GFP expression in the heart, takes place during the first 48 h APF (Fig. 5D compared to F). Later, at 80 h APF, the function of ostia and valves can be monitored in the *hand*-GFP specimens (additional movies available online), allowing the conclusion that the changes in overall heart morphology are finished at this point of time. The second cardiomyocyte posterior of each ostium seems to build the valve and the border to the next chamber. Segment A1 is an exception since it is fused with A2 to form the conical chamber (Curtis et al., 1999; Rizki, 1978).

No significant differences between 90 h APF pupae and adults were detectable. We observed a strong GFP expression that is maintained in the adult heart in cardioblasts and pericardial cells. Additionally, GFP is found in the scutellar pulsatile organ, the garland cells, and the circular visceral muscles (Fig. 8).

We did not quantify the intensity of GFP fluorescence, but the level of expression seems to be constant when newly hatched flies are compared to older ones (up to four weeks). Thus, *hand*-GFP might be useful to investigate age-associated cardiac dysfunction in *Drosophila*, like the decrease of the heart-beating rate (Paternostro et al., 2001). Compared to other available techniques to visualize heart beating in pupae or adults (Johnson et al., 2001; Nichols et al., 1999; Papaefthmiou and Theophilidis, 2001; Wessels and Bodmer, 2004), *hand*-GFP allows genetic screening for mutations involved in heart morphogenesis during metamorphosis and formation of the adult heart, because non-invasive observation of heart morphology and function is possible. As a very exceptional addition, the *hand* C-GFP reporter line could serve to take into account the relevance of the scutellar pulsatile organ for e.g. viability or fitness in correlation with circulatory functions.

1.5. Regulation of cardiac hand expression during embryogenesis

In order to determine where *hand* acts in the genetic hierarchy controlling heart development, we examined its expression in several mutant backgrounds, either by in situ hybridization with a *hand* specific RNA probe or by use of the third intron GFP reporter line (*hand* C-GFP) described above. Tinman, Pannier and its binding partner U-shaped have essential functions in specification of the heart primordium within the mesoderm (Azpiazu and Frasch, 1993; Bodmer, 1993; Gajewski et al., 1999; Gajewski et al., 2001; Klinedinst and Bodmer, 2003). Loss of function mutations in either of these genes cause severe malformations of the heart. In *tinman* mutants the heart is missing completely, whereas in *pannier* and *u-shaped* mutants cardioblasts and pericardial cells are affected in number. The different cardiogenic cell lineages are affected disproportionally resulting in clusters of accumulated heart cell subpopulations at later embryonic stages (Gajewski et al., 1999; Klinedinst and Bodmer, 2003).

In homozygous *tinman* mutants, heart and lymph glands are not formed, therefore no *hand* expression is detected in the heart region (Fig. 9B,D). *hand* expression in the nervous system (arrows in Fig. 9A,B) and the formation of garland cells, which are also labeled by *hand* expression, are unaffected in *tinman* mutants (Fig. 9D, inset).

The zinc finger- and homeobox-containing gene *zfh-1* codes for a transcription factor expressed in a subset of heart or heart associated cell types, namely the pericardial and lymph gland cells. *zfh-1* mutant embryos exhibit occasional kinks in the linear heart tube (Lai et al., 1993), and the Even-skipped expressing pericardial cells (EPCs) are absent (Su et al., 1999). *hand* expression is still detectable in the remaining pericardial cells in *zfh-1* mutants (Fig. 9E). Notably, we found that the lymph glands are not formed and that the garland cells are strongly reduced in number (arrow in Fig. 9E and inset). The garland cells are arranged in a horseshoe-like structure surrounding the posterior foregut (Fig. 9C, inset). They originate bilaterally from the anterior trunk mesoderm and fuse at later stages of development to adopt their final arrangement, clearly seen when *hand* is used as marker (Kölsch and Paululat, 2002). Our results indicate that Zfh-1 is, in addition to its known function for pericardial cell specification, also required for lymph gland cell differentiation and formation of garland cells.

In *pannier* mutant embryos, the number of cardioblasts is strongly reduced, and we found only a few heart cells expressing *hand* mRNA (data not shown) or the *hand*-GFP reporter (Fig. 9L–N). The few remaining cardioblasts (marked by mef2 expression, Fig. 9M,N, white arrow) are still *hand* GFP positive, as well as some pericardial cells (Fig. 9N, white arrowhead). They fail to form a closed heart tube. Interestingly, GFP positive lymph gland cells are totally absent (open arrow in Fig. 9N), while GFP expression in the visceral mesoderm (open arrowhead in Fig. 9N) and the garland cells (Fig. 9L–N, inset) is still present. In contrast, panmesodermal expression of Pannier causes a broader heart with an increased number of *hand* positive heart cells (Fig. 9F–H) and ectopic patches of hand expression (Fig. 9G). Increased *hand* expression is also observable in the nervous system (arrow in Fig. 9H). This indicates that Pannier is a potential positive regulator of *hand,* though cardioblasts are still *hand* GFP positive in *pnr* mutants.

The mutation of the *pnr*-antagonist *ush* leads to an increased number of cardioblasts and a reduction of *pericardin*-expressing cells. The heart fails to form properly with the cardioblasts clustering primarily at a posterior position (Fossett, et al., 2000; Gajewski et al., 1999; Klinedinst and Bodmer, 2003). Nerverless, they do express *hand* (data not shown) as well as *hand*-GFP (Fig. 9O–Q), while no GFP-positive pericardial cells were detectable (no GFP-positive cells without mef2-colocalization, Fig. 9Q). The visceral mesoderm is still labeled by *hand* expression and appears normal (not shown).

We furthermore analyzed *hand*-GFP expression in homozygous *pointed*$^{\Delta 88}$ mutants (Fig. 9R–T). Pointed, an ETS-transcription factor, acts downstream of *pannier* and is crucial for pericardial cell differentiation (Alvarez et al., 2003). In *pointed*$^{\Delta 88}$ mutants, the number of the Seven-up expressing cardioblasts is strongly increased to the expense of pericardial cells. The heart at stage 16 appears broader and a highly organized linear heart tube fails to form (Alvarez et al., 2003). *hand* driven GFP expression is observed in all heart cells of *pointed* mutant embryos (Fig. 9R–T), indicating that Pointed is not a regulator of *hand* in cardiac tissues.

As the exemplary inspection of *hand* C-GFP fluorescence in the mutants described above has proven, the reporter line is an efficient tool to check the relevance of putative regulators as well as to screen for new heart mutants, since it conveniently shows both cardioblasts and pericardial cells without staining

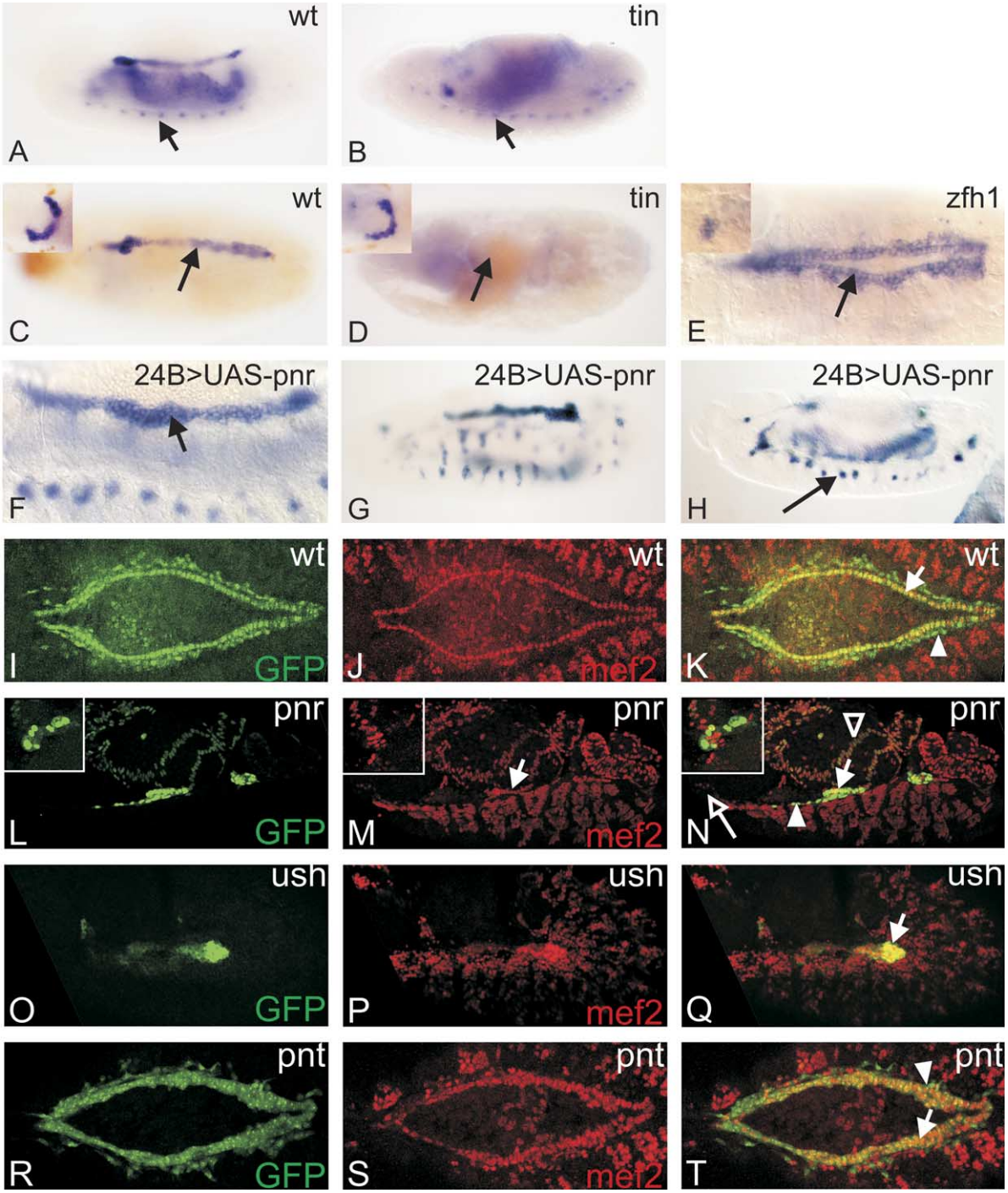

Fig. 9. *hand* mRNA and *hand* GFP expression in selected mutant backgrounds. (A–H) show stainings with an anti *hand* RNA probe. (I–T) show stainings with an anti-GFP antibody (green) and anti-Mef2 antibody (red). (A–D) Compared to wildtype (A and C), *hand* expression in *tinman* mutant embryos (B and D) is absent in cardiac tissues, while the garland cells (insets in C and D) appear normal, as well as *hand* expression in neural cells (compare B–A, arrow). (E) *zfh-1* mutant embryos exhibit a malformed dorsal vessel (compare to D). The expression of *hand* in cardioblasts and pericardial cells is unaffected (arrow). In contrast, the numbers of lymph gland cells and garland cells are strongly reduced in *zfh-1* mutants (E compared to C and insets) and the horseshoe-like arrangement of garland cells is disturbed. (F–H) Ectopic expression of Pannier results in increased expression of *hand* in the heart (F, arrow), ectopic locations (G), and some cells of the CNS (arrow in H), indicating that Pannier is a potential regulator of *hand*. (I–K) shows *hand* C-GFP expression in the wildtype heart. (L–N) In *pannier* mutant embryos, the number of heart cells is strongly reduced, while remaining cardioblasts (filled arrow in M and N) and pericardial cells (filled arrowhead) still express *hand* GFP. They do not meet at the dorsal midline to form a regular heart tube. The lymph gland cells are missing (open arrow in N). Expression of *hand* C-GFP in the visceral mesoderm is still present (open arrowhead in N). (O–Q) The formation of a linear heart tube fails to form in *u-shaped* mutant embryos. Clustering of *hand*-GFP expressing cells that coexpress *mef2* in posterior regions (arrow in Q) indicates that some cardioblasts are still specified in *u-shaped*. (R–T) Compared to wildtype, *pointed* mutant embryos exhibit an increased number of cardioblasts accompanied by a reduction of pericardial cells. *hand*-GFP expression is unaffected in cardioblasts (arrow in T), and some remaining pericardial cells are GFP positive as well (arrowhead in T).

or even fixation of embryos. This allowed us the detection of so far unknown *zfh1*-phenotypes in heart associated tissues (lymph glands) and the garland cells as well as the evaluation of the influence of several putative regulators on *hand* expression.

2. Experimental procedures

2.1. Drosophila Stocks

Oregon R was the wild type used. The following mutant stocks were used: tin^{34B} (from Manfred Frasch), $zfh\text{-}1^{1}$ (from Mike Taylor), $pnt^{\Delta 88}$, ush^{2}, pnr^{1} (Bloomington stock center). For overexpression studies the following lines were used: UAS-*pnr* (from Pat Simpson), UAS-*ush* (from Robert Schulz), 24B-Gal4 (Bloomington stock center). All transgenic *Drosophila* lines were established by use of the w^{1118}-line.

2.2. Generation of lacZ reporter gene constructs

Specific regions of the *hand* gene were amplified and cloned into pCRII-Topo (Invitrogen) and verified by sequencing. LacZ reporter constructs were made by subcloning the fragments into pCaSpeR-AUG-ßGal or pCaSpeR-hs43-ßGal (Thummel and Pirrotta, 1992) and verified by partial sequencing. P-element-mediated germline transformations were performed as described (Rubin and Spradling, 1982). GFP constructs were made using the pH-Stinger vector of the Pelican series of P-element vectors (Barolo et al., 2000). Construct plasmid DNA was coinjected with Δ2-3 helper plasmid DNA (Robertson et al., 1988) into w^{1118} embryos. After backcrossing, four to five independent lines per construct were examined for reporter expression to exclude position effects.

2.3. Immunocytochemistry of whole-mount embryos

Processing and immunostaining of whole-mount embryos for ß-galactosidase was done following standard protocols, using the Vectastain Elite ABC Kit (VectorLabs). The following antibodies were used: mouse anti-ß-Galactosidase primary antibody 1:2000 (Promega-Z378A), rabbit anti-Tinman 1:500 (Rolf Bodmer), rabbit anti-Eve 1:3000 (Manfred Frasch), mouse anti-Zfh-1 (Zhi-Chun Lai), rabbit anti-Odd 1:500 (Jim Skeath), rabbit anti-Mef2 1:1500 (Hanh Nguyen). To detect GFP in embryos we used a rabbit polyclonal anti-GFP antibody (Abcam-ab6556, Cambridge, UK) or a mouse anti-GFP antibody (Invitrogen) at 1:600–1:2000 dilutions. All documentations were done with digital cameras. For confocal analysis we used a Zeiss LSM5 Pascal. Whole mount in-situ hybridization was performed as described previously (Kölsch and Paululat, 2002).

2.4. Dissections

Dissections were performed under a Leica MZ16 FA stereomicroscope using fine forceps, iridectomy shears and microneedles. Larvae, pupae, and adult flies were pinned ventral side up on Sylgard 184 plates (Sasco, Munich, Germany) and perfused with 1 × PBT. Individuals were cut open at the midline and the body wall was pinned by additional needles. The visceral organs were removed.

2.5. Time-lapse studies, GFP assessment in larvae, pupae and adults

Direct GFP fluorescence was observed with a Leica MZ16FA-stereo microscope equipped with UV-illumination and a Zeiss Axioscope2 epifluorescence microscope. Image Capturing was done using a SIS ColorView12 digital camera. Pictures and movies were assessed with the software package AnalySIS (SIS software, Münster, Germany). Stage 16 and 17 embryos were collected under a UV-equipped stereomicroscope and dechorionated in 50% DanKlorix in water (Colgate-Palmolive, Hamburg, Germany). Larvae were timed by hours after egg deposition (h AED): every 2 h, eggs were collected and then incubated for additional 22–76 h at 25 °C. For GFP image capturing, larval movement was stopped as follows: A commercial refrigerator cool-package was preadjusted to −20 °C. Next, a microscope slide with an individual larva was placed on the cooling block. Under these conditions, larvae stop movement within minutes. For image capturing a drop of microscopic immersion oil (precooled to 4 °C) was placed directly onto the larva.

To visualize the entire heart at high resolution, some pictures were composed by merging two to eight individual images using a commercial photo editing software (Canon Photo Stitch).

Acknowledgements

Work in the laboratory of A.P. is supported by grants from the DFG (European PhD program 767: Transcriptional Control in Development), DFG Pa 517/10-1 and the SFB 431: Membranproteine - Funktionelle Dynamik und Kopplung an Reaktionsketten.

Supplementary Data

Supplementary data associated with this article can be found at 10.1016/j.jmb.2005.09.079

References

Alvarez, A.D., Shi, W., Wilson, B.A., Skeath, J.B., 2003. *pannier and pointedP2* act sequentially to regulate *Drosophila* heart development. Development 130, 3015–3026.

Angelo, S., Lohr, J., Lee, K.H., Ticho, B.S., Breitbart, R.E., Hill, S., et al., 2000. Conservation of sequence and expression of *Xenopus* and zebrafish dHAND during cardiac, branchial arch and lateral mesoderm development. Mech. Dev. 95, 231–237.

Azpiazu, N., Frasch, M., 1993. *tinman and bagpipe*: two homeo box genes that determine cell fates in the dorsal mesoderm of *Drosophila*. Genes Dev. 7, 1325–1340.

Barolo, S., Carver, L.A., Posakony, J.W., 2000. GFP and ß-Galactosidase transformation vectors for promoter/enhancer analysis in *Drosophila*. BioTechniques 29, 726–732.

Bodmer, R., 1993. The gene *tinman* is required for specification of the heart and visceral muscles in *Drosophila*. Development 118, 719–729.

Charité, J., McFadden, D.G., Olson, E.N., 2000. The bHLH transcription factor dHAND controls Sonic *hedgehog* expression and establishment of the zone of polarizing activity during limb development. Development 127, 2461–2470.

Cross, J.C., Flannery, M.L., Blanar, M.A., Steingrimsson, E., Jenkins, N.A., Copeland, N.G., et al., 1995. *Hxt* encodes a basic helix-loop-helix transcription factor that regulates trophoblast cell development. Development 121, 2513–2523.

Curtis, N.J., Ringo, J.M., Dowse, H.B., 1999. Morphology of the pupal heart, adult heart, and associated tissues in the fruit fly, *Drosophila melanogaster*. J. Morphol. 240, 225–235.

Fernandez-Teran, M., Piedra, M.E., Kathiriya, I.S., Srivastava, D., Rodriguez-Rey, J.C., Ros, M.A., 2000. Role of dHAND in the anterior-posterior polarization of the limb bud: implications for the Sonic hedgehog pathway. Development 127, 2133–2142.

Firulli, A.B., 2003. A HANDful of questions: the molecular biology of the heart and neural crest derivatives (HAND)-subclass of basic helix–loop–helix transcription factors. Gene 312, 27–40.

Firulli, A.B., McFadden, D.G., Lin, Q., Srivastava, D., Olson, E.N., 1998. Heart and extra-embryonic mesodermal defects in mouse embryos lacking the bHLH transcription factor Hand1. Nat. Genet. 18, 266–270.

Fossett, N., Zhang, Q., Gajewski, K., Choi, C.Y., Kim, Y., Schulz, R.A., 2000. The multitype zinc-finger protein U-shaped functions in heart cell specification in the *Drosophila* embryo. Proc. Natl Acad. Sci. (USA) 97, 7348–7353.

Gajewski, K., Fossett, N., Molkentin, J.D., Schulz, R.A., 1999. The zinc finger proteins Pannier and GATA4 function as cardiogenic factors in *Drosophila*. Development 126, 5679–5688.

Gajewski, K., Choi, C.Y., Kim, Y., 2000. Genetically distinct heart cells within the *Drosophila* heart. Genesis 28, 36–43.

Gajewski, K., Zhang, Q., Choi, C.Y., Fossett, N., Dang, A., Kim, Y.H., et al., 2001. Pannier is a transcriptional target and partner of Tinman during *Drosophila* cardiogenesis. Dev. Biol. 233, 425–436.

Han, Z., Bodmer, R., 2003. Myogenic cells fates are antagonized by Notch only in asymmetric lineages of the *Drosophila* heart, with or without cell division. Development 130, 3039–3051.

Han, Z., Olson, E., 2005. *Hand* is a direct target of Tinman and GATA factors during *Drosophila* cardiogenesis and hematopoiesis. Development 132, 3525–3536.

Hollenberg, S.M., Sternglanz, R., Cheng, P.F., Weintraub, H., 1995. Identification of a new family of tissue-specific basic helix–loop–helix proteins with a two-hybrid system. Mol. Cell. Biol. 15, 3813–3822.

Howard, M., Foster, D.N., Cserjesi, P., 1999. Expression of *HAND* gene products may be sufficient for the differentiation of avian neural crest-derived cells into catecholaminergic neurons in culture. Dev. Biol. 215, 62–77.

Jensen, P.V., 1973. Structure and metamorphosis of the larval heart of Calliphora *erythrocephala*. Biologiske Skrifter/Kongelige Danske Videnskabernes Selskab 20, 2–19.

Johnson, E., Ringo, J., Dowse, H., 2001. Dynamin, encoded by shibire, is central to cardiac function. J. Exp. Biol. 289, 81–89.

Kambysellis, M.P., Wheeler, M.R., 1972. Banded polytene chromosomes in pericardial cells of *Drosophila*. J. Hered. 63, 214–215.

Klinedinst, S.L., Bodmer, R., 2003. Gata factor Pannier is required to establish competence for heart progenitor formation. Development 130, 3027–3038.

Knöfler, M., Meinhardt, G., Vasicek, R., Husslein, P., Egarter, C., 1998. Molecular cloning of the human Hand1 gene/cDNA and its tissue-restricted expression in cytotrophoblastic cells and heart. Gene 224, 77–86.

Kölsch, V., Paululat, A., 2002. The highly conserved cardiogenic bHLH factor Hand is specifically expressed in circular visceral muscle progenitor cells and in all cell types of the dorsal vessel during *Drosophila* embryogenesis. Dev. Genes Evol. 212, 473–485.

Krenn, H.W., Pass, G., 1994. Morphological diversity and phylogenetic analysis of wing circulatory organs in insects. 1. Non-holometabola. Zoology—Analysis of Complex Systems 98, 7–22.

Krenn, H.W., Pass, G., 1994. Morphological diversity and phylogenetic analysis of wing circulatory organs in insects. 2. Holometabola. Zoology—Analysis of Complex Systems 98, 147–164.

Lai, Z.C., Rushton, E., Bate, M., Rubin, G.M., 1993. Loss of function of the *Drosophila zfh-1* gene results in abnormal development of mesodermally derived tissues. Proc. Natl Acad. Sci. (USA) 90, 4122–4126.

Lo, P.C., Frasch, M., 2001. A role for the COUP-TF-related gene *seven-up* in the diversification of cardioblast identities in the dorsal vessel of *Drosophila*. Mech. Dev. 104, 49–60.

Lo, P.C.H., Skeath, J.B., Gajewski, K., Schulz, R.A., Frasch, M., 2002. Homeotic genes autonomously specify the anteroposterior subdivision of the *Drosophila* dorsal vessel into aorta and heart. Dev. Biol. 251, 307–319.

Lovato, T.L., Nguyen, T.P., Molina, M.R., Cripps, R.M., 2002. The Hox gene abdominal-A specifies heart cell fate in the *Drosophila* dorsal vessel. Development 129, 5019–5027.

Miller, A., 1965. The internal anatomy and histology of the imago. In: Demerec, M. (Ed.), Biology of Drosophila. Hafner Pub. Co., New York, pp. 420–534.

Molina, M.R., Cripps, R.M., 2001. Ostia, the inflow tracts of the *Drosophila* heart, develop from a genetically distinct subset of cardial cells. Mech. Dev. 109, 51–59.

Moore, A.W., Barbel, S., Jan, L.Y., Jan, Y.N., 2000. A genomewide survey of basic helix–loop–helix factors in *Drosophila*. Proc. Natl Acad. Sci. (USA) 97, 10436–10441.

Nichols, R., McCormick, J., Cohen, M., Howe, E., Jean, C., Paisley, K., Rosario, C., 1999. Differential processing of neuropeptides influences *Drosophila* heart rate. J. Neurogenet. 13, 89–104.

Papaefthmiou, C., Theophilidis, G., 2001. An in vitro method for recording the electrical activity of the isolated heart of the adult *Drosophila melanogaster*. In Vitro Cell. Dev. Biol. 37, 445–449.

Pass, G., 1998. Accessory pulsatile organs. In: Harrison, F., Locke, M. (Eds.), Microscopic Anatomy of Invertebrates, vol. 11/1. Wiley, New York, pp. 621–640.

Pass, G., 2000. Accessory pulsatile organs: evolutionary innovations in insects. Annu. Rev. Entomol. 45, 495–518.

Paternostro, G., Vignola, C., Bartsch, D.U., Omens, J.H., McCulloch, A.D., Reed, J.C., 2001. Age-associated cardiac dysfunction in *Drosophila melanogaster*. Circ. Res. 88, 1053–1058.

Perrin, L., Monier, B., Ponzielli, R., Astier, M., Semeriva, M., 2004. Drosophila cardiac tube organogenesis requires multiple phases of Hox activity. Dev. Biol. 272, 419–431.

Perttunen, V., 1955. The blood circulation and the accessory pulsatile organs in the wings of D*rosophila funebris* and *D. melanogaster* (Dipt Drosophilidae). Ann. Entomol. Fenn. 21, 78–88.

Ponzielli, R., Astier, M., Chartier, A., Gallet, A., Therond, P., Semeriva, M., 2002. Heart tube patterning in Drosophila requires integration of axial and segmental information provided by the Bithorax Complex genes and hedgehog signaling. Development 129, 4021–4509.

Riley, P., Anson-Cartwright, L., Cross, J.C., 1998. The Hand1 bHLH transcription factor is essential for placentation and cardiac morphogenesis. Nat. Genet. 18, 271–275.

Rizki, T.M., 1978. The circulatory system and associated cells and tissues. In: Ashburner, M., Wright, T.R.F. (Eds.), The Genetics and Biology of Drosophila, vol. 2b. Academic Press, New York, NY, pp. 397–452.

Robertson, H.M., Preston, C.R., Phillis, R.W., Johnson-Schlitz, D.M., Benz, W.K., Engels, W.R., 1988. A stable genomic source of P-element transposase in *Drosophila melanogaster*. Genetics 118, 461–470.

Rubin, G.M., Spradling, A.C., 1982. Genetic transformation of *Drosophila* with transposable element vectors. Science 218, 348–353.

Russell, M.W., Baker, P., Izumo, S., 1997. Cloning, chromosomal mapping, and expression of the human eHAND gene. Mamm. Genome 8, 863–865.

Russell, M.W., Kemp, P., Wang, L., Brody, L.C., Izumo, S., 1998. Molecular cloning of the human HAND2 gene. Biochim. Biophys. Acta. 1443, 393–399.

Sparrow, D.B., Kotecha, S., Towers, N., Mohun, T.J., 1998. *Xenopus eHAND*: a marker for the developing cardiovascular system of the embryo that is regulated by bone morphogenetic proteins. Mech. Dev. 71, 151–163.

Srivastava, D., Cserjesi, P., Olson, E.N., 1995. A subclass of bHLH proteins required for cardiac morphogenesis. Science 270, 1995–1999.

Srivastava, D., Thomas, T., Lin, Q., Kirby, M.L., Brown, D., Olson, E.N., 1997. Regulation of cardiac mesodermal and neural crest development by the bHLH transcription factor, dHAND. Nat. Genet. 16, 154–160.

Su, M.T., Fujioka, M., Goto, T., Bodmer, R., 1999. The *Drosophila* homeobox genes *zfh-1* and *even-skipped* are required for cardiac-specific differentiation of a numb-dependent lineage decision. Development 126, 3241–3251.

Tanaka, M., Munsterberg, A., Anderson, W.G., Prescott, A.R., Hazon, N., Tickle, C., 2002. Fin development in a cartilaginous fish and the origin of vertebrate limbs. Nature 416, 527–531.

Thattaliyath, B.D., Livi, C.B., Steinhelper, M.E., Toney, G.M., Firulli, A.B., 2002. HAND1 and HAND2 are expressed in the adult-rodent heart and are modulated during cardiac hypertrophy. Biochem. Biophys. Res. Commun. 297, 870–875.

Thomas, T., Yamagishi, H., Overbeek, P.A., Olson, E.N., Srivastava, D., 1998. The bHLH factors, dHAND and eHAND, specify pulmonary and systemic cardiac ventricles independent of left–right sidedness. Dev. Biol. 196, 228–236.

Thummel, C.S., Pirrotta, V., 1992. New pCasper P-element vectors. Drosophila Information Service 71, 150.

Wang, J., Tao, Y., Reim, I., Gajewski, K., Frasch, M., Schulz, R.A., 2005. Expression, regulation, and requirement of the toll transmembrane protein during dorsal vessel formation in *Drosophila melanogaster*. Mol. Cell. Biol. 25, 4200–4210.

Ward, E.J., Skeath, J.B., 2000. Characterization of a novel subset of cardiac cells and their progenitors in the *Drosophila* embryo. Development 127, 4959–4969.

Wessels, R.J., Bodmer, R., 2004. Screening assays for heart function mutants in *Drosophila*. Biotechniques 37, 58–66.

Yamagishi, H., Olson, E.N., Srivastava, D., 2000. The basic helix–loop–helix transcription factor, dHAND, is required for vascular development. J. Clin. Invest. 105, 261–270.

Yarnitzky, T., Volk, T., 1995. Laminin is required for heart, somatic muscles, and gut development in the *Drosophila* embryo. Dev. Biol. 169, 609–618.

Yelon, D., Ticho, B., Halpern, M.E., Ruvinsky, I., Ho, R.K., Silver, L.M., Stainier, D.Y., 2000. The bHLH transcription factor Hand2 plays parallel roles in zebrafish heart and pectoral fin development. Development 127, 2573–2582.

Zaffran, S., Frasch, M., 2002. Early signals in cardiac development. Circ. Res. 91, 457–469.

Zaffran, S., Astier, M., Gratecos, D., Guillen, A., Semeriva, M., 1995. Cellular interactions during heart morphogenesis in the *Drosophila* embryo. Biol. Cell 84, 13–24.

Zikova, M., Da Ponte, J.P., Dastugue, B., Jagla, K., 2003. Patterning of the cardiac outflow region in *Drosophila*. Proc. Natl Acad. Sci. (USA) 100, 12189–12194.

ELSEVIER

Mechanisms of Development 123 (2006) 372–387

www.elsevier.com/locate/modo

The ADAM metalloprotease Kuzbanian is crucial for proper heart formation in *Drosophila melanogaster*

Stefanie Albrecht [a], Shuoshuo Wang [a], Anne Holz [b], Annette Bergter [a], Achim Paululat [a,*]

[a] *Universität Osnabrück, Fachbereich Biologie/Chemie, Zoologie, Barbarastraße 11, D-49069 Osnabrück, Germany*
[b] *Justus Liebig Universität Gießen, Institut für Allgemeine und Spezielle Zoologie, Entwicklungsbiologie, Stephanstr. 24, D-35390 Gießen, Germany*

Received 18 January 2006; received in revised form 7 March 2006; accepted 9 March 2006
Available online 27 March 2006

Abstract

We have screened a collection of EMS mutagenized fly lines in order to identify genes involved in cardiogenesis. In the present work, we have studied a group of alleles exhibiting a hypertrophic heart. Our analysis revealed that the ADAM protein (A Disintegrin And Metalloprotease) Kuzbanian, which is the functional homologue of the vertebrate ADAM10, is crucial for proper heart formation. ADAMs are a family of transmembrane proteins that play a critical role during the proteolytic conversion (shedding) of membrane bound proteins to soluble forms. Enzymes harboring a sheddase function recently became candidates for causing several congenital diseases, like distinct forms of the Alzheimer disease. ADAMs play also a pivotal role during heart formation and vascularisation in vertebrates, therefore mutations in ADAM genes potentially could cause congenital heart defects in humans. In *Drosophila*, the zygotic loss of an active form of the Kuzbanian protein results in a dramatic excess of cardiomyocytes, accompanied by a loss of pericardial cells. Our data presented herein suggest that Kuzbanian acts during lateral inhibition within the cardiac primordium. Furthermore we discuss a second function of Kuzbanian in heart cell morphogenesis.

Keywords: Cardiogenesis; Heart; Dorsal vessel; *Kuzbanian*; ADAM; Metalloprotease; *Drosophila*; Lateral inhibition; *Mastermind*; Morphogenesis

1. Introduction

Heart development in vertebrates and flies share astonishing similarities, for instance during the early steps of heart primordium induction and during the first steps of heart cell differentiation (Bodmer and Venkatesh, 1998; Bodmer and Frasch, 1999; Cripps and Olson, 2002; Zaffran and Frasch, 2002; Brand, 2003). In both systems, Nkx and GATA factors are present in a subset of mesodermal cells that become competent to receive external signals from the overlaying ectoderm in flies, or from the underlying endoderm in vertebrates. Decapentaplegic (Dpp)/BMP and Wingless (Wg)/Wnt signalling is essential to promote differentiation of *tinman* expressing cells into cardiac primordium. Nkx and GATA factors as well as the signal molecules Dpp and Wg are required for the specification of both subtypes of heart cells in the fly, the myogenic contractile cardiomyocytes and the non-contractile pericardial cells. Mutations in the *tinman* gene, or an interruption of Dpp or Wg signalling, result in the complete absence of heart structures in the fly (Azpiazu and Frasch, 1993; Bodmer, 1993; Frasch, 1995; Wu et al., 1995; Yin and Frasch, 1998; Lockwood and Bodmer, 2002). The activity of Tinman within the cardiac primordium, combined with the activity of the *Drosophila* GATA factor Pannier, promotes further specification of cardioblasts (Azpiazu and Frasch, 1993; Bodmer, 1993; Xu et al., 1998; Gajewski et al., 1999, 2001; Alvarez et al., 2003; Klinedinst and Bodmer, 2003; Reim et al., 2003; Reim and Frasch, 2005; Sorrentino et al., 2005). Specification of different subtypes of cardiac progenitors is accompanied by the combinatorial expression of particular transcription factors, including the homeobox factor Ladybird and the COUP nuclear hormone receptor Seven-up (Jagla et al., 1997, 2002; Lo and Frasch, 2001; Han et al., 2002; Ryan et al., 2005). Likely, these factors are required for the appropriate specification of individual heart progenitors and their proper differentiation, e.g. into ostia (Lo and Frasch, 2001; Molina and Cripps, 2001). Studies of Hartenstein, Bodmer and others have

* Corresponding author. Tel.: +49 541 9692861; fax: +49 541 9692587.
E-mail address: paululat@biologie.uni-osnabrueck.de (A. Paululat).

0925-4773/$ - see front matter © 2006 Elsevier Ireland Ltd. All rights reserved.
doi:10.1016/j.mod.2006.03.005

shown that the differentiation of heart cells within the dorsal mesoderm also depends on Notch–Delta signalling. Early elimination of Notch activity using a temperature-sensitive allele causes hypertrophy of cardiac cells, due to a failure of lateral inhibition within the dorsal mesoderm (Hartenstein et al., 1992; Mandal et al., 2004). Notch has at least a second function during asymmetric cell division in the heart cell lineage and thus a biphasic requirement during heart development. The heart progenitors forming the ostia arise from asymmetric cell divisions, dependent on Notch function, as well as on the function of other components of the asymmetric cell division machinery including Sanpodo, Numb and Inscuteable (Ward and Skeath, 2000; Alvarez et al., 2003; Han and Bodmer, 2003; Popichenko and Paululat, 2004).

In a search for novel genes involved in heart differentiation, we screened a collection of EMS-induced lethal mutations (Hummel et al., 1999a,b). We identified several mutant lines displaying strong malformations of the embryonic heart, which we grouped into different phenotypic classes (Fig. 1). The molecular characterization of these mutants will be described elsewhere. Among the mutants displaying heart defects, we identified five alleles of the metalloprotease-disintegrin Kuzbanian and three alleles of the Notch downstream effector Mastermind, all of them displaying a hyperplasic heart. Embryos, stained for β3Tubulin, Mef2 and other markers, revealed an approximately twofold excess of cardioblasts concomitant by a loss of pericardial and lymph gland cells. The excess of cardioblasts in *kuzbanian* affects all subtypes of cardioblasts, e.g. the *tinman* and the *seven-up* expressing cells. According to this observation, we assume a functional role for Kuzbanian during Notch dependent lateral inhibition within the early cardiac mesoderm, likely in conjunction with a later function during asymmetric cell division in the heart cell lineage. In *kuzbanian* mutants, we furthermore observed a misarrangement of heart cells and the failure of cardioblasts to adopt their final cell morphology, while specification and initial differentiation of heart cells still occurs, indicated by the expression of genes that label specific cell types in the heart, and the attempts of cardioblasts to form lumen-like structures.

Metalloprotease-disintegrins (ADAMs) are membrane-anchored proteases, which have a critical function for proteolytic release of soluble forms of membrane bound target proteins (shedding). Recently, it has been shown that distinct members of the vertebrate ADAM family are crucial for cardiogenesis and vascularisation (Dibbs et al., 2003; Jackson et al., 2003; Shi et al., 2003; Zhou et al., 2004; Horiuchi et al., 2005), therefore mutations in ADAM genes potentially could cause congenital heart defects in humans. *Drosophila* has five known ADAMs. DmTace is the homologue of the human TNF-α converting enzyme Hs-TACE (TACE; tumor necrosis factor-alpha converting enzyme), Dm-Mmd and Dm-Meltrin are closely related to the human Meltrin-alpha gene. Kuzbanian (*kuz*) and Kuzbanian-like (*kul*) reveal strong similarities to human ADAM10 (Sapir et al., 2004). So far, for none of them a function for embryonic heart formation was described. Herein, we show that the metalloprotease Kuzbanian is crucial for proper cardiogenesis in *Drosophila*.

2. Results

2.1. A screen for genes required in cardiogenesis revealed several heart phentoypes

About 500 balanced lines from mutagenized second or third chromosomes (Hummel et al., 1999a,b) were examined for mutations affecting the morphology of the embryonic heart. For the first round of screening, we used an anti-β3Tubulin antibody (Leiss et al., 1988), which turned out to be a particularly useful marker, allowing the visualisation of heart cells and the majority of the mesodermal tissue simultaneously (Burchard et al., 1995; Rau et al., 2001; Schröter et al., 2004). Therefore, not only the morphology of the dorsal vessel itself, but also the architecture of the heart in its tissue context is clearly visible. Within the dorsal vessel, β3Tubulin is expressed in four out of six cardioblasts per hemisegment, regulated by the transcription factor Tinman, which is active in the same subset of cardioblasts (Buttgereit et al., 1996; Damm et al., 1998; Kremser et al., 1999). Subsequently, a second round of screening was performed with an antibody against Mef2, which visualises the nuclei of all six cardioblasts in a hemisegment (Lilly et al., 1994; Nguyen et al., 1994; Taylor et al., 1995). Finally, we identified several mutants with malformations of the dorsal vessel (Fig. 1). One group of mutants is characterized by the absence of the majority of cardioblasts or the heart at all (Fig. 1C). These mutants exhibit additional defects in the somatic mesoderm, indicating that the mutated genes have a more general role during mesoderm or dorsal mesoderm differentiation. The second group of mutants shows a misarrangement of cardioblasts (Fig. 1D). A closer microscopic inspection revealed that cardioblasts obviously fail to undergo cytokinesis upon embryonic mitosis 16. The third group of mutants is characterized by appearance of kinks, gaps or cardioblast alignment defects (Fig. 1E). The fourth group (Fig. 1F) exhibits phenotypes reminiscent to defects typically observed in asymmetric cell division mutants like, e.g. *inscuteable* (Popichenko and Paululat, 2004). The analysis of these mutants will be described elsewhere, while the fifth group (see below, Fig. 1H–J) is described herein.

Eight mutant fly lines identified in our screen show a nearly identical phenotype, characterized by the appearance of an approximately twofold excess of cardiomyocytes (Fig. 1G and H, Table 1). They fall into two complementation groups, representing three *mastermind* (*mam*) and five *kuzbanian* (*kuz*) alleles (see methods section for details of the genetics). Mam is a modulator of Notch signalling and crucial for mesodermal and neuronal differentiation (Petcherski and Kimble, 2000; Yedvobnick et al., 2004), including cardiogenesis (Hartenstein et al., 1992). In contrast, a functional role of Kuzbanian during cardiogenesis was not investigated so far, although the embryonic phenotype of *kuzbanian* mutant embryos was extensively analysed (Fambrough et al., 1996; Rooke et al., 1996; Pan and Rubin, 1997; Sotillos et al., 1997; Qi et al., 1999;

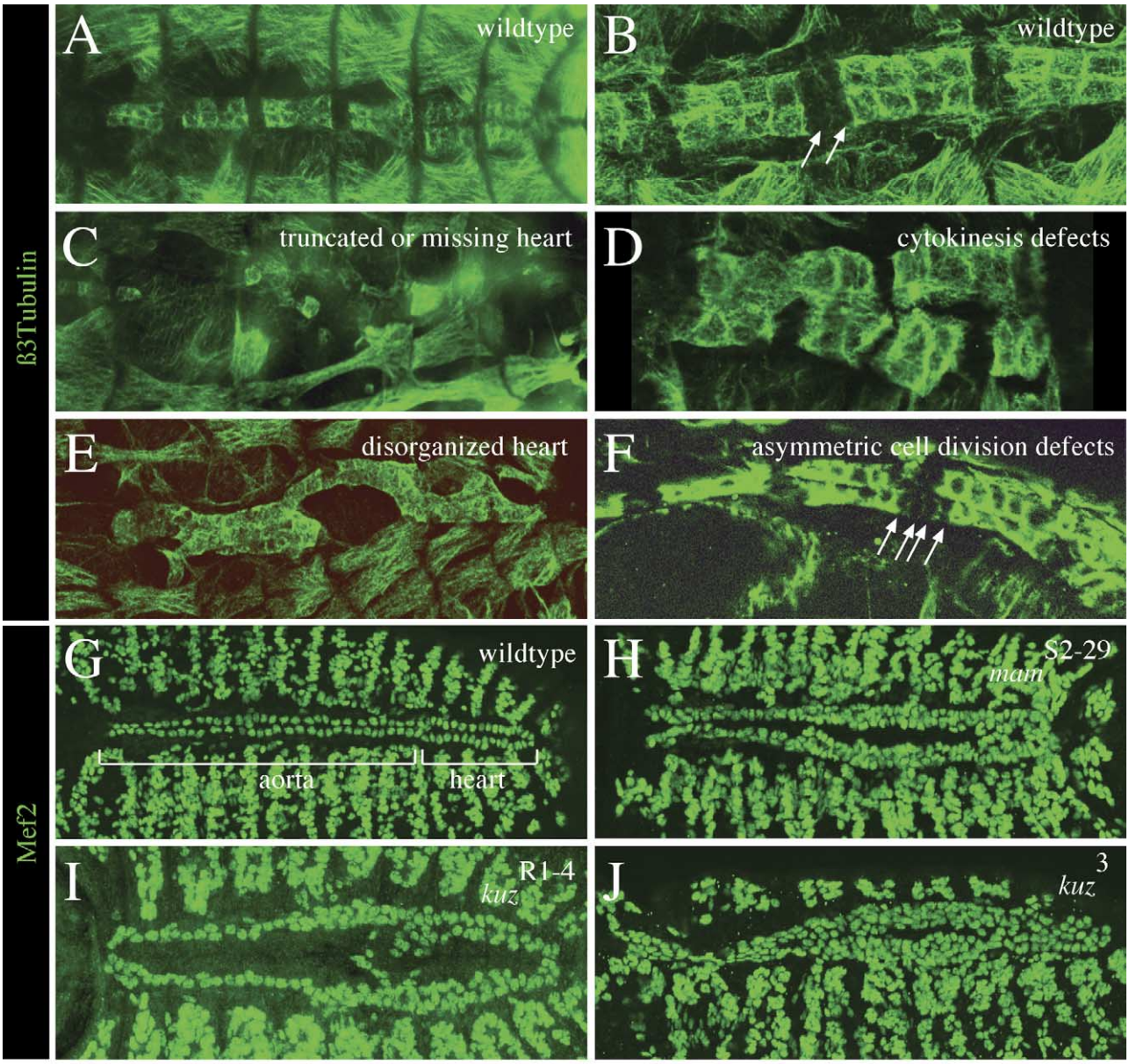

Summary of the observed heart phenotypes

Phenotype	Number of Lines
Rudimentary or missing heart	4
Cell cycle / cytokinesis defects	4
Disorganized heart	7
Asymmetric cell division phenotype	2
Hyperplasic heart	8

Fig. 1. A screen of EMS-induced embryonic lethals identifies mutations affecting heart development. The dorsal vessel is visualised using an antibody against β3Tubulin (A–F) or Mef2 (G–J). Wildtype embryos are shown in A, B and G for comparison. In embryos belonging to the first group of mutants, the heart is missing or only a few remaining cardioblasts can be detected (C). The second group reveals cytokinesis defects, characterised by cardioblasts that fail to separate during mitosis and to align properly (D). The third group shows a disorganized heart with gaps or cardioblast alignment defects (E). The fourth group displays asymmetric cell division phenotypes (F). We identified the EMS-mutant shown in F as being a *sanpodo* allele (own observation). The fifth group shows a strong excess of cardioblasts (H–J, compared to G). In wildtype embryos Mef2 labels all cardioblasts, six per hemisegment. In total, the embryonic heart of a wildtype embryos consists of 104 Mef2-positive cardioblasts (G). We identified three EMS-induced *mastermind* alleles in our screen, which roughly exhibit a twofold excess of cardioblasts (see Table 1). As an example, $mam^{S2\text{-}29}$ is shown in (H). Similarily, the five *kuzbanian* alleles depicted in our screen display a similar phenotype (see Table1). At late stages, the heart in *kuzbanian* embryos appears to be closed. As an example, $kuz^{R1\text{-}4}$ (I) and kuz^{3} (J) are shown. Pictures were made using the maximum projection algorithm using a stack of confocal pictures.

Table 1
Kuzbanian and *mastermind* regulate cell number in the heart

Cell type	Wildtype	kuz^{R1-4}	*Tw*iGal4 > *Kuz*DN	mam^{S2-29}
Mef2-expressing cardioblasts/embryo	105.8 ± 5.4 ($n=8$)	183.6 ± 19.1 ($n=7$)	138.8 ± 10.9 ($n=6$)	201.3 ± 24.6 ($n=12$)
Svp-expressing cardioblasts/embryo	28.5 ± 1.2 ($n=4$)	40 ± 2.4 ($n=6$)	n.d.	45.1 ± 4.6 ($n=9$)
Zfh1-expressing pericardial cells/embryo	119.5 ± 22.3 ($n=8$)	75 ± 5.7 ($n=2$)	n.d.	53 ± 22.6 ($n=2$)
Odd-expressing pericardial cells/embryo	85.5 ± 2.4 ($n=8$)	41.3 ± 7.2 ($n=9$)	40.3 ± 5.4 ($n=11$)	21.2 ± 1.5 ($n=9$)
Eve-expressing pericardial cells/embryo	29.6 ± 0.6 ($n=3$)	32.6 ± 3.0 ($n=3$)	n.d., see Fig. 4	0.7 ± 0.95 ($n=7$)

Numbers in parentheses indicate number of embryos scored; n.d., not determined.

Schimmelpfeng et al., 2001; Klein, 2002; Lieber et al., 2002). To verify that mutations in the *kuzbanian* gene are responsible for the observed heart phenotype, we added two independently detected amorphic *kuzbanian* alleles, kuz^{3} and kuz^{e29-4}, to our phenotypic analysis. Indeed, all alleles exhibit an approximate twofold increase in cardioblast number. The severity of the heart phenotype varies only slightly between each allele, indicating that all mutations are likely to be null mutations. As an entry point to elucidate the molecular nature of the EMS-induced mutations, we have sequenced the *kuzbanian* locus, which consists of 13 exons spanning a region of about 88 KB, from selected mutant chromosomes. The R1-4 allele indeed carries a mutation within the *kuzbanian* gene. The mutation in kuz^{R1-4} arises from a splice-donor-site mutation in the 4th intron (see Fig. 2A–D, the point mutation is five base pairs downstream of the 4th exon). This results in a failure to splice a 68 bp intron, which finally causes a truncation within the prodomain of Kuzbanian due to a frameshift (see Fig. 2E). The predicted protein lacks any recognizable domains, and therefore we consider this allele to be a *kuzbanian* null allele. The characterization of the other EMS-induced *kuzbanian* alleles is in progress.

2.2. Loss of kuzbanian function results in an excess of cardioblasts in all subregions of the dorsal vessel

The embryonic dorsal vessel of *Drosophila* is composed of three morphologically distinguishable regions, the posterior 'heart' with a wider lumen and functional ostia, the posterior aorta with ostia precursor cells and the anterior aorta, which lacks ostia or ostia precursors. The 'heart' is separated by a valve-like structure from the aorta-region (Jensen, 1973; Rizki, 1978; Alvarez et al., 2003; Perrin et al., 2004). Recent studies have shown that the specification of distinct heart regions along the anterior–posterior (a–p) axis depends on the activity of the homeobox factors Antennapedia (Antp), Ultrabithorax (Ubx), Abdominal-A (Abd-A), and Abdominal-B (Abd-B) (Lo et al., 2002; Lovato et al., 2002; Ponzielli et al., 2002). Consequently, mutations were observed, which affect heart cell differentiation in specific regions, e.g. mutations in the transcription factor *pointed-P2* result in cardioblast proliferation restricted to the posterior seven segments (Alvarez et al., 2003). In contrast, *kuzbanian* mutant embryos display an excess of cardioblasts along the whole a–p axis of the dorsal vessel (see Fig. 1), although the phenotype is more prominent in the posterior segments. To examine whether the observed excess of cardioblasts is restricted to a specific subtype of heart cells, we used various markers to visualise individual cardioblast identities. Double-labellings for Seven-up/Mef2, Seven-up/Tinman, and Ladybird/Tinman clearly show that all types of cardioblasts in an abdominal hemisegment are increased in number, although to different extend (Fig. 3A–F, Table 1, see also Section 3). Thus, the *kuzbanian* phenotype is not restricted to a particular subset of cardioblasts. Other parts of the dorsal mesoderm, for instance the dorsal somatic muscles, are obviously not affected in zygotic loss-of-function *kuzbanian* mutant embryos. Nevertheless, mesodermal expression of a dominant negative construct shows that Kuzbanian is crucial for the differentation of the somatic muscles (see below, Fig. 4). The time of lethality was examined for selected amorphic *kuzbanian* alleles (kuz^{F2-16}, kuz^{J2-11}, kuz^{P2-108}, kuz^{R1-4}, kuz^{S5-65} and kuz^{3}) utilising a GFP balancer chromosome. We found that homozygous *kuzbanian* embryos display muscle contraction but fail to hatch and die approximately 2 days after egg deposition. Likely, lethality is caused by the combination of various embryonic defects observed in *kuzbanian* mutant embryos, including neuronal and potentially heart defects.

2.3. Kuzbanian is required for pericardial cell and lymph gland development

Pericardial and lymph gland cells, like cardioblasts, arise from the dorsal mesoderm. Using antibodies against even-skipped (Frasch and Levine, 1987), Odd-skipped (Ward and Skeath, 2000), Zfh1 (Lai et al., 1993) and a *hand*-GFP reporter line (Kölsch and Paululat, 2002; Sellin et al., 2006), that visualise all or a specific subset of pericardial cells, we observed a strongly reduced number of pericardial cells in the *kuzbanian* mutant background (Fig. 3G–L, Table 1). For example, the four Odd-skipped expressing pericardial cells visible in a wildtype hemisegment were sometimes completely missing in *kuzbanian* embryos (Fig. 3L). Because two of the four Odd cells derive from asymmetric cell division

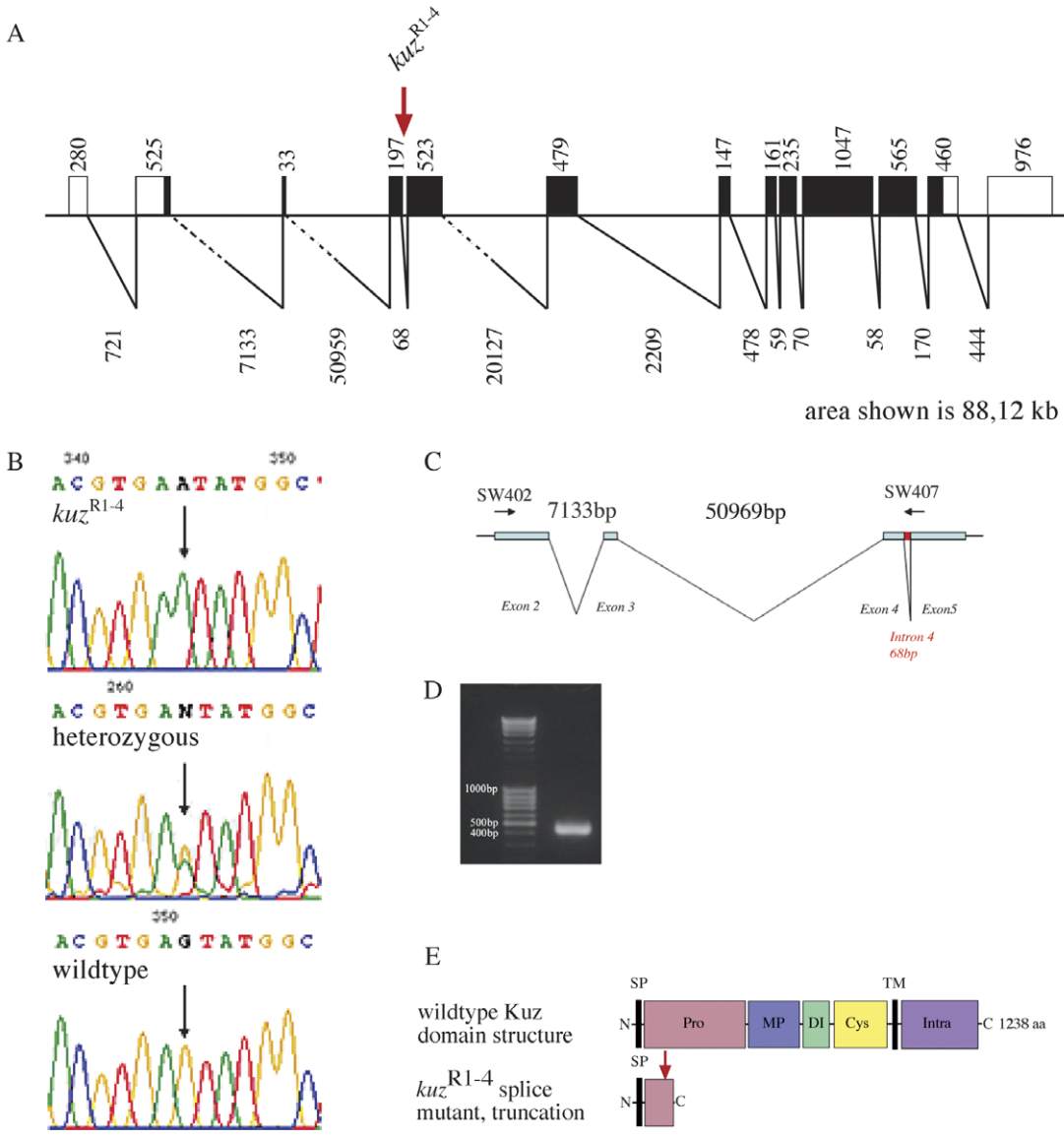

Fig. 2. Organization of the *kuzbanian* locus and molecular characterization of the *kuzbanian* allele kuz^{R1-4}. (A) Schematic representation of the genomic structure of the *kuzbanian* gene showing the exon–intron structure and open reading frame. Black and white boxes represent coding and non-coding sequences. The location of the ethylmethane sulfonate (EMS) induced mutation in kuz^{R1-4} is indicated by an arrow. (B) The sequence alteration in kuz^{R1-4} (A→G) was detected when DNA from homozygous mutants (upper panel), heterozygous (mid panel) and wildtype animals (lower panel) was sequenced. In heterozygous embryos, a double peak is visible. (C) As a further proof, we designed a RT-PCR experiment. The forward primer SW402 is located within exon 2; the reverse primer SW407 matches the intron–exon boundary of the fourth intron/fifth exon. Thus, the reverse primer SW407 binds solely to an mRNA that harbors the 4th intron. This primer combination avoids artificial amplification from genomic DNA due to the distance of the primer binding sites to the *kuzbanian* locus (>58 kb). As template for PCR, RNA isolated from heterozygous animals was used. We expected an amplicon of about 456 bp instead of 388 bp, resulting from correct splicing of intron 2 and 3, but presence of intron 4 in the mRNA. (D) An amplicon of about 450 bp was observed. The band was extracted from the gel, cloned and sequenced. We found that the 4th intron is present in the amplified cDNA. As shown in B, a single point mutation (A→G) is present in direct neighborhood to the intron–exon boundary within the intron. This result indicates, that the mutation in kuz^{R1-4} is a splice site mutation. (E) Schematic representation of the domain structure of Kuzbanian and the postulated alteration in kuz^{R1-4}. The presence of the forth intron causes a premature truncation due to a frame shift induced stop codon within the prodomain. The Kuz^{R1-4} protein lacks any recognizable domain and is thought to be a strong loss of function mutation. Abbr.: SP, signal peptide; Pro, prodomain; MP, metalloprotease domain; DI, disintegrin domain; Cys, cystein-rich domain; TM, transmembrane domain; Intra, intracellular domain.

whereas the other two cells originate from symmetric cell division, the absence of all four cells in a hemisegment indicates that Kuzbanian function is not restricted to one of these lineage types. Furthermore, we observe that the remaining pericardial cells in *kuzbanian* mutant embryos appear in an irregular fashion along the a–p axis of the heart. We do recognise specific regions where the pericardial cell pattern appears normal, neither with respect to the location nor to the number of pericardial cells. The *even-skipped* expressing pericardial cells (EPCs), which share a common lineage with a dorsal body wall muscle (Buff et al., 1998; Carmena et al., 1998, 2002; Su et al., 1999) are not affected in *kuzbanian* mutant embryos (Fig. 3M, Table 1), whereas a dominant negative form of Kuzbanian, driven by *twist*-Gal4

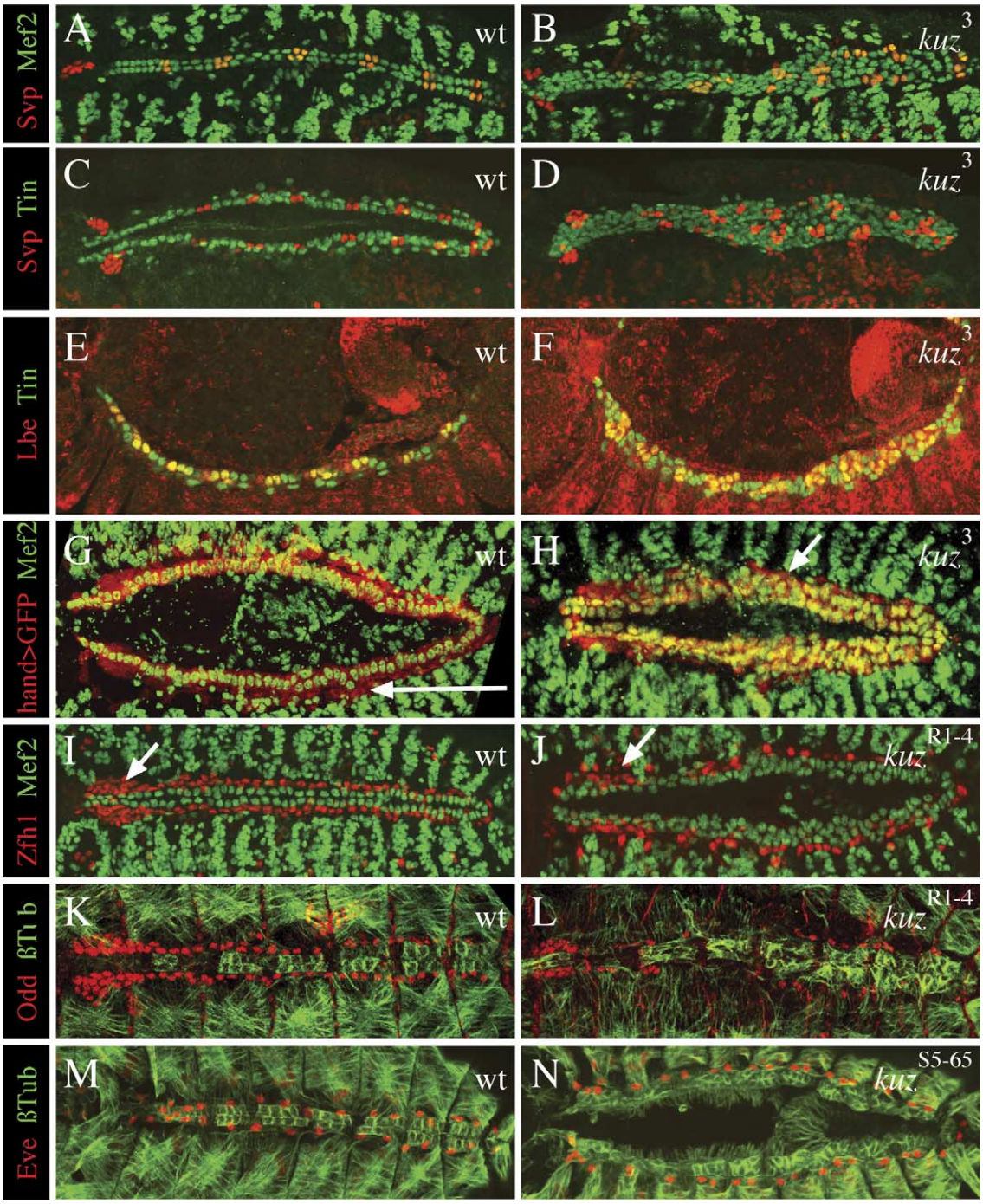

Fig. 3. The dorsal vessel consists of different cell types, characterized by the specific expression of molecular markers. A–F shows confocal images of wildtype embryos (A, C and E) and *kuzbanian* mutant embryos (B, D and F). The alleles we used were kuz^{3} (B, D, F, H), kuz^{R1-4} (J, L) and kuz^{S5-65} (N). The six cells in an abdominal hemisegment express Mef2; four out of six cardioblasts express *tinman*, two of which coexpress *tinman* and *ladybird*. The remaining two cardioblasts express *svp*-lacZ but not *tinman* or *ladybird*. *svp*-lacZ identifies the cardioblasts that form ostia or ostia precursors and which derive from asymmetric cell division (Ward and Skeath, 2000). Compared to wildtype (A), the number of *svp*-lacZ expressing cells is increased approximately twofold in *kuzbanian* (B). Double labelling for *svp*-lacZ/Tinman and Ladybird/Tinman in wildtype (C and E) and *kuzbanian* mutant embryos (D and F) reveals that the *tinman, ladybird* and *svp*-lacZ expressing cardioblasts contribute all to the increased total number of cardioblasts in *kuzbanian*. The pericardial cells, some of which express *tinman*, are reduced in *kuzbanian* mutant embryos. Therefore, the *tinman* positive cells in *kuzbanian* embryos (D and F) represent predominantly cardioblasts. Double labelling with Mef2/*hand*-GFP (G and H), Mef2/Zfh1 (I and J) and β3Tub/Odd (K and L) reveals that the number of pericardial cells is reduced in *kuzbanian* mutant embryos (H, J, and L) compared to wildtype (G, I, and K). In addition, the number of lymph gland cells is reduced (arrow in I and J). The Even-skipped expressing pericardial cells (EPCs) are not affected in *kuzbanian* (compare M and N). All pictures were made using the maximum projection algorithm on a stack of confocal pictures.

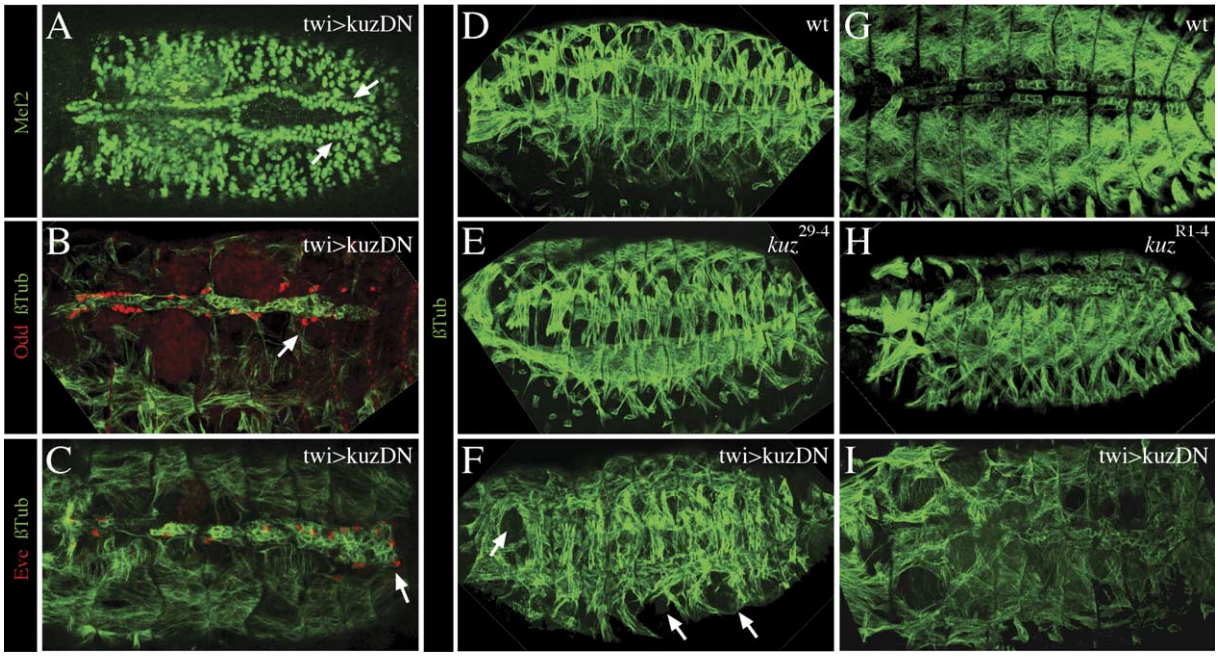

Fig. 4. Expression of a dominant negative *kuzbanian* transgene (UAS-KuzDN), driven by *twist*-Gal4, mimics the phenotype of *kuzbanian* loss of function mutant embryos (compare A with Fig. 1I) and indicates a function of Kuzbanian in the somatic mesoderm. (A) shows a representative embryo, stained for Mef2. The hyperplasic heart is clearly visible (arrows). (B) double staining for β3Tubulin (green) and Odd (red) reveals a significant loss of pericardial cells (arrow). KuzDN, when driven with *twi*-Gal4, causes severe defects in the somatic mesoderm as well (B and C). In contrast to the zygotic *kuzbanian* mutant embryos, which show a normal number of Eve-expressing pericardial cells (see Fig. 3M,N), the *twi* > KuzDN embryos exhibit only a few Eve-expressing cells (arrow in C), likely due to the early inhibition of the maternal Kuzbanian function. Furthermore, panmesodermal expression of KuzDN causes patterning defects in the somatic mesoderm. (D–I) show embryos stained for β3Tubulin to visualise somatic muscles. For comparision wildtype embryos are shown in lateral (D) or dorsal view (G). Whereas homozygous *kuzbanian* mutant embryos ($kuz^{29\text{-}4}$ in E, lateral view, $kuz^{R1\text{-}4}$ in H, dorsal view) exhibit a fairly normal muscle pattern, embryos in which KuzDN is driven in the mesoderm by *twist*-Gal4 display severe muscle malformation defects, indicating that Kuzbanian plays a role in muscle formation.

(see Section 2.4 and Fig. 4), causes a reduction of EPC cells. The number of EPCs is also strongly reduced in *mastermind* mutant embryos (see Table 1). The progenitors of the various subsets of pericardial cells are specified during different time windows. Double-staining for Eve and Odd has shown that Eve-mesodermal cells giving rise to the EPCs appear at stage 10, whereas the Odd-skipped expressing pericardial cell progenitors are not detectable until stage 12/2 (Ward and Skeath, 2000). Therefore we assume, that in zygotic *kuzbanian* mutant embryos the maternal component is sufficient for proper differentiation of the EPCs, but not for the Odd-skipped pericardial cells. The EPCs constitute a subset of the Zfh1 positive pericardial cells, of which—beside the EPCs—only a small number is still present in *kuzbanian* mutant embryos. Our results indicate that Kuzbanian is required for the coordinated specification of pericardial cells. In addition, we observe defects in lymph gland differentiation. The lymph glands, which are a source for larval hemocytes, appear as two bilateral located cell cluster flanking the anterior part of the dorsal vessel at stage 16 embryos (Mandal et al., 2004; Jung et al., 2005). Each cluster harbors about 20 cells that express, e.g. Odd-skipped and Zfh-1, two markers we have already used to determine the consequences of mutations in the *kuzbanian* gene on pericardial cell development (see above). We found a reduced number of lymph gland cells in *kuzbanian* mutant embryos (e.g. Fig. 3J, compared to 3I).

2.4. The excess of cardioblasts in kuzbanian mutant embryos is caused by a requirement of Kuzbanian prior to heart cell specification

As an entry point to elucidate the time of Kuzbanian requirement during heart development, we expressed a dominant negative *kuzbanian* variant (KuzDN) in the mesoderm at different time points of embryonic development. The transgene KuzDN lacks the extracellular metalloprotease domain and was successfully used to mimic *kuzbanian* phenotypes, e.g. in bristle development, eye development (Pan and Rubin, 1997), and the embryonic nervous system (Schimmelpfeng et al., 2001). Utilising the UAS-Gal4 system we choose *twist*-Gal4, *tinman*-Gal4 (*tin*CΔ4-Gal4) and *hand*-Gal4 as drivers. *twist*-Gal4 allows the activation of UAS-KuzDN in the entire early mesoderm, covering the time when heart progenitors are selected within the dorsal mesoderm by lateral inhibition. *tin*CΔ4-Gal4 drives expression in differentiating cardioblasts from embryonic stage 11 to 12 onwards, but lacks the early tinman expression domain (Lo and Frasch, 2001; Perrin et al., 2004). As a third driver we used *hand*-Gal4. The bHLH factor Hand is expressed from stage 12 onwards in all heart cells (cardioblasts and pericardial cells) after the selection of heart progenitors (Moore et al., 2000; Kölsch and Paululat, 2002; Han and Olson, 2005; Sellin et al., 2006). Thus, *hand*-Gal4 provides the Gal4 activator later then *twi*-Gal4 and *tin*-Gal4. The dominant negative Kuzbanian transgene

(KuzDN) phenocopies the loss of function phenotype, but only when driven by *twi*-Gal4 (Fig. 4, Table 1). The number of cardioblasts is increased approximately twofold, as seen in all loss of function alleles. The number of pericardial cells appears to be reduced. Furthermore, we observe strong muscle patterning defects (Fig. 4), indicating that Kuzbanian is important for the development of the somatic mesoderm. We assume that the panmesodermal expression of KuzDN inhibits the maternally contributed wildtype Kuzbanian protein in this tissue, causing a severe muscle phenotype not visible in the zygotic mutants. KuzDN expression, driven by *tin*-Gal4 and *hand*-Gal4 does not cause a significant excess of cardioblasts. As mentioned above, both drivers are active predominantly after the selection of the cardiac primordial cells.

2.5. Terminal heart cell differentiation is affected in kuzbanian mutants

Heart formation during embryogenesis requires the migration of heart precursors towards a dorsal position. From stage 15 to 17, cardiac precursors become flattened, polarized cells that align in a highly organized longitudinal row (Rugendorff et al., 1994; Fremion et al., 1999). At dorsal closure, the leading edges of the cardioblasts meet their contralateral counterparts. Finally, the lumen is formed when the trailing edges of the cardioblasts of either side bend around and contact each other (Rugendorff et al., 1994). In *kuzbanian* mutant embryos, the migration of heart precursors towards the dorsalmost position is not affected, whereas the final alignment of heart precursors and cardioblasts is considerably disturbed. All analysed mutant alleles finish dorsal closure and cardiac cells appear as a three to six cell wide band, extending from anterior to posterior, indicating that the contralateral counterparts of the developing heart contact each other. α-Spectrin staining (Zarnescu and Thomas, 1999) allows to distinguish between the ostia-forming cardioblasts that exhibit a characteristic double-bean like morphology at late embryonic stages and the *tinman*-expressing cardioblasts that show a cube-like, polarized appearance at stage 16 (Fig. 5A). In *kuzbanian* mutant embryos, cardioblasts fail to adopt the final cell morphology. For example, the characteristic bean-like shape of cardioblasts, that normally form the ostia at stage 16/17, is not recognizable (compare Fig. 5A,B). Also, the four *tinman*-expressing cardioblasts, which usually have a flattened, cube-like morphology with a distinct polarisation, exhibit an abnormal morphology (Fig. 5A,B). In *kuzbanian* mutant embryos the majority of cardioblasts show a triangle or parallelogram-like shape; the characteristic cube-like appearance, as seen in stage 16/17 wildtype embryos, is aberrant. In the posterior region of the heart, Wingless (Wg) is expressed specifically in three double pairs of cardioblasts (Wg, see Fig. 5C,D). These cells coexpress Seven-up and differentiate into ostia (Molina and Cripps, 2001; Lo et al., 2002). In *kuzbanian* mutant embryos, we observe an increased number of Wg-positive cardioblasts that fail to form the typically double pairs and exhibit an abnormal morphology, indicating that final cell differentiation is abolished (Fig. 5D). At stages before the contralateral cardioblasts meet each other at the dorsal midline, we observe in *kuzbanian* mutants embryos occasionally regions, in which short stretches of pair-wise organised cardioblasts are prominent (Fig. 5F). The arrangement of the pair-wise organized cardioblasts at stage 14 or 15 resembles the highly organised dorsal vessel of wildtype embryos at stage 16/17 (Fig. 5E). We assume that cardiac cell differentiation is initiated in *kuzbanian* mutant embryos, as cardioblasts on both sides of the embryo attempt to align along the a-p axis to form a two cell wide row of cardioblasts.

Rugendorff and colleagues have shown that heart lumen formation is a late step during cardiogenesis, requiring the contact of the contralateral located cardioblasts when they meet each other at the midline (Rugendorff et al., 1994). Therefore, we have analysed whether lumen formation is abolished in the heart of *kuzbanian* mutants. Light and transmission electron microscopic analysis of sectioned embryos revealed that the cardioblasts in *kuzbanian* mutants occasionally attempt to form a lumen-like structure (Fig. 5G–I), when cardioblasts align correctly along the a–p axis and establish a pair-wise organisation in restricted small areas. The lumina, shown in Fig. 5H, appear to be formed by ipsilateral cardioblasts instead of contralateral cardioblasts, consistent with the observation of bilateral located two cell rows of cardioblasts at stage 14/15 mentioned above. Our results indicate that heart lumen formation does not require the correct position of two bilateral located one cell wide rows of cardioblasts at the dorsal midline rather than any two adjacent rows of specified cardioblasts that can communicate directly.

The larval heart in *Drosophila* lacks neuronal innervation, suggesting that heart beating is totally myogenic (Dulcis and Levine, 2003). This particular aspect of heart function should be not influenced by the neuronal defects occurring in *kuzbanian* embryos, but being dependent on cell autonomous mechanisms. Therefore we have analysed, whether the *kuzbanian* heart is able to beat, using a GFP-reporter gene, specifically driven in the whole heart by an enhancer element cloned from the bHLH transcription factor gene *hand* (Sellin et al., 2006). In wildtype embryos, heart beating can be observed at late stage 17 embryos shortly before hatching. However, heart beating is observed in homozygous *kuzbanian* embryos, although beating is irregular, probably due to the misarrangement of cardioblasts. Nevertheless, the result indicates that cells bearing pacemaker activity are specified and active.

3. Discussion

Kuzbanian, and its vertebrate homologue ADAM10, belong to the large family of membrane anchored glycoproteins that show a characteristic conserved domain structure: an amino-terminal signal sequence followed by pro-, metalloprotease, and disintegrin domains, a cysteine-rich domain, usually containing an EGF repeat, and finally a transmembrane domain and cytoplasmic tail (see Fig. 2E, reviewed in, e.g. Becherer and Blobel, 2003). The complex protein structure suggests a widespread function of this class of molecules. Indeed, ADAMs act in many biological processes, including

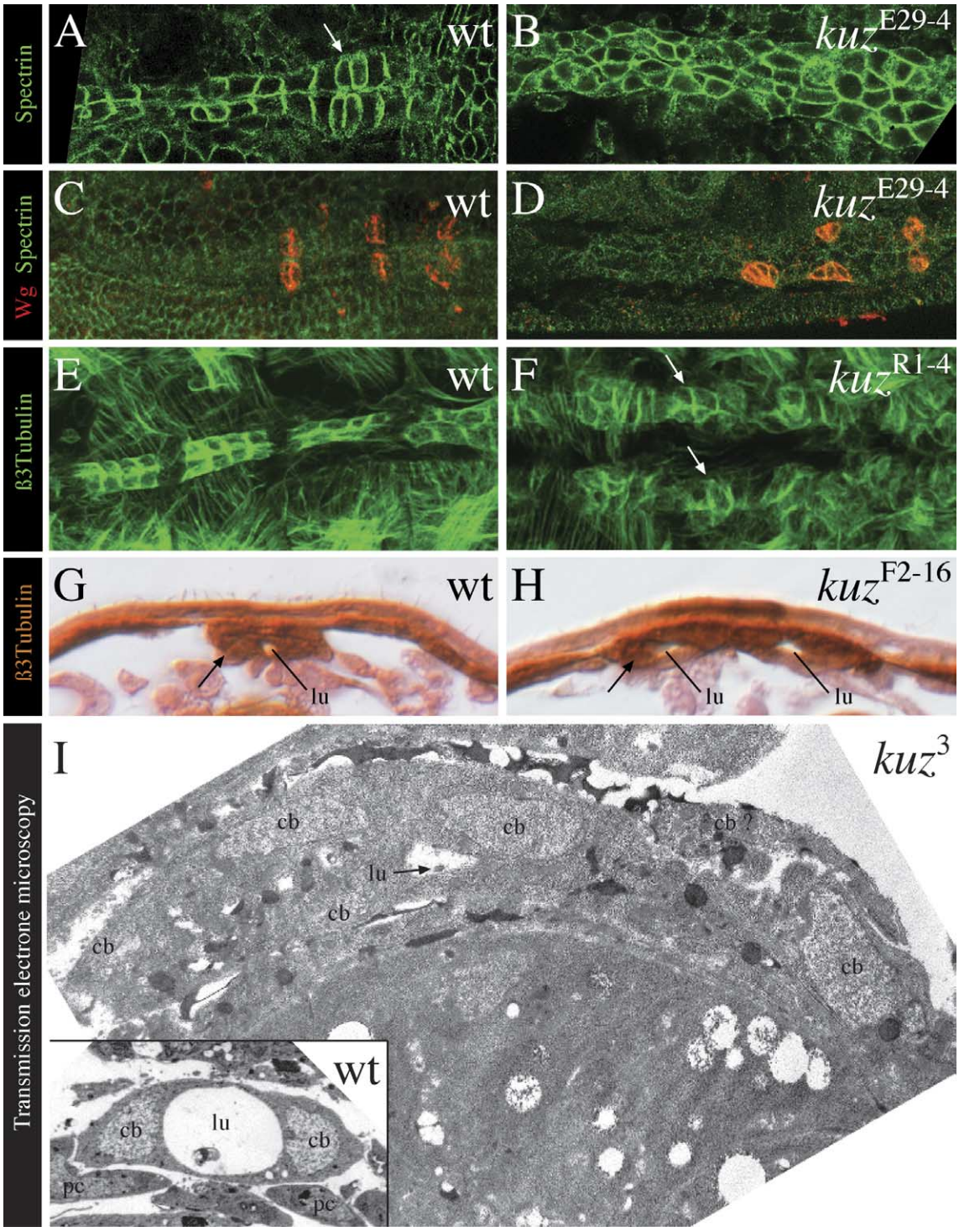

Fig. 5. Alignment of cardioblasts and cell polarity defects in *kuzbanian*. A, C, E and G show wildtype embryos, B, D, F and H *kuzbanian* mutant embryos. Alleles we used are $kuz^{29\text{-}4}$ (B), $kuz^{R1\text{-}4}$ (D and F) and $kuz^{F2\text{-}16}$ (H). Embryos in A and B are stained for α-Spectrin, which visualises cell polarity and cell morphology. In wildtype, the ostia-forming cardioblasts are visible by their characteristic shape (arrow in A). *kuzbanian* embryos at a similar stage of development complete dorsal closure (B). Cardioblasts from contralaterally located cardiac tissue on both sides of the embryo meet each other at the dorsal midline and form a broad compact band of cardioblasts. We do not observe cells that adopt the typical morphology of the ostia-forming cardioblasts (arrow in A), indicating that final cell differentiation seems to be blocked, although the typical markers for ostia-forming cardioblasts are expressed (compare with Fig. 3). Embryos in (C) and (D) are stained for Wingless and α-Spectrin. Wingless is expressed in three double pairs of ostia-forming cells within the heart proper and labels the surface of the cells. In *kuzbanian* mutant embryos (D), cell number and cell morphology is aberrant, compared to wildtype (C). Note that one cluster of Wg-expressing cells is out of focus in (D). Embryos in (E) and (F) are stained for β3tubulin. (F) shows a *kuzbanian* embryo slightly before dorsal closure. Occasionally, properly aligned and pair-wise orientated assemblies of cardioblasts appear on both sides of the embryo (arrow in F). This situation resembles the appearance of the final heart at late stage wildtype embryos (E). (G) and (H) show cross-sections through an abdominal segment (A5 or A6, respectively), of a wildtype (G) or a $kuz^{F2\text{-}16}$ (H) embryo. Prior to section, embryos were stained for β3tubulin (brown color) and selected under a dissecting microscope. Sections were counterstained with eosin (red). The cardioblasts are

neurogenesis, myogenesis, angiogenesis, fertilisation and others (reviewed in, e.g. Blobel, 2000; Primakoff and Myles, 2000), and they are involved in the shedding of various membrane bound proteins, including growth factors and cell adhesion molecules (examples are given in White et al., 2001; Moss and Lambert, 2002; Seals and Courtneidge, 2003; White, 2003; Blobel, 2005; Reiß et al., 2005). For the majority of ADAMs, the substrates are not known and due to the widespread functions many aspects of their biological role are poorly understood.

3.1. ADAMs are crucial for cardiogenesis

Studies on the function of ADAMs in vertebrates indicate that some of the members of the gene family are involved in cardiac development. Mice, lacking functional ADAM19, exhibit severe defects in cardiac morphogenesis, e.g. ventral septal defects, abnormal formation of the aortic and pulmonic valves and abnormalities of the cardiac vasculature (Zhou et al., 2004). Recently, it was shown that TACE (ADAM17) is essential for cardiac valvulogenesis in mice, likely by its sheddase function on EGFR (Jackson et al., 2003). Interestingly, mice lacking a functional TACE die at birth with an enlarged fetal heart with increased myocardial trabeculation and reduced cell compaction, mimicking the pathological changes of noncompaction of ventricular myocardium. In addition, larger cardiomyocyte cell size and increased cell proliferation were reported in ventricles of the TACE knockout mouse hearts (Shi et al., 2003). Cardiac restricted overexpression of a non-cleavable, transmembrane TNF/tumor necrosis factor, a major substrate of TACE, in mice provokes a hypertrophic cardiac phenotype (Dibbs et al., 2003).

Although it is clear that some mammalian ADAMs are crucial for heart development (Horiuchi et al., 2005), a role for ADAM metalloproteases during *Drosophila* heart formation was not reported so far. Here, we have provided multiple lines of evidence that the metalloprotease Kuzbanian/ADAM10 is crucial for cardiogenesis in flies. Screening a collection of mutagenized *Drosophila* lines for displaying heart phenotypes and the subsequent analysis of selected alleles revealed that mutations in the *kuzbanian* genes cause a hyperplasic heart.

3.2. A potential role for Kuzbanian in heart cell specification

One of the best-studied Kuzbanian functions on the molecular level is the activation of the Notch receptor. The Notch receptor is processed throughout three proteolytic steps, likely two in *Drosophila* (Kidd and Lieber, 2002). First, mediated by a furin-like convertase, Notch is cleaved in its extracellular domain. The two halves of the Notch molecules form an intramolecular heterodimer. Interaction with a ligand induces the second cleavage event mediated by a disintegrin metalloprotease (ADAM17/TACE in vertebrates, Kuzbanian/ADAM10 in *Drosophila*), generating a Notch extracellular truncation. Finally, Notch is processed by a *y*-secretase complex to release an active intracellular Notch fragment that translocates to the nucleus (reviewed, e.g. in Lai, 2002). Genetic and molecular experiments have shown that Notch is a major substrate of Kuzbanian in *Drosophila* (Rooke et al., 1996; Pan and Rubin, 1997; Sotillos et al., 1997; Kidd and Lieber, 2002; Klein, 2002; Lieber et al., 2002), but likely not the only one (Qi et al., 1999; Mishra-Gorur et al., 2002; Yan et al., 2002).

Loss of Kuzbanian function and subsequently abrogation of Notch signalling explains the heart phenotype of *kuzbanian* mutant embryos. Notch activity was found between 6 and 10 h of development in the dorsal mesoderm, from which the cardioblasts, the pericardial cells, and the lymph glands arise. During this time, Notch-dependant lateral inhibition is responsible for selecting cardiac precursors within the dorsal mesoderm. Hartenstein and colleagues have shown that elimination of Notch during the first half of this period, using a temperature-sensitive Notch mutant, results in substantially more cardioblasts, pericardial cells and lymph gland progenitors. Reducing Notch function between 8 and 10 h causes an excess of cardioblasts and a concomitant loss of pericardial cells, reflecting a crucial function of Notch for cell fate specification (Hartenstein et al., 1992; Mandal et al., 2004). In embryos carrying a deficiency for Notch ($Df(1)N^{81K1}$), the number of heart cells is strongly increased, pericardial cells are missing, and cardioblasts fail to assemble into a regular tube (Hartenstein et al., 1992), reflecting a combined effect on cell number and cell fate (Mandal et al., 2004). Park and coworkers investigated the role of Notch for a particular subset of pericardial cells, the EPCs. Mutants lacking the maternal and zygotic Notch revealed initially enlarged clusters of EPC progenitors (late stage 11), while EPCs fail to form later on (Park et al., 1998). This finding is consistent with our observation, where panmesodermal driven KuzDN causes a loss of Even-skipped expressing pericardial cells at later stages, a phenotype, which we also found in embryos mutant for *mastermind*, a downstream effector of Notch signalling (see Section 2). Hypertrophy of cardioblasts was also reported by Tian et al., who used $N^{ts\text{-}1}/Df(1)N^{81K1}$ embryos (Tian et al., 2004), but in this case the number of pericardial cells (Zfh1-expressing cells) was reported as being normal. These studies have shown that Notch is required in the dorsal mesoderm (stage 11 to 12) to regulate the initial commitment of cells to the cardioblasts and pericardial cell fate, but also to regulate the choice between the cardioblast and pericardial fate. In addition, Han and coworkers propose a biphasic recruitment of Notch signalling in heart development (Han and Bodmer, 2003). First, Notch is needed during lateral inhibition for selecting heart precursors in a field of equally competent cells within the

clearly visible (arrows in G and H). In *kuzbanian* embryos (H) lumen-like structures appear (marked as 'lu' in G and H), indicating, that cardioblasts in *kuzbanian* are able to bend, to adopt a bean-like morphology and to form lumen-like structures. (I) shows a TEM micrograph of a transverse section of a kuz^3 mutant embryo at about 50% egg length. The inset shows a wildtype embryo. Cardioblast-like cells (cb) are increased in number and form an irregular cluster. The formation of a lumen-like structure (lu) is indicated. Cb, cardioblast; pc, pericardial cell; lu, lumen.

dorsal mesoderm, which essentially covers the function of Notch described above. Second, Notch is involved in asymmetric cell division giving rise to specific heart progenitors. The second requirement of Notch is restricted to those heart cells that arise from asymmetric cell division (Ward and Skeath, 2000; Alvarez et al., 2003; Han and Bodmer, 2003), in conjunction with additional components of the asymmetric cell division machinery, including Sanpodo, Numb and Inscuteable (Park et al., 1998; Su et al., 1999; Ward and Skeath, 2000; Alvarez et al., 2003; Han and Bodmer, 2003; Popichenko and Paululat, 2004).

Previous reports have shown that the Notch receptor is a main substrate of Kuzbanian (Rooke et al., 1996; Pan and Rubin, 1997; Sotillos et al., 1997; Lieber et al., 2002). Proteolytic cleavage of the membrane anchored Notch receptor is interrupted in the absence of Kuzbanian, which finally results in inactivation of Notch signalling (Pan and Rubin, 1997; Lieber et al., 2002). Thus, the observed heart phenotype of the identified EMS-induced *kuzbanian* alleles is caused by interruption of Notch signalling in the cardiac primordium, respectively. Therefore, a similar phenotype of *kuzbanian*, *mastermind* and *Notch* mutant embryos is expected. Indeed, the five *kuzbanian* and the three *mastermind* EMS alleles identified in our screen for heart mutants as well as the previously described *kuzbanian* alleles kuz^{3} and $kuz^{29\text{-}4}$ exhibit cardiac malformations resembling particular aspects of cardiac defects described for Notch mutants. The phenotypes are not completely identical, which can be explained by the maternal product that masks most of the very early recruitments of Kuzbanian. Indeed, Rooke and colleagues have shown that embryos lacking any maternally derived Kuzbanian product and contain no zygotic copies of *kuzbanian* have a early neurogenic phenotype, which is even more severe than strong Notch phenotypes (Rooke et al., 1996). Therefore, we assume that the zygotic *kuzbanian* mutants reflect a later requirement of Kuzbanian, manifested in the cardiac mesoderm when the maternal product is diminished in this tissue. The cardiac mesoderm develops as cardioblasts to the expense of pericardial cells (and lymph gland cells) in *kuzbanian* mutant embryos. We postulate that Kuzbanian plays a dual role during cardiogenesis, first for the selection of cardiac progenitors during Notch dependent lateral inhibition and second for cell fate specification during Notch dependent asymmetric cell division. This explains the strong excess of all subtypes of heart cells and the significant loss of pericardial cells. The excess of cardioblasts firstly arises, because in the absence of Notch dependent lateral inhibition too many progenitors are selected within the dorsal mesoderm. This phenotype is further enhanced in later development when remaining pericardial cells (those that arise from the asymmetric lineage) are transformed into cardioblasts as a consequence of an abrogated Notch dependent asymmetric cell division. This explains why the hyperplasia of the heart is more prominent in segments A2–A8 than in T3 to A1, because the anterior cardioblasts arise from symmetric cell divisions only (Ward and Skeath, 2000; Alvarez et al., 2003; Han and Bodmer, 2003). If conversion of the pericardial cell fate into the cardioblast cell fate takes place, it occurs in the posterior heart lineage, resulting in a stronger hyperplasia in this heart region as seen in *kuzbanian* mutant embryos.

Our model predicts that Kuzbanian is essential for heart development by effecting Notch signalling, which is further supported by the fact, that we retrieved another key component of Notch signalling from our screen, based on a nearly identical phenotype. We found three alleles of the *mastermind* gene, which encodes a downstream effector of the Notch signalling pathway. Mastermind was previously isolated in various screens as a modifier of Notch signalling and acts on the molecular level via a direct interaction to the ankyrin repeats of the intracellular form of Notch (Wu et al., 2000; Giraldez et al., 2002; Hall et al., 2004). As in *kuzbanian*, we observe in *mastermind* mutant alleles a strong excess of cardioblasts and a reduced number of pericardial cells (Table 1, see also Hartenstein et al., 1992).

Interestingly, mutations in another component of Notch signalling pathway reveals a slightly different phenotype. *liquid facets*, which encodes a *Drosophila* Epsin orthologue, is reported to be responsible for endocytosis and trafficking of the Notch ligand Delta in the signalling cell. *Liquid facets* homozygous embryos reveal a hyperplasic heart, but a normal number of pericardial cells. The excess of cardioblasts in *liquid facets* arises due to a preferential expansion of the *tinman* expressing subtype of cardioblasts (which arise from symmetric cell division), whereas the number of *seven-up* expressing cardioblasts (which arise from asymmetric cell division) is normal. Moreover, the additional cardioblasts presumably develop at the expense of fusion competent myoblasts from the dorsal mesoderm (Tian et al., 2004). In contrast, *kuzbanian* mutant embryos show an increased number of *seven-up* expressing cardioblast, although the overall excess of cardioblasts is, similar to the findings in *liquid facets* mutants, preferentially due to the expansion of the *tinman* expressing cardioblasts (see Table1, Fig. 3). One explanation is that Kuzbanian is required for the selection of both cardioblast cell types, whereas Liquid facets is not. Additionally, the maternal contribution of Kuzbanian present in *kuzbanian* mutant embryos might be sufficient for the selection of the correct number of the Seven-up (Svp) progenitors, but not for the symmetrically derived Tinman cardioblast progenitors. Shortly later, absence of Kuzbanian then affects the Notch dependent asymmetric cell division in the Seven-up lineage, resulting in a moderately increased number of Seven-up cardioblasts. This hypothesis is confirmed by our observation of a maximum of four Svp cells per hemisegment in the *kuzbanian* mutant background (Figs. 3B,D and 5D), fully explainable by an effect on asymmetric cell division in this cell lineage (Park et al., 1998; Ward and Skeath, 2000; Alvarez et al., 2003; Han and Bodmer, 2003; Popichenko and Paululat, 2004). It should also be mentioned that Liquid facets is reported to be critical for endocytosis and trafficking of Delta in the signalling cells, whereas Kuzbanian is crucial not only for proteolytic processing of Notch, but presumably also for processing Delta as well. As for *kuzbanian*, maternal contribution of *liquid facets* likely masks some requirements

of this molecule and hampers a direct comparison of the zygotic phenotypes (Tian et al., 2004).

3.3. Heart morphogenesis in kuzbanian

Morphogenesis of cardiac cells is not very well understood so far. After specification, cardioblasts align bilaterally along the a–p axis and migrate together with the overlaying ectoderm towards the dorsal midline. During this process, all cardioblasts become flattened, polarised cells (Rugendorff et al., 1994; Chartier et al., 2002). Rugendorff and colleagues found that the heart lumen is formed when the trailing edges of the cardioblasts of either side bend around and contact each other at the dorsalmost position (Rugendorff et al., 1994). Recently, a growing number of genes controlling morphogenesis of cardioblasts was identified. Among these, cell adhesion molecules play a pivotal role during the alignment of cardioblasts (faint sausage), adhesion of opposing cardioblasts and lumen formation (E-cadherin), and maintenance of the normal heart morphology at late embryonic stages (laminin A) (Haag et al., 1999). For the alignment and migration of cardioblasts towards the dorsal midline, the Toll receptor act as a critical cell adhesion component (Wang et al., 2005). The *Drosophila* type IV collagen-like protein Pericardin is a crucial factor for the alignment of cardioblasts and the formation of an organised heart epithelium (Chartier et al., 2002). The polarity of cardioblasts is a prerequisite to form the organised heart tube. Recently, it was shown that the T-box transcription factor neuromancer (Nmr1/H15 and Nmr2/Midline) is required for establishing the polarity of heart cells, most likely by regulating genes that are responsible for the transition of an unpolarised cardioblast progenitor into a flattened polarised cardioblast (Miskolczi-McCallum et al., 2005; Qian et al., 2005a; Reim et al., 2005). A number of studies have shown that Kuzbanian/ADAM10 plays a role in cell–cell communication and cell adhesion. For example, ADAM10 binds Ephrin2A, a protein with a role in neuronal repulsion (Hattori et al., 2000), is necessary for shedding EGFR ligands (Sahin et al., 2004) and is involved in cleavage of N-cadherin and regulation of cell–cell adhesion (Reiß et al., 2005). In *Drosophila*, Kuzbanian mediates the transactivation of EGF receptor as shown by *in vivo* studies (Yan et al., 2002). Recently, Wang and coworkers found that Kuzbanian is also important for border cell migration in the *Drosophila* ovary (Wang et al., 2006).

We found that in *kuzbanian* mutant embryos initial heart cell differentiation takes place. This includes the specification of different subtypes of heart cell, as shown by the use of specific molecular markers, the alignment of cardioblasts on both sides of the heart primordium and the initiation of heart beating. In late embryos (stage 16/17), we observe an abnormal morphology of cardioblasts, an uncoordinated arrangement of ostia-forming cardioblasts and, instead of a single heart lumen, additional lumen-like structures. These findings point to the possibility that Kuzbanian might have a function for final heart cell morphogenesis, e.g. by processing substrates other then Notch. Schimmelpfeng and collegues provided evidences that Kuzbanian is involved in the repulsive guidance system in the CNS and interacts genetically with Slit (Schimmelpfeng et al., 2001). Interestingly, the Slit/Robo signalling pathway plays a pivotal role in polarity and morphogenesis control of cardioblasts as well (Qian et al., 2005b), pointing to the possibility that one of these molecules might be a substrate for Kuzbanian. This would explain the heart cell morphogenesis phenotypes seen in *kuzbanian* mutant embryos. In embryos that express a dominant negative Kuzbanian form driven late in the heart cardioblast morphogenesis is not significantly affected. This indicates that the drivers we used so far are inappropriate to separate different functions of Kuzbanian. Furthermore, we cannot exclude that the induction of morphogenetic processes requires the Kuzbanian-dependant Notch signalling pathway quite early. This would hamper significantly the separation of Kuzbanian functions using various driver lines and the dominant negative Kuzbanian form. Nevertheless, it remains to be clarified if the described effects on heart cell morphology are primarily due to the absence of Kuzbanian function or occur as a secondary consequence of hyperplasia.

In this paper, we have shown that Kuzbanian (ADAM10) plays an essential role in heart development. Members of the ADAM gene family in vertebrates are also known to be critical for cardiogenesis. Interestingly, mice lacking ADAM17 exhibit a cardioblast proliferation phenotype as well, besides other defects, indicating a conserved function of ADAM proteins in heart development. Here, we discuss a model for Kuzbanian function in Notch signalling, which can fully explain the observed phenotype in mutant embryos. We assume that Kuzbanian might have additional functions, e.g. as a sheddase on unknown substrates in the cardiac mesoderm, which has to be proven in future studies.

4. Experimental procedures

4.1. Drosophila strains

Oregon R was the wild type used. *kuz*^{3}, *kuz*$^{e29\text{-}4}$, *kuz*^{1403}, UAS-KuzDN, Df(2R)CX1, Df(2R)BSC18, *mam*^{8}, 24B-Gal4 and CyO-ActGFP were obtained from Bloomington Stock Center. *svp*-lacZ is an enhancer trap insert in the *seven-up* gene (Mlodzik et al., 1990). *hand*-GFP is a reporter line made in our laboratory (Sellin et al., 2006). The collection of EMS-induced mutant alleles was generated in the laboratory of Christian Klämbt, Münster, Germany (Hummel et al., 1999a,b). Gene misexpression was achieved with the UAS-Gal4 system using the following driver lines: *twi*-Gal4 (from Michelson), *tin*-cΔ4-Gal4 (from Frasch) and *hand*-Gal4 (our laboratory).

4.2. Immunocytochemistry of whole-mount embryos

Processing and immunostaining of whole-mount embryos for β-galactosidase was done following standard protocols, using the Vectastain Elite ABC Kit (Vector). A monoclonal anti-β-galactosidase primary antibody (Promega-Z378A) was used at a 1:2000 dilution. As primary antibodies we used anti-β3Tubulin at 1:1500 (Leiss et al., 1988), anti-Mef2 at 1:500 (Bour et al., 1995), anti-Eve at 1:3000 (Frasch and Levine, 1987), anti-Tin at 1: 500 (Bodmer, 1993), anti-Zfh1 at 1:1500 (Lai et al., 1991), anti-Odd at 1:500 (Ward and Coulter, 2000), anti-Mab3 at 1:5 (Yarnitzky and Volk, 1995) and anti-Lbe at 1:30 (Jagla et al., 1997). Mouse anti α-Spectrin (1:5) and mouse anti-Wg (1:4, TSA amplification kit) was from Hybridoma Bank, University of Iowa. Rabbit anti-GFP and mouse anti-GFP was obtained from Abcam (ab6556) and Invitrogen. All secondary antibodies were used at 1:200 (Dianova).

4.3. Complementation tests

We identified eight EMS-induced embryonic lethals exhibiting a cardiac hypertrophy phenotype. They fall into two complementation groups, which were further characterized. The first group includes the three EMS-alleles J1-202, J2-202 and S2-29. A systematic complementation analysis with S2-29 and deficiencies for the second chromosome reveals, that S2-29 fails to complement the deficiencies Df(2R)CX1 with breakpoints at 49C1-4 and 50C23-D1 and Df(2R)BSC18 with breakpoints at 50D1 and 50D2-7. Both deficiencies remove the *mastermind* gene. We found that S2-29 is allelic to a characterized *mam* allele (mam^8); therefore we concluded that the newly identified heart mutants J1-202, J2-202 and S2-29 belong to the same complementation group and represent new *mam* alleles. The second complementation group includes the five EMS-alleles F2-16, J2-11, P2-108, R1-4 and S5-65. These EMS-mutant lines were identified as being *kuzbanian*-alleles (Schimmelpfeng et al., 2001). As expected, a complementation analysis of the five EMS alleles and two *kuzbanian* alleles generated independently, kuz^3 and $kuz^{29\text{-}4}$ (Rooke et al., 1996), showed, that all lines are allelic to each other.

4.4. Identification of kuzbanian mutants

kuzbanian (*kuz*) mutants were identified by sequence analysis. Genomic DNA from heterozygous and/or selected homozygous flies was prepared, and sequence analysis was carried out. Point mutations in the *kuzbanian* gene were identified from double peaks in the sequencing trace, and this was subsequently confirmed by cloning into the TOPO vector (Invitrogen) followed by further sequence analysis. These sequences showed single peaks in the sequencing trace, corresponding to either mutant or wild-type DNA. We detect a single point mutation at a splice-donor-site in the 4th intron in the R1-4 allele. To further proof the existence of this mutation, we amplified a cDNA from R1-4 RNA that contains the expected unspliced 68 bp intron. The amplicon was cloned and sequenced and a point mutation was detected at the predicted position.

4.5. Histological analysis of kuzbanian mutant embryos

Embryos were stained with anti-β3Tubulin antibody (made in rabbits) at 1:1000 and kept in PBS buffer. Stage 16 to 17 *kuzbanian* mutant and wildtype embryos were individually selected under a dissecting microscope. The embryos were transferred into an Eppendorf cup and PBS was stepwise replaced by liquid 0.8% agarose at 50 °C (agarose in PBS). After cooling down to room temperature and hardening, the agarose pieces were dehydrated through a graded series of ethanol (each incubation took 15 min) into 100% ethanol, repeating the last step three times. Afterwards the agarose pieces were washed two times with Technovit 8100 (Kulzer, Germany). Finally, the embryos were incubated overnight in Technovit 8100.The agarose pieces were trimmed and used for embedding in Technovit 8100, following the manufacture's protocol with a few modifications. Sections of 4 μm each were performed on a crank microtome (Leitz, Wetzlar, Germany) and collected on microscopic slides coated with poly-L-lysin (Sigma, Germany). After drying overnight at 37 °C, sections were counterstained with 1% eosin in aqua dest. (Romeis, 1968) and mounted in DPX (Fluka, Germany).

4.6. Electron microscopy

Embryos were dechorionated, fixed in 12.5% glutaraldehyde in PBS and heptane for 20 min, then placed on double-side tape and devitellinised by hand. Embryos were further prepared for transmission electron microscopy as described (Hartenstein, 1988; Rugendorff et al., 1994). The allele we used was kuz^3.

Acknowledgements

We are especially grateful to Christian Klämbt and the members of his lab for the opportunity to screen the EMS mutants generated in his lab. We thank the Bloomington Stock Center, R. Bodmer, M. Frasch, K. Jagla, Z.C. Lai, A. Michelson, M. Mlodzik, H.T. Nguyen, R. Renkawitz-Pohl, J. Skeath, M. Taylor and T. Volk for sharing antibodies and fly stocks. This work was supported by the Deutsche Forschungsgemeinschaft to A.P. (PA517/10-1) and the SFB 431: Membrane proteins—Functional dynamics and coupling to cellular networks.

References

Alvarez, A.D., Shi, W., Wilson, B.A., Skeath, J.B., 2003. *pannier* and *pointedP2* act sequentially to regulate *Drosophila* heart development. Development 130, 3015–3026.

Azpiazu, N., Frasch, M., 1993. *tinman* and *bagpipe*: two homeo box genes that determine cell fates in the dorsal mesoderm of *Drosophila*. Genes & Development 7, 1325–1340.

Becherer, J.D., Blobel, C.P., 2003. Biochemical properties and functions of membrane-anchored metalloprotease-disintegrin proteins (ADAMs). Current Topics in Developmental Biology 54, 101–123.

Blobel, C.P., 2000. Remarkable roles of proteolysis on and beyond the cell surface. Current Opinion in Cell Biology 12, 606–612.

Blobel, C.P., 2005. ADAMs: key components in EGFR signalling and development. Nature Reviews/Molecular Cell Biology 6, 32–43.

Bodmer, R., 1993. The gene *tinman* is required for specification of the heart and visceral muscles in *Drosophila*.. Development 118, 719–729.

Bodmer, R., Venkatesh, T.V., 1998. Heart development in *Drosophila* and vertebrates: conservation of molecular mechanisms. Developmental Genetics 22, 181–186.

Bodmer, R., Frasch, M., 1999. Genetic determination of *Drosophila* heart development. In: Harvey, R.P., Rosenthal, N. (Eds.), Heart development. Academic Press, San Diego, pp. 65–90.

Bour, B.A., O'Brien, M.A., Lockwood, W.L., Goldstein, E.S., Bodmer, R., Taghert, P.H., et al., 1995. *Drosophila* MEF2, a transcription factor that is essential for myogenesis. Genes & Development 9, 730–741.

Brand, T., 2003. Heart development: molecular insights into cardiac specification and early morphogenesis. Developmental Biology 258, 1–19.

Buff, E., Carmena, A., Gisselbrecht, S., Jiménez, F., Michelson, A.M., 1998. Signalling by the *Drosophila* epidermal growth factor receptor is required for the specification and diversification of embryonic muscle progenitors. Development 125, 2075–2086.

Burchard, S., Paululat, A., Hinz, U., Renkawitz-Pohl, R., 1995. The mutant *not enough muscles* (*nem*) reveals reduction of the *Drosophila* embryonic muscle pattern. Journal of Cell Science 108, 1443–1454.

Buttgereit, D., Paululat, A., Renkawitz-Pohl, R., 1996. Muscle development and attachment to the epidermis is accompanied by expression of ß3 and ß1 tubulin isotypes, respectively. International Journal of Developmental Biology 40, 189–196.

Carmena, A., Murugasu-Oei, B., Menon, D., Jimenez, F., Chia, W., 1998. *inscuteable* and *numb* mediate asymmetric muscle progenitor cell divisions during *Drosophila* myogenesis. Genes & Development 12, 304–315.

Carmena, A., Buff, E., Halfon, M.S., Gisselbrecht, S., Jimenez, F., Baylies, M.K., Michelson, A.M., 2002. Reciprocal regulatory interactions between the Notch and Ras signalling pathways in the *Drosophila* embryonic mesoderm. Developmental Biology 244, 226–242.

Chartier, A., Zaffran, S., Astier, M., Semeriva, M., Gratecos, D., 2002. Pericardin, a *Drosophila* type IV collagen-like protein is involved in the morphogenesis and maintenance of the heart epithelium during dorsal ectoderm closure. Development 129, 3241–3253.

Cripps, R.M., Olson, E.N., 2002. Control of cardiac development by an evolutionarily conserved transcriptional network. Developmental Biology 246, 14–28.

Damm, C., Wolk, A., Buttgereit, D., Löher, K., Wagner, E., Lilly, B., et al., 1998. Independent regulatory elements in the upstream region of the *Drosophila ß3 tubulin* gene (*ß3Tub60D*) guide expression in the dorsal vessel and the somatic muscles. Developmental Biology 199, 138–149.

Dibbs, Z.I., Diwan, A., Nemoto, S., DeFreitas, G., Abdellatif, M., Carabello, B.A., et al., 2003. Targeted overexpression of transmembrane tumor necrosis factor provokes a concentric cardiac hypertrophic phenotype. Circulation 108, 1002–1008.

Dulcis, D., Levine, R.B., 2003. Innervation of the heart of the adult fruit fly, *Drosophila melanogaster*. Journal of Comparative Neurology 465, 560–578.

Fambrough, D., Pan, D., Rubin, G.M., Goodman, C.S., 1996. The cell surface metalloprotease/disintegrin Kuzbanian is required for axonal extension in *Drosophila*. Proceedings of the National Academy of Sciences (USA) 93, 13233–13238.

Frasch, M., 1995. Induction of visceral and cardiac mesoderm by ectodermal Dpp in the early *Drosophila* embryo. Nature 374, 464–467.

Frasch, M., Levine, M., 1987. Complementary patterns of *even-skipped* and *fushi tarazu* expression involve their differential regulation by a common set of segmentation genes in *Drosophila*. Genes & Development 1, 981–995.

Fremion, F., Astier, M., Zaffran, S., Guillen, A., Homburger, V., Semeriva, M., 1999. The heterotrimeric protein Go is required for the formation of heart epithelium in *Drosophila*. Journal of Cell Biology 145, 1063–1076.

Gajewski, K., Fossett, N., Molkentin, J.D., Schulz, R.A., 1999. The zinc finger proteins Pannier and GATA4 function as cardiogenic factors in *Drosophila*. Development 126, 5679–5688.

Gajewski, K., Zhang, Q., Choi, C.Y., Fossett, N., Dang, A., Kim, Y.H., et al., 2001. Pannier is a transcriptional target and partner of Tinman during *Drosophila* cardiogenesis. Developmental Biology 233, 425–436.

Giraldez, A.J., Perez, L., Cohen, S.M., 2002. A naturally occurring alternative product of the *mastermind* locus that represses Notch signalling. Mechanisms of Development 115, 101–105.

Haag, T.A., Haag, N.P., Lekven, A.C., Hartenstein, V., 1999. The role of cell adhesion molecules in *Drosophila* heart morphogenesis: *faint sausage*, *shotgun*/*D*E-cadherin, and *laminin A* are required for discrete stages in heart development. Developmental Biology 208, 56–69.

Hall, L.E., Alexander, S.J., Chang, M., Woodling, N.S., Yedvobnick, B., 2004. An EP overexpression screen for genetic modifiers of Notch pathway function in *Drosophila melanogaster*. Genetical Research 83, 71–82.

Han, Z., Bodmer, R., 2003. Myogenic cells fates are antagonized by notch only in asymmetric lineages of the *Drosophila* heart, with or without cell division. Development 130, 3039–3051.

Han, Z., Olson, E.N., 2005. Hand is a direct target of tinman and GATA factors during *Drosophila* cardiogenesis and hematopoiesis. Development 132, 3525–3536.

Han, Z., Fujioka, M., Su, M., Liu, M., Jaynes, J.B., Bodmer, R., 2002. Transcriptional integration of competence modulated by mutual repression generates cell-type specificity within the cardiogenic mesoderm. Developmental Biology 252, 225–240.

Hartenstein, V., 1988. Development of *Drosophila* larval sensory organs in spatiotemporal pattern of sensory neurones, peripheral axonal pathways and sensilla differentiation. Development 102, 869–886.

Hartenstein, A.Y., Rugendorff, A., Tepass, U., Hartenstein, V., 1992. The function of the neurogenic genes during epithelial development in the *Drosophila* embryo. Development 116, 1203–1220.

Hattori, M., Osterfield, M., Flanagan, J.G., 2000. Regulated cleavage of a contact-mediated axon repellent. Science 289, 1360–1365.

Horiuchi, K., Zhou, H.M., Kelly, K., Manova, K., Blobel, C.P., 2005. Evaluation of the contributions of ADAMs 9, 12, 15, 17, and 19 to heart development and ectodomain shedding of neuregulins ß1 and ß2. Developmental Biology 283, 459–471.

Hummel, T., Schimmelpfeng, K., Klämbt, C., 1999a. Commissure formation in the embryonic CNS of *Drosophila*. Developmental Biology 209, 381–398.

Hummel, T., Schimmelpfeng, K., Klämbt, C., 1999b. Commissure formation in the embryonic CNS of *Drosophila*. Development 126, 771–779.

Jackson, L.F., Qiu, T.H., Sunnarborg, S.W., Chang, A., Zhang, C., Patterson, C., Lee, D.C., 2003. Defective valvulogenesis in HB-EGF and TACE-null mice is associated with aberrant BMP signaling. EMBO Journal 22, 2704–2716.

Jagla, K., Frasch, M., Jagla, T., Dretzen, G., Bellard, F., Bellard, M., 1997. *ladybird*, a new component of the cardiogenic pathway in *Drosophila* required for diversification of heart precursors. Development 124, 3471–3479.

Jagla, T., Bidet, Y., Da Ponte, J.P., Dastugue, B., Jagla, K., 2002. Cross-repressive interactions of identity genes are essential for proper specification of cardiac and muscular fates in *Drosophila*. Development 129, 1037–1047.

Jensen, P.V., 1973. Structure and metamorphosis of the larval heart of *calliphora erythrocephala*. Biologiske skrifter/Kongelige Danske Videnskabernes Selskab 20, 2–19.

Jung, S.H., Evans, C.J., Uemura, C., Banerjee, U., 2005. The *Drosophila* lymph gland as a developmental model of hematopoiesis. Development 132; 2521–2533.

Kidd, S., Lieber, T., 2002. Furin cleavage is not a requirement for *Drosophila* Notch function. Mechanisms of Development 115, 41–51.

Klein, T., 2002. *kuzbanian* is required cell autonomously during Notch signalling in the *Drosophila* wing. Development Genes and Evolution 212, 251–255.

Klinedinst, S.L., Bodmer, R., 2003. Gata factor Pannier is required to establish competence for heart progenitor formation. Development 130, 3027–3038.

Kölsch, V., Paululat, A., 2002. The highly conserved cardiogenic bHLH factor Hand is specifically expressed in circular visceral muscle progenitor cells and in all cell types of the dorsal vessel during *Drosophila* embryogenesis. Development Genes and Evolution 212, 473–485.

Kremser, T., Gajewski, K., Schulz, R.A., Renkawitz-Pohl, R., 1999. Tinman regulates the transcription of the ß3 *tubulin* gene (*ßTub60D*) in the dorsal vessel of *Drosophila*. Developmental Biology 216, 327–339.

Lai, E.C., 2002. Notch cleavage: Nicastrin helps Presenilin make the final cut. Current Biology 12, R200–R202.

Lai, Z.C., Fortini, M.E., Rubin, G.M., 1991. The embryonic expression patterns of *zfh-1* and *zfh-2*, two *Drosophila* genes encoding novel zinc-finger homeodomain proteins. Mechanisms of Development 34, 123–134.

Lai, Z.C., Rushton, E., Bate, M., Rubin, G.M., 1993. Loss of function of the *Drosophila zfh-1* gene results in abnormal development of mesodermally derived tissues. Proceedings of the National Academy of Sciences (USA) 90, 4122–4126.

Leiss, D., Hinz, U., Gasch, A., Mertz, R., Renkawitz-Pohl, R., 1988. ß3-*tubulin* expression characterizes the differentiating mesodermal germ layer during *Drosophila* embryogenesis. Development 104, 525–531.

Lieber, T., Kidd, S., Young, M.W., 2002. *kuzbanian-mediated* cleavage of *Drosophila* Notch. Genes & Development 16, 209–221.

Lilly, B., Galewsky, S., Firulli, A.B., Schulz, R.A., Olson, E.N., 1994. D-MEF2: a MADS box transcription factor expressed in differentiating mesoderm and muscle cell lineages during *Drosophila* embryogenesis. Proceedings of the National Academy of Sciences (USA) 91, 5662–5666.

Lo, P.C., Frasch, M., 2001. A role for the COUP-TF-related gene *seven-up* in the diversification of cardioblast identities in the dorsal vessel of *Drosophila*. Mechanisms of Development 104, 49–60.

Lo, P.C.H., Skeath, J.B., Gajewski, K., Schulz, R.A., Frasch, M., 2002. Homeotic genes autonomously specify the anteroposterior subdivision of the drosophila dorsal vessel into aorta and heart. Developmental Biology 251, 307–319.

Lockwood, W.K., Bodmer, R., 2002. The patterns of *wingless*, *decapentaplegic*, and *tinman* position the *Drosophila* heart. Mechanisms of Development 114, 13–26.

Lovato, T.L., Nguyen, T.P., Molina, M.R., Cripps, R.M., 2002. The Hox gene *abdominal-a* specifies heart cell fate in the *Drosophila* dorsal vessel. Development 129, 5019–5027.

Mandal, L., Banerjee, U., Hartenstein, V., 2004. Evidence for a fruit fly hemangioblast and similarities between lymph-gland hematopoiesis in fruit fly and mammal aorta-gonadal-mesonephros mesoderm. Nature Genetics 36, 1019–1023.

Mishra-Gorur, K., Rand, M.D., Perez-Villamil, B., Artavanis-Tsakonas, S., 2002. Down-regulation of Delta by proteolytic processing. Journal of Cell Biology 159, 313–324.

Miskolczi-McCallum, C.M., Scavetta, R.J., Svendsen, P.C., Soanes, K.H., Brook, W.J., 2005. The *Drosophila melanogaster* T-box genes *midline* and *H15* are conserved regulators of heart development. Developmental Biology 278, 459–472.

Mlodzik, M., Hiromi, Y., Weber, U., Goodman, C.S., Rubin, G.M., 1990. The *Drosophila seven-up* gene, a member of the steroid receptor gene superfamily, controls photoreceptor cell fates. Cell 60, 211–224.

Molina, M.R., Cripps, R.M., 2001. Ostia, the inflow tracts of the *Drosophila* heart, develop from a genetically distinct subset of cardial cells. Mechanisms of Development 109, 51–59.

Moore, A.W., Barbel, S., Jan, L.Y., Jan, Y.N., 2000. A genomewide survey of basic helix-loop-helix factors in *Drosophila*. Proceedings of the National Academy of Sciences (USA) 97, 10436–10441.

Moss, M.L., Lambert, M.H., 2002. Shedding of membrane proteins by ADAM family proteases. Essays in Biochemistry 38, 141–153.

Nguyen, H.T., Bodmer, R., Abmayr, S.M., McDermott, J.C., Spoerel, N.A., 1994. *D-mef2*: a *Drosophila* mesoderm-specific MADS box-containing gene with a biphasic expression profile during embryogenesis. Proceedings of the National Academy of Sciences (USA) 91, 7520–7524.

Pan, D., Rubin, G.M., 1997. Kuzbanian controls proteolytic processing of Notch and mediates lateral inhibition during *Drosophila* and vertebrate neurogenesis. Cell 90, 271–280.

Park, M., Yaich, L.E., Bodmer, R., 1998. Mesodermal cell fate decisions in *Drosophila* are under the control of the lineage genes *numb*, *Notch*, and *sanpodo*. Mechanisms of Development 75, 117–126.

Perrin, L., Monier, B., Ponzielli, R., Astier, M., Semeriva, M., 2004. *Drosophila* cardiac tube organogenesis requires multiple phases of Hox activity. Developmental Biology 272, 419–431.

Petcherski, A.G., Kimble, J., 2000. Mastermind is a putative activator for Notch. Current Biology 10, R471–R473.

Ponzielli, R., Astier, M., Chartier, A., Gallet, A., Therond, P., Semeriva, M., 2002. Heart tube patterning in *Drosophila* requires integration of axial and segmental information provided by the Bithorax Complex genes and hedgehog signaling. Development 129, 4509–4521.

Popichenko, D., Paululat, A., 2004. Cell fate decisions in the *Drosophila* dorsal vessel depend on the multiadapter protein Inscuteable. Genesis 40, 218–222.

Primakoff, P., Myles, D.G., 2000. The ADAM gene family: surface proteins with adhesion and protease activity. Trends in Genetics 16, 83–87.

Qi, H., Rand, M.D., Wu, X., Sestan, N., Wang, W., Rakic, P., Xu, T., Artavanis-Tsakonas, S., 1999. Processing of the Notch ligand Delta by the metalloprotease Kuzbanian. Science 283, 91–94.

Qian, L., Liu, J., Bodmer, R., 2005a. *Neuromancer* Tbx20-related genes (*H15/midline*) promote cell fate specification and morphogenesis of the *Drosophila* heart. Developmental Biology 279, 509–524.

Qian, L., Liu, J., Bodmer, R., 2005b. Slit and Robo control cardiac cell polarity and morphogenesis. Current Biology 15, 2271–2278.

Rau, A., Buttgereit, D., Holz, A., Fetter, R., Doberstein, S.K., Paululat, A., Staudt, N., Skeath, J., Micheslon, A.M., Renkawitz-Pohl, R., 2001. *rolling pebbles* (*rols*) is required in *Drosophila* muscle precursors for recruitment of myoblasts for fusion. Development 128, 5061–5073.

Reim, I., Frasch, M., 2005. The Dorsocross T-box genes are key components of the regulatory network controlling early cardiogenesis in *Drosophila*. Development 132, 4911–4925.

Reim, I., Lee, H.H., Frasch, M., 2003. The T-box-encoding dorsocross genes function in amnioserosa development and the patterning of the dorsolateral germ band downstream of Dpp. Development 130, 3187–3204.

Reim, I., Mohler, J.P., Frasch, M., 2005. Tbx20-related genes, *mid* and *H15*, are required for *tinman* expression, proper patterning, and normal differentiation of cardioblasts in *Drosophila*. Mechanisms of Development 122, 1056–1069.

Reiß, K., Maretzky, T., Ludwig, A., Tousseyn, T., de Strooper, B., Hartmann, D., Saftig, P., 2005. ADAM10 cleavage of N-cadherin and regulation of cell-cell adhesion and beta-catenin nuclear signalling. EMBO Journal 24, 742–752.

Rizki, T.M., 1978. The circulatory system and associated cells and tissues. In: Ashburner, M., Wright, T.R.F. (Eds.), The Genetics and Biology of Drosophila, vol. 2b. Academic Press, New York, pp. 397–452.

Romeis, B., 1968. Mikroskopische Technik. R. Oldenbourg Verlag, München, Wien, pp. 757.

Rooke, J., Pan, D., Xu, T., Rubin, G.M., 1996. KUZ, a conserved metalloprotease-disintegrin protein with two roles in *Drosophila* neurogenesis. Science 273, 1227–1231.

Rugendorff, A., Younossi-Hartenstein, A., Hartenstein, V., 1994. Embryonic origin and differentiation of the *Drosophila* heart. Roux's Archives of Developmental Biology 203, 266–280.

Ryan, K.M., Hoshizaki, D.K., Cripps, R.M., 2005. Homeotic selector genes control the patterning of *seven-up* expressing cells in the *Drosophila* dorsal vessel. Mechanisms of Development 122, 1023–1033.

Sahin, U., Weskamp, G., Kelly, K., Zhou, H.M., Higashiyama, S., Peschon, J., et al., 2004. Distinct roles for ADAM10 and ADAM17 in ectodomain shedding of six EGFR ligands. Journal of Cell Biology 164, 769–779.

Sapir, A., Assa-Kunik, E., Tsruya, R., Schejter, E., Shilo, B.Z., 2004. Unidirectional Notch signaling depends on continuous cleavage of Delta. Development 132, 123–132.

Schimmelpfeng, K., Gogel, S., Klämbt, C., 2001. The function of *leak* and *kuzbanian* during growth cone and cell migration. Mechanisms of Development 106, 25–36.

Schröter, R.H., Lier, S., Holz, A., Bogdan, S., Klämbt, C., Beck, L., Renkawitz-Pohl, R., 2004. *kette* and *blown fuse* interact genetically during the second fusion step of myogenesis in *Drosophila*. Development 131, 4109–4501.

Seals, D.F., Courtneidge, S.A., 2003. The ADAMs family of metalloproteases: multidomain proteins with multiple functions. Genes & Development 17, 7–30.

Sellin, J., Albrecht, S., Kölsch, V., Paululat, A., 2006. Dynamics of heart differentiation, visualized utilizing heart enhancer elements of the *Drosophila melanogaster* bHLH transcription factor Hand. Gene Expression Patterns 6, 360–375.

Shi, W., Chen, H., Sun, J., Buckley, S., Zhao, J., Anderson, K.D., Williams, R.G., Warburton, D., 2003. TACE is required for fetal murine cardiac development and modeling. Developmental Biology 261, 371–380.

Sorrentino, R.P., Gajewski, K.M., Schulz, R.A., 2005. GATA factors in *Drosophila* heart and blood cell development. Seminars in Cell & Developmental Biology 16, 107–116.

Sotillos, S., Roch, F., Campuzano, S., 1997. The metalloprotease-disintegrin Kuzbanian participates in *Notch* activation during growth and patterning of *Drosophila* imaginal discs. Development 124, 4769–4779.

Su, M.T., Fujioka, M., Goto, T., Bodmer, R., 1999. The *Drosophila* homeobox genes *zfh-1* and *even-skipped* are required for cardiac-specific differentiation of a *numb*-dependent lineage decision. Development 126, 3241–3251.

Taylor, M.V., Beatty, K.E., Hunter, H.K., Baylies, M.K., 1995. *Drosophila* MEF2 is regulated by *twist* and is expressed in both the primordia and differentiated cells of the embryonic somatic, visceral and heart musculature. Mechanisms of Development 50, 29–41.

Tian, X., Hansen, D., Schedl, T., Skeath, J.B., 2004. Epsin potentiates notch pathway activity in *Drosophila* and *C. elegans*. Development 131, 5807–5815.

Wang, J., Tao, Y., Reim, I., Gajewski, K., Frasch, M., Schulz, R.A., 2005. Expression, regulation, and requirement of the toll transmembrane protein during dorsal vessel formation in *Drosophila melanogaster*. Molecular and Cellular Biology 25, 4200–4210.

Wang, X., Bo, J., Bridges, T., Dugan, K.D., Pan, T.C., Chodosh, L.A., Montell, D.J., 2006. Analysis of cell migration using whole-genome expression profiling of migratory cells in the *Drosophila* ovary. Developmental Cell 10, 483–495.

Ward, E.J., Coulter, D.E., 2000. *odd-skipped* is expressed in multiple tissues during *Drosophila* embryogenesis. Mechanisms of Development 96, 233–236.

Ward, E.J., Skeath, J.B., 2000. Characterization of a novel subset of cardiac cells and their progenitors in the *Drosophila* embryo. Development 127, 4959–4969.

White, J.M., 2003. ADAMs: modulators of cell-cell and cell-matrix interactions. Current Opinion in Cell Biology 15, 598–606.

White, J.M., Bigler, D., Chen, M., Takahashi, Y., Wolfsberg, T.G., 2001. ADAMs in cell adhesion. In: Beckerle, M. (Ed.), Cell adhesion: Frontiers in Molecular Biology. Oxford University Press, Oxford, pp. 189–216.

Wu, X., Golden, K., Bodmer, R., 1995. Heart development in *Drosophila* requires the segment polarity gene wingless. Developmental Biology 169, 619–628.

Wu, L., Aster, J.C., Blacklow, S.C., Lake, R., Artavanis-Tsakonas, S., Griffin, J.D., 2000. MAML1, a human homologue of *Drosophila mastermind*, is a transcriptional co-activator for NOTCH receptors. Nature Genetics 26, 484–489.

Xu, X., Yin, Z., Hudson, J.B., Ferguson, E.L., Frasch, M., 1998. Smad proteins act in combination with synergistic and antagonistic regulators to target Dpp responses to the *Drosophila* mesoderm. Genes & Development 12, 2354–2370.

Yan, Y., Shirakabe, K., Werb, Z., 2002. The metalloprotease Kuzbanian (ADAM10) mediates the transactivation of EGF receptor by G protein-coupled receptors. Journal of Cell Biology 158, 221–226.

Yarnitzky, T., Volk, T., 1995. Laminin is required for heart, somatic muscles, and gut development in the *Drosophila* embryo. Developmental Biology 169, 609–618.

Yedvobnick, B., Kumar, A., Chaudhury, P., Opraseuth, J., Mortimer, N., Bhat, K.M., 2004. Differential effects of *Drosophila mastermind* on asymmetric cell fate specification and neuroblast formation. Genetics 166, 1281–1289.

Yin, Z., Frasch, M., 1998. Regulation and function of *tinman* during dorsal mesoderm induction and heart specification in *Drosophila*. Developmental Genetics 22, 187–200.

Zaffran, S., Frasch, M., 2002. Early signals in cardiac development. Circulation Research 91, 457–469.

Zarnescu, D.C., Thomas, G.H., 1999. Apical spectrin is essential for epithelial morphogenesis but not apicobasal polarity in *Drosophila*. Journal of Cell Biology 146, 1075–1086.

Zhou, H.M., Weskamp, G., Chesneau, V., Sahin, U., Vortkamp, A., Horiuchi, K., et al., 2004. Essential role for ADAM19 in cardiovascular morphogenesis. Molecular and Cellular Biology 24, 96–104.

The transmembrane receptor Uncoordinated 5 (Unc5) is essential for heart lumen formation in *Drosophila melanogaster*

Stefanie Albrecht[1], Benjamin Altenhein[2] and Achim Paululat[1]*

1 Universität Osnabrück, Fachbereich Biologie/Chemie - Zoologie/Entwicklungsbiologie, Barbarastraße 11, 49069 Osnabrück, Germany

2 Johannes Gutenberg Universität Mainz, Institut für Genetik, J. - J. - Becherweg 32

55099 Mainz, Germany

* Corresponding Author:
Achim Paululat
Universität Osnabrück, Fachbereich Biologie/Chemie – Zoologie/Entwicklungsbiologie,
Barbarastraße 11, 49069 Osnabrück, Germany
Phone: +49 541 969 2285
Fax: +49 541 969 2587
E-mail address: Paululat@biologie.uni-osnabrueck.de

Keywords: Drosophila heart morphogenesis, cardiogenesis, lumen formation, tubulogenesis, Unc5, NetrinB

ABSTRACT

Transport of liquids or gases in biological tubes is fundamental for many physiological processes. Our knowledge on how tubular organs are formed during organogenesis and tissue remodeling has increased dramatically during the last decade. Studies on different animal systems have helped to unravel some of the molecular mechanisms underlying tubulogenesis. Tube architecture varies dramatically in different organs and different species, ranging from tubes formed by several cells constituting the cross section, tubes formed by single cells wrapping an internal luminal space or tubes that are formed within a cell. Some tubes display branching whereas others remain linear without intersections. The modes of shaping, growing and pre-patterning a tube are also different and it is still not known, whether these diverse architectures and modes of differentiation are realized by sharing common signaling pathways or regulatory networks. However, several recent investigations provide evidence for the attractive hypothesis that the *Drosophila* cardiogenesis and heart tube formation shares many similarities with primary angiogenesis in vertebrates. Additionally, another important step to unravel the complex system of lumen formation has been the outcome of recent studies that junctional proteins, matrix components as well as proteins acting as attractant and repellent cues play a role in the formation of the *Drosophila* heart lumen. In this study we show the requirement for the repulsively active Unc5 transmembrane receptor to facilitate tubulogenesis in the dorsal vessel of *Drosophila*. Unc5 is localized in the luminal membrane compartment of cardiomyocytes and animals lacking Unc5 fail to form a heart lumen. Our findings support the idea, that Unc5 is crucial for lumen formation and thereby represents a repulsive cue acting during *Drosophila* heart tube formation.

Introduction

Circulation of hemolymph in *Drosophila* is facilitated by muscular pumps that ensure its distribution throughout the body cavity. The main circulatory organ of the fly is the tube-like heart, or dorsal vessel, which is formed by 104 cardiomyocytes accompanied by about 140 pericardial cells (for recent review see Bryantsev and Cripps (2009) and Reim and Frasch (2005). Additional muscular pumps assure circulation in long body appendages for example the so-called wing hearts are essential for wing maturation and blood circulation in wings (Reim and Frasch, 2005; Tögel et al., 2008). During the last decades, the *Drosophila* heart has been established not only as a powerful model for analyzing fundamental molecular, genetic and cellular mechanisms of organogenesis, exemplarily reviewed in Bryantsev and Cripps, (2009); Cripps and Olson (2002); Medioni et al. (2009); Monier et al. (2007); Tao and Schulz (2007); Zaffran and Frasch (2002), but also as a genetically treatable and pharmacologically relevant system for understanding human cardiac diseases (Bier and Bodmer, 2004; Ocorr et al., 2007; Taghli-Lamallem et al., 2008; Wolf et al., 2006; Wolf and Rockman, 2008). More recently tubulogenesis in the *Drosophila* heart tube has attracted scientists because lumen formation plays a fundamental role in organogenesis such as in kidney or lung differentiation in vertebrates or tracheal or salivary gland differentiation in flies. Tubular organs are made by different modes of differentiation (recently reviewed by Baer et al. (2009)) and *Drosophila* heart tube formation likely represents a new type of tubulogenesis, sharing some similarities with blood vessel formation in vertebrates (Jin et al., 2005). Potentially, studying lumen formation in the *Drosophila* heart might help to understand certain aspects of vertebrate angiogenesis.

Cardiac tube formation in *Drosophila* relies on the regulation of adhesive interactions between cardiomyocytes that originate from bilateral located cardiac primordia. Cardioblasts in each primordium interact with their neighbors to form two linear rows of cells. The pre-patterned tissues migrate towards the dorsal midline to meet their counterpart. Following

newly formed adhesive interactions cardioblasts from both primordia become attached to each other at distinct membrane domains. After joining dorsally, cardioblasts adopt a crescent-like shape that brings their ventral sides into close proximity. Sealing at the ventral side closes the tube and forms a central lumen in between the two cardioblasts (Medioni et al., 2008; Santiago-Martínez et al., 2008). The dynamic change of cell shape resulting in sealing of the ventral contact areas of the two lumen forming cells requires again the involvement of attractant signals and junctional proteins that form the adhesive structures and a regulated crosstalk between signaling and cytoskeletal rearrangements. Furthermore, the luminal wall becomes covered with an extracellular matrix, thereby cell polarity specific ECM formation and remodeling is assumed to occur in the course of cardiogenesis.

Recent work of several laboratories shed light on heart tubulogenesis and the molecular mechanisms underlying this process. Using 3D and time-lapse imaging in combination with studies on the subcellular localization of several molecular markers Medioni and colleagues were able to decipher in great detail, how cardioblasts undergo coordinated morphogenesis during lumen formation (Medioni et al., 2008). They showed that the driving force of lumen formation relies in repulsion of specific membrane domains at the luminal side of cardioblasts in conjunction with cell shape remodeling. After or during the mesenchymal-epithelial transition of cardioblasts, taking place during the migration of the heart primordium towards the dorsal midline (Fremion et al., 1999), proteins required either for cell-cell recognition, cell adhesion, junction formation or proteins required for a repulsive signal that prevents closure of the luminal areas become sub-localized into distinct cardioblast membrane compartments. At dorsal and ventral membrane regions, the so-called Junctional-domains (J-domains), in which sealing of the heart tube occurs, adhesion and junctional proteins, including DE-Cadherin, Armadillo, Discs-large, Lethal Giant Larvae and NeurexinIV, are found to be highly enriched. The membrane compartment in between, the Luminal-domain (L-domain), which encloses the lumen itself, is characterized by the presence of basal membrane matrix

proteins, including Dystroglycan and Trol/Perlecan, and the attractant/repellent proteins Slit and Robo1/2. Mutations in any of these genes result in severe heart malformations and eventually in tube formation defects (Haag et al., 1999; MacMullin and Jacobs, 2006; Medioni et al., 2008; Qian et al., 2005; Santiago-Martinez et al., 2006; Santiago-Martínez et al., 2008). Until know, two proteins were identified to be directly involved in defining and functionalizing the L-domain of differentiating cardioblasts, which are Slit and Robo1/Robo2 (MacMullin and Jacobs, 2006; Medioni et al., 2008; Qian et al., 2005; Santiago-Martinez et al., 2006; Santiago-Martínez et al., 2008). Both proteins are well known as repulsive and/or attractive signals acting in the CNS, trachea and muscles (Englund et al., 2002; Liu et al., 2006; Lundstrom et al., 2004; Simpson et al., 2000; Volohonsky et al., 2007; Wayburn and Volk, 2009). Animals in which either *slit* or *robo1/robo2* is mutated display a misalignment of cardiomyocytes and fail to form a proper heart lumen (MacMullin and Jacobs, 2006; Medioni et al., 2008; Qian et al., 2005; Santiago-Martinez et al., 2006; Santiago-Martínez et al., 2008). Slit and Robo1/Robo2 are co-expressed in the same cardiomyocytes indicating that they play a role, presumably different from those observed in other tissues, in which one cell type provides an attractant/repellant signal by releasing Slit and another cell type (displaying the Robo receptor) receives the signal and uses it for guided migration. As suggested previously, Slit predominantly may have a Robo1/2 independent adhesive function (MacMullin and Jacobs, 2006; Qian et al., 2005). Although the precise role of Slit and Robo1/2 for cardiac lumen formation remains to be fully analyzed, the involvement of attractive and/or repulsive signals in heart lumen formation is obvious.

In this report, we provide evidence that the membrane receptor Unc5 is essential for lumen formation in the *Drosophila* heart. Unc5 was originally identified by Keleman & Dickson as a repulsive Netrin receptor contributing to motor axon guidance. Netrins are expressed by cells of the CNS and muscles cells and they act on axons which display receptors of the DCC and Unc5 family. In this context, Unc5 receptors are required for repulsion of axons (Keleman

and Dickson, 2001). These findings are consistent with the observation, that homozygous *unc5* mutant animals display severe defects in motor axon guidance (Labrador et al., 2005). Recently it was shown that Netrin-mediated signaling via Frazzled or Unc5 acts cell-autonomously in glia cell migration (von Hilchen et al., 2010). We found, that *unc5* mutant embryos fail to form a proper heart lumen. Unc5 is expressed in cardiomyocytes and becomes highly enriched at the luminal membrane compartment during heart tube formation. The determination of J- and L-domains is not altered in $unc5^{8}$ mutants indicated by the correct localization of domain specific proteins like Armadillo (J-domain) or Dystroglycan (L-domain). Our findings indicate that Unc5 is required to facilitate heart lumen formation but is not directly involved in regulation or localization of other tested components at the cardiomyocyte membrane compartments. Addressing the potential Unc5 ligand involved, we furthermore show that NetrinB, which is known to be the Unc5 ligand in nerves, glia cells and muscles, is co-localized with Unc5 and can be found predominantly at the luminal side of cardiomyocytes. *Netrin* deficient embryos fail to form a heart lumen as well, indicating, that the ligand/receptor pair Unc5-Netrin is crucial to promote tubulogenesis in the *Drosophila* heart.

Material and methods

Fly stocks

White^{1118} was the wild type used. The $unc5^{8}$ allele was kindly provided by G. J. Bashaw (Philadelphia). $NetAB^{\Delta}$, $NetA^{\Delta}$ and $NetB^{\Delta}$ flies were kindly provided by B. Dickson (Vienna). Df(1)NP5, Df(2R)ED2426, shg^{2} and sli^{2} alleles were obtained from the Bloomington Stock Center. Following reporter lines were used in this study: *hand*C-GFP, generated in our laboratory using the full-length 3rd intron of the *hand* gene (Sellin et al., 2006), *odd*-lacZ (odd^{rkIII}, Rauskolb et al. (1995)) and *svp*-lacZ (Mlodzik et al., 1990). Gene mis-expression

was achieved with the UAS-Gal4 system (Brand and Perrimon, 1993) using the following lines: *mef2*-Gal4 (H. Nguyen, Erlangen), UAS-*unc5* (Labrador et al., 2005), *hemese*-Gal4, UAS-GFP (Zettervall et al., 2004), kindly provided by J. Royet (Marseille).

Immunocytochemistry and in situ hybridization

Processing and immunostaining of whole-mount embryos was done as previously described (Sellin et al., 2009). Mutant animals were identified by the absence of a lacZ or GFP balancer signal. Antibodies used in this study include monoclonal anti-ßGalactosidase at 1:1000 (Promega Z378A), rabbit anti-ßGalactosidase at 1:2000 (Cappel 55976), rabbit anti-GFP at 1:1000 (Abcam ab6556), mouse anti-GFP at 1:500 (Invitrogen), guinea pig anti-ß3Tubulin at 1:1000 (newly generated based on a previously characterized antigenic peptide sequence by Leiss et al. (1988)), rabbit anti-Myocyte enhancing factor2 at 1:500 (Bour et al., 1995), rabbit anti-Tinman at 1:500 (Bodmer, 1993) and anti-Dystroglycan at 1:200 (Deng et al., 2003). Anti-Pericardin used at 1:5 (Yarnitzky and Volk, 1995), anti-Armadillo at 1:3, anti-αSpectrin at 1:5, anti-Roundabout at 1:3 and anti-Slit at 1:5 were obtained from the Developmental Studies Hybridoma Bank, Iowa. The rabbit anti-Uncoordinated5 and rabbit anti-NetrinB Sera were used at 1:100 (Altenhein, unpublished, this report). All secondary antibodies were used at 1:200 (Dianova and Molecular Probes). *In situ*-hybridizations on whole-mount embryos were performed according to (Duan et al., 2001).

Heat fixation

All antibody staining for Uncoordinated5, Armadillo, Silt and NetrinB were performed on embryos prepared by heat fixation to improve antigen preservation (Kesper et al., 2007; Medioni et al., 2008; Miller et al., 1989). Briefly, embryos were dechorionized in 50% Chlorix, washed several times in TNX (0.7% NaCl and 0.01% Triton X-100). Afterwards embryos were placed into perforated cups and incubated 5-7 seconds in boiling buffer (68mM

NaCl + 0.04% Triton X-100), followed by recovery washes in the same buffer (ice cooled). Embryos were then transferred into Eppendorf-cups with 50:50 heptan/methanol. Shaking for 30 seconds results in devitellinization. This step was repeated ones. Afterwards embryos were washes two times in methanol each for 10 minutes, and at least two times in ethanol for at least 20 minutes. Embryos were stored in ethanol at 4°C before staining.

Generation of Unc5 and Netrin antisera

Unc5 and NetB antisera are directed against single peptides of the two *Drosophila melanogaster* protein sequences at amino acids 983-1000 (GALDPPRADERDWRLLAK) and 294-312 (NLQDNDSADAGYDEYEEPK), respectively. Synthetic peptides were coupled to Keyhole limpet hemocyanin (KLH) and injected into rabbits. Booster injections were performed every four weeks starting at day 61 after the first injection. Animals were sacrificed and sera were captured at day 195 after the first injection and affinity purified against the synthetic peptide on Protein-A-Sepharose columns. Peptide synthesis, immunization of rabbits, and antibody purification were performed by Pineda antibody service (Berlin, Germany).

Histological sections

Embryos were stained with anti-ß3Tubulin antibody and kept in PBS buffer. Stage 17 mutant and wild type embryos were individually selected under a dissecting microscope. The embryos were transferred into an Eppendorf cup and dehydrated through a graded series of ethanol (each incubation took 15 min) into 100% ethanol, repeating the last step three times. Afterwards the embryos were incubated in to 100% ethanol/propylenoxid (10 minutes) and 2 times in 100% propylenoxid (each 10 minutes). Afterwards the embryos were kept overnight in propylenoxid/Epon 3:1. Finally, the embyos were embedded in Epon 812 resin. Semi-thin cross sections of 4 µm each were performed on a Leica Ultracut UCT ultramicrotome using

histological diamond knife. Sections were stained with toluidine blue at 70 °C for 2 min. Image acquisition were performed using a Nikon Eclipse TE2000U microscope equipped with a 100x Plan Fluo objective and a Vosskühler Cool 1300 digital camera.

Electron microscopy

Embryos were prepared for TEM analysis essentially as described (Lehmacher et al., 2009; Tepass and Hartenstein, 1994) with minor modification. A detailed protocol is available upon request. After fixation the specimens were embedded in Epon 812. Ultra-thin sections (70 nm) for transmission electron microscopy were performed with a diamond knife on a Leica Ultracut UCT ultramicrotome. Sections were mounted on single slot grids, contrasted with uranyl acetate (40 min; 20 °C) and lead citrate (6 min; 20 °C) using a Leica EMstain. Specimens were investigated with a Zeiss 902 transmission electron microscope (60kV).

Live video microscopy and time lapse analysis

For monitoring heart beating activity and hemocyte streaming, 1st instar larvae with the genotype *unc5*^{8} / *unc5*^{8}; *hand*C-GFP / *hemese*-Gal4, UAS-GFP and, as control, animals with the genotype *unc5*^{8} / CyO, *kr*-GFP ; *hand*C-GFP / *hemese*-Gal4, UAS-GFP were selected and glued with their ventral side on a microscopic slide (slides were prepared in advance using stripes of double-sided adhesive tape). The slide was placed into a closed chamber containing filter paper impregnated with a few drops of an anesthetic (50% triethylamin, 50% ethanol). Successfully anesthetized larvae showed no locomotion activity and muscle contractions (usually after 30-90 seconds). The anesthetized larvae were covered with Voltalef oil S10. After placing spacers at both sides of the larvae, the animal was covered with a coverslip. For capturing heart beating and hemocyte movements we used a Zeiss Axioplan 2 Imaging microscope equipped with a Hamamatsu C9100 digital camera, controlled by Zeiss Axiovision software. We used a 20x planapochromatic objective (Zeiss) for imaging.

Results

Unc5 was first identified by Keleman & Dickson as a repulsive Netrin receptor important for motorneuron guidance (Keleman and Dickson, 2001). During embryogenesis, *unc5* expression was predominantly found in peripheral and exit glia and in individual motoneurons during stage 14-17. The authors noticed an embryonic *unc5* expression in the cardiac primordium and later in the differentiation heart (Keleman and Dickson, 2001), but a potential role of Unc5 in cardiogenesis was not described.

Expression of Unc5 in the dorsal vessel

We reexamined the cardiac expression of *unc5* using RNA antisense probes to visualize the mRNA and a newly derived Unc5 specific antiserum to stain for the protein. *Unc5* transcripts are first detectable in cells of the heart primordium at stage 14. During further development *unc5* mRNA accumulates in heart cells and becomes most prominent at the end of embryogenesis (Fig. 1 A inset). Double staining against *unc5* mRNA and Mef2 (Bour et al., 1995; Lilly et al., 1994; Taylor and Braude, 1995; Taylor et al., 1995), *seven up*-LacZ (Gajewski et al., 2000; Lo and Frasch, 2001; Molina and Cripps, 2001) and Tinman (Azpiazu and Frasch, 1993; Bodmer, 1993) revealed that *unc5* is expressed in all 104 cardiomyocytes of the heart (Fig. 1 A-C). The mRNA level observed in the ostia forming Tinman negative cardiomyocytes might be slightly reduced in some animals (compare Fig. 1 A to C). We also observed *unc5* expression in pericardial cells as shown by co-expression of *odd skipped*-LacZ (Ward and Coulter, 2000) and Tinman (Fig. 1 C-D). In accordance with this observation Unc5 protein accumulates in cardioblasts during heart differentiation at membranes in a polar fashion (Fig. 1 E-G). At stage 15, the Unc5 protein concentrates in the luminal membrane of the cardioblasts, while weaker signal is seen at the abluminal side (Fig. 1 E). At late stage 16/17, the Unc5 protein is localized at the luminal and abluminal side in equal amounts. Essentially no protein is found on lateral sides of cardiomyocytes. We overexpressed Unc5 in

all cardiomyocytes (*mef2>unc5*) to verify the specificity of the antiserum. Under these conditions we detect Unc5 protein at all membrane regions, including at the lateral side of the cardiomyoblast, where under wild type conditions no significant amounts of Unc5 protein can be detected (Fig. 1 H). This, and the observation that no Unc5 protein is detectable in *unc5* mutant embryos (Fig. 4 B'), demonstrates that the generated antiserum specifically detects Unc5.

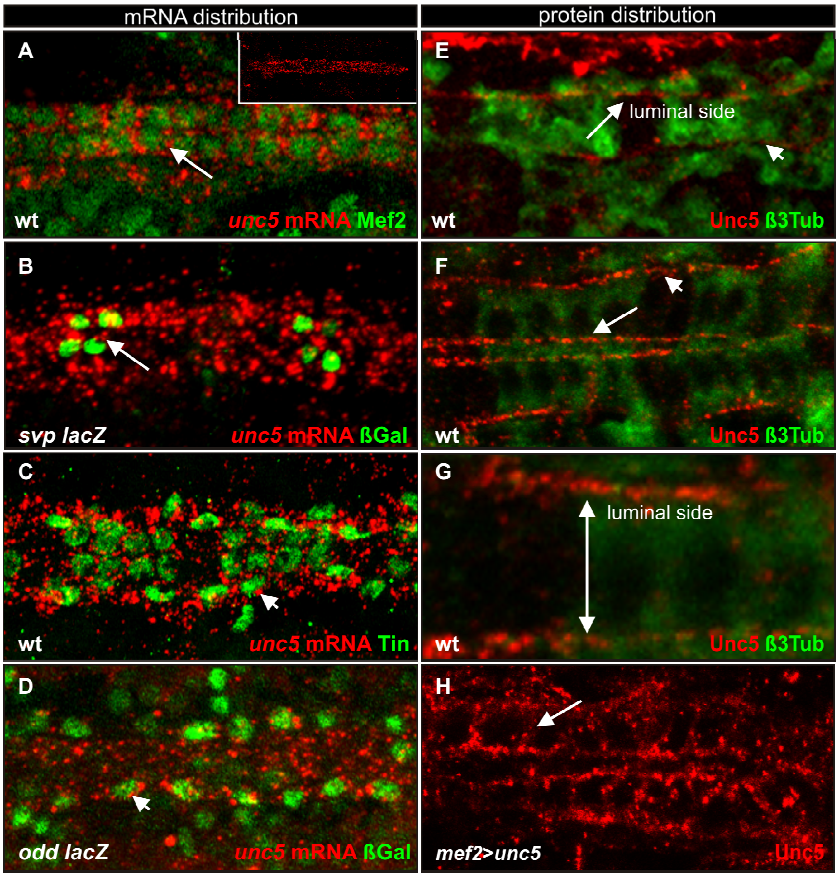

Fig. 1 Expression of *unc5* during embryogenesis and localization of Unc5 protein. (A-D) digoxigenin labeled *unc5* antisense RNA probe hybridized to late stage embryos. (A inset) Expression of *unc5* at stage 16 is highly enriched in cells constituting the dorsal vessel. Co-staining for anti-Mef2, which labels the nucleus of all cardiomyocytes (CBs) (A) and *svp*-lacZ (anti-ßGal), which marks the nucleus of the ostia forming cells (arrow) of the heart (B) reveals presence of *unc5* mRNA in the cytoplasm of all CBs. Co-staining for anti-Tinman (C) and *odd*-lacZ (anti-ßGal) (D) show expression of *unc5* in the majority of pericardial cells (PCs) (exemplarily one PC is labeled by an arrow in C and D). (E-H) Embryos were stained with an anti-Unc5 polyclonal antibody. (E) At stage 15, before CBs from the bilateral primordia meet at the dorsal midline, Unc5 is localized in a polarized fashion. CBs exhibit a strong Unc5 signal on their prospective lumen forming side (large arrow) and a slightly weaker signal at the opposite membrane region (short arrow). (F) Co-staining with anti-ß3Tubulin (expressed in four out of six CBs per hemisegment) in late stage 16 embryos, when the dorsal vessel is already formed, reveals the distinct Unc5 localization. Unc5 is predominantly enriched at the prospective luminal (large arrow) and at the opposite side (short arrow), but not at lateral positions. (G) Enlargement of F demonstrates the polarized Unc5 location. The arrow indicates the extension of the CB. (H) Anti-Unc5 antibody staining of embryos with the genotype *mef2>unc5*. Overexpression of Unc5 in CBs causes ectopic localization of Unc5 at lateral membranes (arrow). It demonstrates the specificity of the antibody (see also text).

Unc5 is essential for cardioblast alignment and heart lumen formation

To investigate the role of Unc5 in the developing heart we used the molecularly characterized EMS-induced *unc5*^{8} allele (Labrador et al., 2005). The *unc5*^{8} allele contains a nonsense mutation at position Q19 resulting in a premature stop codon at this position. *Unc5*^{8} is therefore considered as a null allele (Labrador et al., 2005).

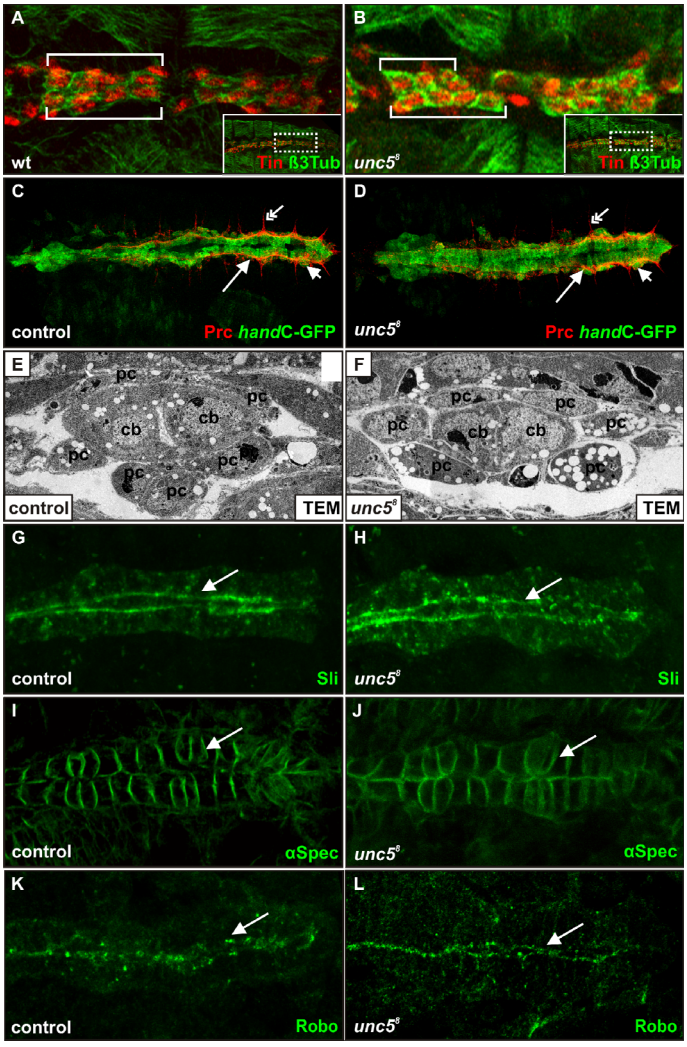

Fig. 2 *Unc5* mutants exhibit heart alignment defects but unchanged cell polarity. (A-B) Wild type (A) and *unc5* mutant embryos (B) stained for Tinman and ß3Tubulin. Insets show overviews of the enlargements (indicated by rectangles). Note, that the bilateral primordia of the dorsal vessel meet their counterpart correctly at the dorsal midline in *unc5* mutant embryos, but anterio-posterior alignment defects are visible. The brackets in A and B mark adjacent cardiomyocytes (CBs) (Tinman and ß3Tubulin positive) anterior to the pair of ostia forming cells (Tinman and ß3Tubulin negative). Note the misalignment of CBs in *unc5* mutant animals (B). The polarity of cardiomyocytes (CBs) and the attachment of adjacent pericardial cells (PCs) are not altered in *unc5* mutants. (C, D) A wild type (C) and an *unc5* mutant (D) stained for Pericardin and *hand*C-GFP (anti-GFP). The type IV collagen-like ECM protein Pericardin marks the outer surface of the heart tube, the ECM of PCs and the surface of the alary muscles. *Hand*C-GFP labels all CBs and PCs. Note, that organization and localization of the Pericardin fiber network appears to be normal (large arrows in C and D). PCs are attached to the heart tube (short arrows in D), comparable to the wild type situation (short arrows in C). Alary muscles are present and attached to the heart tube (compare double arrow in D to C). The presence and correct localization of PCs (pc) in relation to the heart forming CBs (cb) is shown in TEM sections of wild type (E) and mutant animals (F). (G-H) We exemplarily verified the localization of the polarity markers Slit, Roundabout (Robo) and αSpectrin in CBs of wild type (G, I, K) and mutant animals (H, J, L). Slit and αSpectrin are localized to the luminal and lateral (arrows) membrane compartment of CBs, both in the wild type and *unc5* mutant animals. The Robo distribution, most prominent at the luminal membrane compartment of the CBs, is unaffected in *unc5*^{8} mutants compared to wild type (K-L).

Homozygous *unc5* mutant animals show severe heart formation defects. The most prominent malformation is a shifted alignment of the two rows of cardiomyocytes that form the heart tube. The cardiomyocyte misplacement phenotype is seen in about 32% of *unc5* homozygous animals (table 1). We found, that the misalignment ranges between 1 to 3 cell dimensions along the anterior-posterior axis (Fig. 2 A-B). Neither the specification of different heart cell types nor the overall number of cardiomyocytes is affected in *unc5* mutants (table1). We also do not observe a measurable delay in the migration of the cardiac primordia towards the dorsal midline. Pericardial cells are, similar to the situation in wild type, directly associated to the heart tube (Fig. 2 C-F). Due to the polarized expression of Unc5 in heart cells we wondered if the overall cardiomyocyte polarity is affected in *unc5* mutants. Therefore we performed antibody staining against different polarity markers. Exemplarily, the guidance molecule Slit is located at the luminal and lateral side of cardiomyocytes in *unc5* mutants as well as in wild type. The localization of the Slit receptor Roundabout (Robo) at the luminal side of the cardiomyocytes is also not affected in *unc5* mutants. In addition the cytoskeletal linker protein αSpectrin, which is localized in the baso-lateral cell cortex, showed no particular mislocalization in *unc5* mutants compared to wild type (Fig. 2 G-L).

Table 1
Quantification of heart phenotypes in *unc5*^{8} mutants

	wt	***unc5*^{8}**
Cardiomyocyte alignment defects	3% (n=3/102)	32% (n=29/89)
Svp-lacZ expressing ostia cells	28 (n=10)	28 (n=10)
Tinman expressing heart cells	130 (n=10)	130 (n=10)
Lumen present (TEM)	100% (n=4/4)	0% (n=5/5)

n = numbers of embryos counted

Lethal phase analysis revealed that essentially all *unc5*^{8} homozygous mutant embryos hatch, while all 1st instar larvae fail to molt. The survival rate of animals, arrested at 1st larval stage, is about 50% at 2 days (AED) and about 8% after 4 days (AED). To visualize heart

function in living animals we introduced our *hand*C-GFP reporter into the *unc5*^{8} mutant (Sellin et al., 2006; Tögel et al., 2008). In addition we used *hemese*-driven GFP to label floating hemocytes in the hemolymph (Zettervall et al., 2004). Real time video microscopy revealed, that *unc5*^{8} mutant 1st instar larvae lack any sign of hemolymph streaming within the heart tube while the cardiomyocytes are contracting normally (Fig. 3 A, B and supplemental data). Hemocytes, which reside by chance in the neighborhood of the dorsal vessel, are not sucked into the heart, indicating, that the heart fails to establish diastolic sucking power (supplemental movie 2).

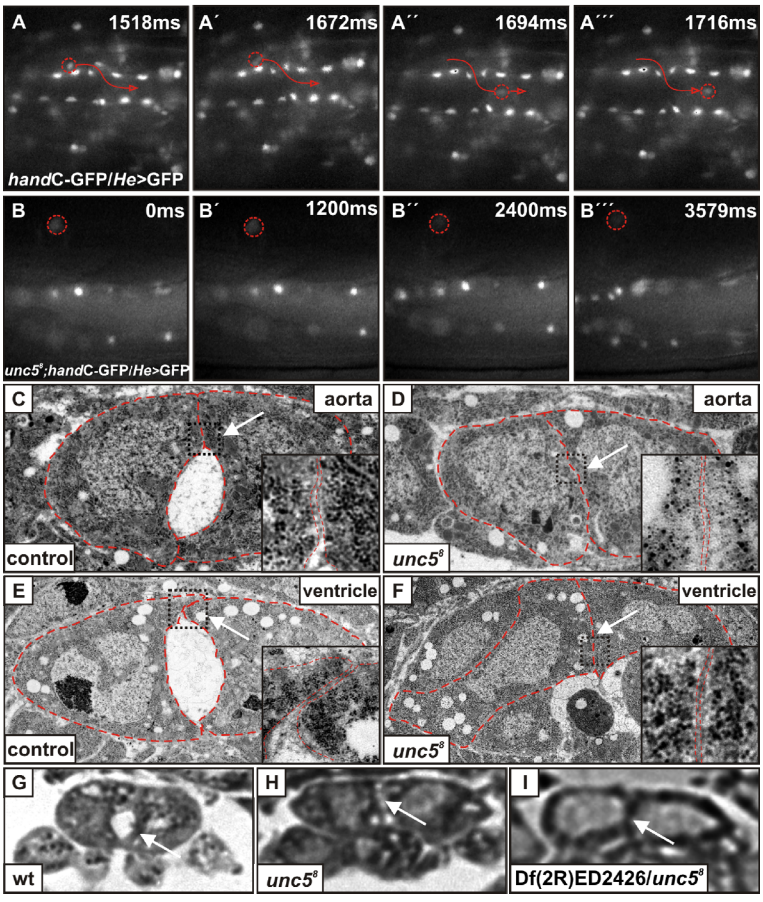

Fig. 3 Unc5 is required for heart lumen formation. (A, B) Still frames selected from two movies (available as supplemental material) to visualize loss of pumping activity of the heart of *unc5* mutant animals. (A) The relative position of a hemocyte (red circle) during heart beating activity in the wild type. Note, that the hemocyte is sucked into the heart lumen within an interval of about 20 milliseconds (one frame). (B) In contrast, there is no hemocyte movement seen in *unc5* mutant animals. The pictures in A and B were selected from videos with duration of about 1 minute. For video capturing 1st instar larvae were used. For details see the material and methods section. (C-F) Transmission electron micrographs of ultra thin sections display the dorsal vessel of wild type (C, E) and *unc5*^{8} homozygous embryos (D, F). CBs are circled by a dotted line. Arrows mark the dorsal contact zone between CBs (insets show enlargements of this membrane region). Sections through the aorta (C, D) and the ventricle region (E-F) are shown. *Unc5* mutant animals lack any sign of lumen formation. Note, that the cross section forming CBs adhere at dorsal positions. Serial sections covering two segments indicate that the lack of lumen formation is independent of cardiomyocyte alignment. (G-I) Semi-thin cross sections through the heart of wild type (G), *unc5*^{8} mutant (H) and transheterozygote Df(2R)ED2426/*unc5*^{8} embryos (I). The phenotype caused by the point mutation in the *unc5*^{8} allele (H) is mimicked in transheterozygote conditions with a deficiency covering the *unc5* gene over *unc5*^{8} (I).

Since the formation of ostia was not detailed investigated in *unc5*^{8} mutants we cannot exclude an additional contribution of ostia malformations to the observed phenotype. Overall this points to a complete loss of heart function in *unc5*^{8} mutants although the myogenic function of the cardiomyocytes is not affected. A detailed inspection of five individual *unc5* mutant embryos (stage 17) by transmission electron microscopy revealed that *unc5* mutants lack a heart lumen. Serial sectioning (70 nm per cross section) allowed us to analyze the shape and size of cardiac cells in detail. In wild type animals, from dorsal to ventral, a junctional zone is followed by the luminal zone and a second junctional region. Junctional membrane areas display zonulae adherens and the luminal area displays a characteristic luminal matrix. We found, that the cardiomyocytes in *unc5* mutants, originating from their bilateral primordia, met each other at the dorsal midline and form adherens junctions along the entire contact zone. The cardiomyocytes also lack the characteristic crescent-like shape and fail to form a morphologic distinguishable L-domain. This phenotype can be observed throughout the entire heart tube, in the aorta as well as in the ventricle region (Fig. 3 E-H). To exclude the possibility that secondary mutations interfere with the observed phenotypes, we performed semi-thin cross sections on transheterozygote embryos (*unc5*^{8} over a *unc5* lacking deficiency (Df(2R)ED2426). These embryos lack a heart lumen and display the same failure in cell shape change as seen in *unc5*^{8} mutants (Fig. 3 G-I). Interestingly, overexpression of Unc5 in all cardiomyocytes using a *mef2*-Gal4 driver does not lead to obvious heart lumen defects (supplemental Fig. S1 B). We conclude, that an increased presence of the Unc5 receptor, even at the lateral sides of the cardiomyocytes (Fig. 1 H), is not sufficient to prevent the attachment of the cardiomyocytes as it is known from overexpression of other repulsive acting receptors (Santiago-Martínez et al., 2008). The function of Unc5 appears to be restricted to the position at the luminal and abluminal side of the cardiomyoblasts and may be due to the exclusive presence of the corresponding ligand (potentially NetrinB, present study and Harris et al. (1996)).

Our data raised the question whether the failure to form a heart lumen is due to an enlarged J-domain or to an absence of repulsive signals at the luminal side of the cells.

Unc5 is localized to the L-domain of cardiomyocytes

The lumen of the heart tube is formed from the migration of two bilateral rows of polarized cardiomyocytes, which join at the dorsal midline (Fremion et al., 1999; Haag et al., 1999; Medioni et al., 2009; Rugendorff et al., 1994). Cardiomyocytes display distinct membrane sub-compartments crucial for tubulogenesis, which are the so-called L-domain (enclosing the lumen) and the adjacent J-domains (where adherens junctions seal the opposing cardiomyocytes at dorsal and ventral positions) (Medioni et al., 2008). Each domain is characterized by the accumulation of either adherens junction proteins (DE-Cadherin, Discs-Large, Armadillo in the J-domain) or proteins known to be involved in repellant/attractant mechanisms or in ECM formation (Dystroglycan, Perlecan, Slit, Robo in the L-domain) (Medioni et al., 2008; Qian et al., 2005; Santiago-Martinez et al., 2006). Mutations in *slit* or *robo1/robo2* cause severe tubulogenesis defects, essentially an absence of the heart lumen. Because *unc5* mutant animals show comparable defects in heart lumen formation, we investigated, whether Unc5 protein reveals a sub-compartmental localization in cardiomyocytes. Z view reconstruction of heart tubes, stained for the J-domain marker Armadillo and Unc5, revealed a specific localization of Unc5 in the luminal membrane domain (Fig. 4 A-A´). As expected, in $unc5^{8}$ mutants no Unc5 protein can be detected in the L-domain. Interestingly, the localization of Armadillo protein is not altered in the same animals indicating the correct establishment of the J-domains (Fig. 4 B-B´). To examine whether the establishment of the L-domain is affected in $unc5^{8}$ mutants, we performed a staining against the LamininA receptor Dystroglycan that shows a specific localization in the L-domain (Medioni et al., 2008). In $unc5^{8}$ mutants, Dystroglycan revealed a wild typic distribution in the L-domain of the cardiomyocytes (Fig. 4 C-D). The Z views display a clear

alternation of the distinct membrane domains (Fig. 4 C´-D´). From this we conclude that the molecular defined domains are established in *unc5*^{8} mutants giving evidence that Unc5 is not involved in the establishment of distinct domains within the cardiomyocyte cell membrane.

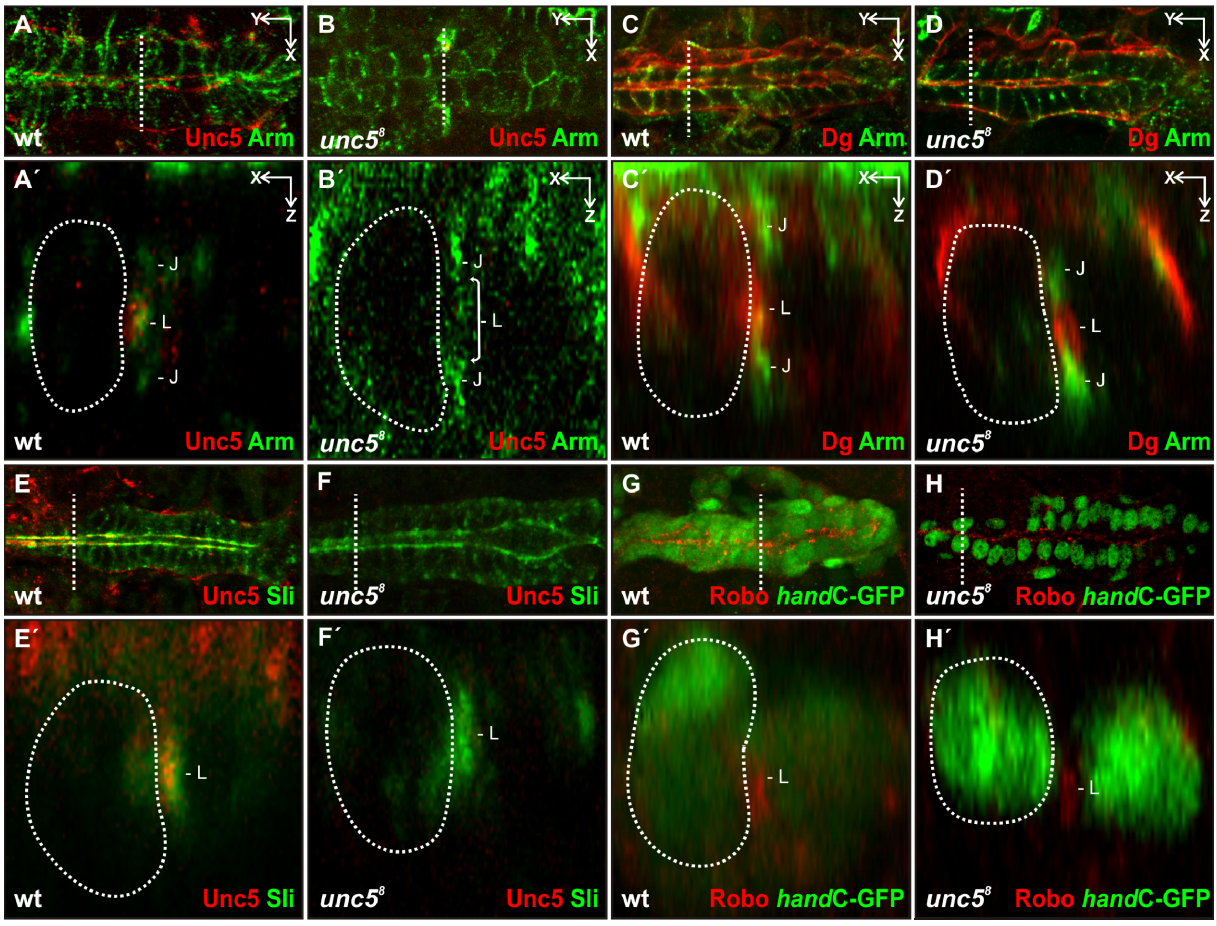

Fig. 4 Cardiac membrane domains in wild type and *unc5* mutants. On the left side late stage 16 wild type animals are shown (A, C, E, G). *Unc5* homozygotes are presented on the right side of the figure (B, D, F, H). The sectional planes of the corresponding Z views (A´-H´) are indicated by a dotted line. The cell shape of a cardiomyoblast (CB) in Z view is marked by a dotted cycle and the membrane domain regions are labeled as J for junctional or L for luminal. (A, B) In wild type, Armadillo (ß-catenin), an adherens junction marker, is localized at the luminal and lateral membranes of the CBs as well as in *unc5*^{8} mutants. (A´, B´) Z views of A & B display the localization of Armadillo at the dorsal and ventral J-domains on the luminal side of CBs. In wild type Unc5 protein can be localized to the L-domain between the two J-domains (A´). In *unc5*^{8} mutants no Unc5 protein is detectable (B´). (C, D) In wild type as in *unc5*^{8} mutants, Dystroglycan is clearly present at the luminal and abluminal side of the CBs while Armadillo is also enriched at the lateral membranes. The Z views display a restriction of Dystroglycan to the L-domain, while Armadillo is present at the attachment points between the CBs (C´, D´). (E, F) Unc5 protein can be co-localized to the luminal distribution of the soluble ligand Slit (E, E´) whereas is *unc5*^{8} mutants only Slit is accumulated at the L-domain. (F, F´). (G, H) The localization of the Robo receptor to the L-domain is unchanged in *unc5*^{8} mutants (H´) compared to wild type (G´). Due to heat fixation nuclear targeted GFP sometimes accumulate in the whole cell (G, G´).

To clarify if Unc5 acts as an independent repellent during heart lumen formation we tested the localization of the known repulsive protein Slit. In the wild type Slit and Unc5 are both localized at the luminal side of the cardiomyocytes (Fig. 4 E-E´). In the absence of Unc5 Slit is still localized at the luminal side of the cardiomyocyte membrane (Fig. 4 F-F´). An additional analysis of the distribution of the Slit receptor Robo in wild type and *unc5*^{8} mutant hearts revealed a wild typic localization of Robo to the L-domain in *unc5*^{8} mutants (compare Fig. 4 G-G´ to 4 H-H´). In agreement with this, animals transheterozygous for *unc5* and *slit* (*unc5/slit*) form a proper heart lumen (compare supplemental Fig. S1 A to C). From these data we conclude, that the heart lumen defect seen in unc5 is not caused by the mislocalization of known tubulogenesis components (like Slit and Robo) and points to alternative or at least additional functions of Unc5 in heart lumen formation independent of the Robo/Slit pathway.

The questions aroused, whether the capacity of Unc5 to promote proper heart lumen formation is linked to the described involvement of DE-Cadherin/Shotgun (Shg) in lumen formation. DE-Cadherin/Shg is controlled via the Slit/Robo pathway to enable proper cell adhesion at the J-domains (Santiago-Martínez et al., 2008). In order to clarify the influence of Unc5 on the DE-Cadherin function we looked at semi-thin cross sections of *unc5*/*shg* transheterozygote embryos. Since in all observed embryos the cardiomyocytes enclose a wild typic luminal space (compare supplemental Fig. S1 A to D) we conclude a different requirement for Unc5 in establishing a correct heart lumen than acting in collaboration with the detailed described Slit/Robo pathway.

The Unc5 ligand Netrin is essential for heart tube formation

Unc5 is known to act as a repulsive receptor for both Netrins (NetrinA & NetrinB) present in *Drosophila melanogaster* (Bashaw and Goodman, 1999; Brankatschk and Dickson, 2006; Gong et al., 1999; Harris et al., 1996; Keleman and Dickson, 2001; Labrador et al., 2005;

Mitchell et al., 1996; von Hilchen et al., 2010). Therefore we were interested to know, whether Netrins play a role in heart tubulogenesis as well.

In situ hybridization experiments using several antisense probes raised against *netrinA* and *netrinB* revealed mRNA expression in the nervous system, the early mesoderm and in a distinct pattern in the dorsal ectoderm (data not shown). However, no *netrinA* or *netrinB in situ* signal could be observed in the heart. In contrast, a detailed analysis of the protein distribution using a NetrinB specific antibody revealed that NetB is localized in a polar fashion with the highest concentration at the lumen forming side of cardiomyocytes (Fig. 5 A). A view in Z direction clearly shows an accumulation of NetB protein at the luminal side while Armadillo localizes at both J-domains (Fig. 5 A inset). As expected, the used antiserum gave no specific staining signal applied on embryos carrying a deletion for *netrin*A and *B* (compare Fig 5 B-C).

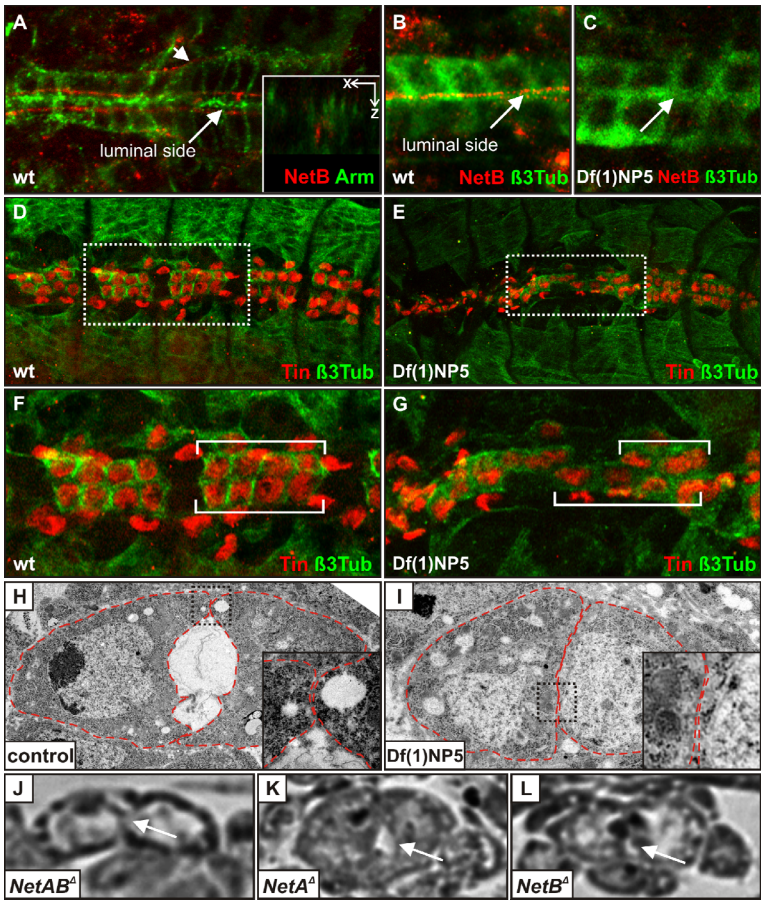

Fig. 5 Netrin is required for heart lumen formation. (A, B, D, F) Show wild type and *netrin* deficient embryos (C, E, G) stained for heart cell markers. (A) Wild type stage 16 embryo stained with an anti-NetrinB specific antibody reveals protein localization in a polarized fashion. NetrinB accumulates at the luminal and abluminal side of cardiomyocytes (CBs), while Armadillo is also present lateral at the CBs. A view in the Z direction displays the localization of NetrinB at the L-domain and Armadillo at the junctional membrane domain of a CB (inset). (B, C) Cardiac specific NetrinB staining is absent in embryos carrying a deletion for *netrinA* and *netrinB* (compare B to C). (D-G) Wild typic and *netrin* deficient embryos stained for Tinman and ß3Tubulin. F is an enlargement of D (rectangle), G an enlargement of E (rectangle). *Netrin* deficient embryos (E, G) reveal CB alignment defects. The brackets in F label four Tinman expressing CBs. The brackets

in G indicate the same positions; note the misalignment and shifting of CBs. (H, I) TEM analysis of ultra thin sectioned hearts from *netrin* deficient embryos (I) reveals an lack of lumen formation compared to wild type (H). Shown are sections in the posterior region (heart chamber) of the dorsal vessel. CBs are circled by a dotted line. Insets show the dorsal contact region (rectangles) of cardiomyocytes at higher magnification. (J-L) Semi-thin cross sections through the heart of *NetAB*$^{\Delta}$ (J) and NetrinB mutant embryos (L) reveal a failure to form a proper heart lumen. Embryos lacking NetrinA display a clear luminal space between their cardiomyocytes (K).

These *netrin* deficient embryos fail to form a proper heart lumen (Fig. 5 D-I). Staining for the heart specific marker ß3Tubulin revealed a misalignment of cardiomyocytes similar to the phenotype visible in *unc5*^{8} mutants (compare Fig. 5 G to Fig. 2 B). TEM analysis of *netrin* deficient embryos displayed an absence of the luminal space between the cardiomyocytes which becomes manifested in all three analyzed individuals (Fig. 5 H-I). To elucidate whether NetrinA and NetrinB display different functions in heart lumen formation, we analyzed semi-thin cross sections of embryos lacking either NetrinA (*Net*A$^{\Delta}$) or NetrinB (*Net*B$^{\Delta}$) in comparison to embryos lacking both genes (*Net*AB$^{\Delta}$) (Brankatschk and Dickson, 2006). We found, that the *netrin* deficient embryos Df(1)NP5, the molecular defined double mutant *Net*AB$^{\Delta}$ and the NetrinB specific allele *Net*B$^{\Delta}$ fail to form a proper heart lumen, whereas NetrinA mutants (*Net*A$^{\Delta}$) display a clear luminal space (Fig. 5 I-L).

The observed phenotypes and the NetrinB localization to the L-domain of cardiomyocytes is consistent with the findings of a previous analysis from Harris and colleagues who found NetrinB accumulation in cardiac cells at late stage 16/17 embryos as well (Harris et al., 1996). Based on the high similarity of the phenotypes observed for *netrinB* deficient embryos and *unc5*^{8} mutant animals, we believe that NetrinB might be a potential ligand for Unc5 in heart cells, similar to the situation in the nervous system. The absence of *netrinB* transcripts in heart cells points to the possibility that *netrinB* mRNA is expressed by a so far unknown non-cardiac cell type and regulates the activity of the Unc5 receptor as a paracrine ligand, since the NetB protein can be co-localized to the cardiomyocytes.

Discussion

The cross section of the *Drosophila* heart tube is constituted by opposing cardiomyocytes that cover the periphery of an inner luminal space (Fig. 3 C, E and Rugendorff et al. (1994)). At the dorsal and ventral side of two facing cardiomyocytes, adherens junctions seal the lumen. Work of several laboratories recently raised evidence, that the secreted extracellular matrix component Slit and its receptor Robo1/2, are specifically co-expressed at the luminal side of cardiomyocytes and provide essential cues for the process of heart lumen formation (MacMullin and Jacobs, 2006; Medioni et al., 2008; Qian et al., 2005; Santiago-Martinez et al., 2006; Santiago-Martínez et al., 2008).

In the present study we demonstrate that the *Drosophila* single-pass transmembrane receptor Unc5, together with its ligand Netrin, ensures heart lumen formation. Unc5 represents the single *Drosophila* homologue of a conserved receptor family, exhibiting an extracellular domain consisting of two Ig domains (both of which are essential for Netrin binding as shown for the C. elegans and the human Unc5 orthologue) (Geisbrecht et al., 2003; Kruger et al., 2004) and two thrombospondin type I (TSP) repeats. The Ig domains of Unc5 share homology with the first two Ig domains of Robo, which are critical for binding its ligand Slit (Liu et al., 2004). As shown by Kruger and colleagues, the binding properties of the Unc5 Ig domains are specific, and Netrin binding therefore is unique to Unc5 (Kruger et al., 2004). Conserved motifs found within the intracellular domain of Unc5 are a ZU5 motif, a DB motif and a carboxy-terminal death domain. The three vertebrate Unc5 orthologs and the single known C. elegans orthologue exhibit a similar organization.

Expression of Unc5 and Netrin in cardiomyocytes

Expression of Unc5 and NetrinB in the heart has been described (Harris et al., 1996; Keleman and Dickson, 2001) but not connected to cardiogenesis. We therefore analyzed in which cells that constitute the *Drosophila* heart, Unc5 and NetrinB are expressed. Transcripts

of *unc5*, Unc5 protein and NetrinB protein were found in all cardiomyocytes forming the cardiac tube (Fig. 1+5). Because no *netrinB* mRNA can be detected in heart cells, the hypothesis arises that NetrinB is synthesized by non-cardiac cells and transported actively or passively to its target site as a soluble protein. Since all other proteins, known to be involved in heart lumen formation (for example Slit, Robo, Dg, Arm, DE-Cadherin), are expressed as autocrine factors by cardiac cells themselves, the Unc5/NetB system likely represents a new mode of tube size regulation during *Drosophila* cardiogenesis (Medioni et al., 2008; Santiago-Martínez et al., 2008). Both proteins accumulate in a polar fashion at the luminal surface of the cardiomyocytes. From stage 15 onwards, when the two bilateral cardiac primordia migrate towards the dorsal midline, Unc5 and NetrinB appear to be exclusively enriched at the prospective luminal and the abluminal side. Transverse Z views of cardiac tubes, stained for Unc5 and specific polarity markers revealed a highly enriched localization of Unc5 in the luminal compartment of cardiomyocyte membranes. Unc5 is excluded from the junctional domains that are responsible for sealing the lumen of the heart. The same distribution is seen for NetrinB. Unc5 and NetrinB are clearly co-localized in the same cells and in the same membrane compartment. This observation argues for a cell autonomous function of the proteins Unc5 and NetrinB.

Unc5 function in the heart

The most prominent cardiac defect seen in homozygous *unc5* or *netrin* mutant animals is the lack of a heart lumen. Additionally, we found frequently defects in the alignment of cardiomyocytes along the anterio-posterior axis. In contrast to mutants of the Slit/Robo pathway, we never observed defects that can be clearly attributed to early adhesion functions or a potential role of Unc5 for specifying the polarity of the cells (MacMullin and Jacobs, 2006). Therefore we interpret the defects seen in *unc5* mutants as being specific for a late role in tubulogenesis rather than for a more general role in cell adhesion. This assumption is

supported by the presence of a dorsal adherens zone between cardiomyocytes that demonstrates that a loss of Unc5 neither does prevent the migration of cardioblasts from the cardiac primordium towards the midline nor the initial recognition and adhesion of cardioblasts at the dorsal midline. The unchanged cell shape of the cardiomyoblasts in *unc5* mutants and in *netrin* deficient embryos however point to an affected remodeling process of the cytoskeleton which normally occurs during the process of lumen formation (as summary Fig. 6). But since downstream factors of the Netrin/Unc5 signaling cascade in *Drosophila* are yet not known this issue has to be further analyzed in the future. Data focusing on Slit and Robo suggests that components regulating actin dynamics (like Enabled) may be effectors of this system during lumen formation (Santiago-Martínez et al., 2008). Work of Colavita & Culotti on potential interactors of the Unc5/Netrin pathway in *C. elegans* indicates that the Enabled homolog in worms Unc-34 can function as a suppressor of ectopic Unc-5 during pioneer axon guidance (Colavita and Culotti, 1998). These observations recommend a closer inspection on the actin filament formation and actin distribution in *unc5* mutants as well as an analysis of altered heart lumen formation in mutants of different cytoskeletal components or their regulators.

The overall polarity of the cardiomyocytes is not affected by the loss of Unc5 (Fig. 2) even the highly specific sub-compartmental organization of the contact sides of the contralateral cardiomyocytes is correctly determined in *unc5* mutants (Fig. 4). Staining of *unc5* mutant animals for junctional and luminal markers revealed that neither the localization of polarity markers nor the specification of the prospective J- and the L-domain is changed by the loss of Unc5 function.

Our findings suggest that Unc5 is specifically required for lumen formation and the necessary processes of cell shape change rather than for general adhesion properties of the cardiomyocytes.

Potential role for Unc5 for tubulogenesis

Lumen formation by cell assembly, as in the *Drosophila* heart, is mechanistically different from tubulogenesis in other tubular organs in which the luminal space is generated by budding, cell hollowing or wrapping (Baer et al., 2009; Bryant and Mostov, 2008) and literature cited therein. Slit and Robo1/2 are considered as being key components that define a luminal membrane compartment in cardiomyocytes and restrict the domains of junctional proteins that mediate the sealing of the heart tube (Medioni et al., 2008; Santiago-Martínez et al., 2008). Our findings indicate that the Unc5/Netrin receptor-ligand system acts at the matrix compartment of cardiomyocytes and promotes lumen formation.

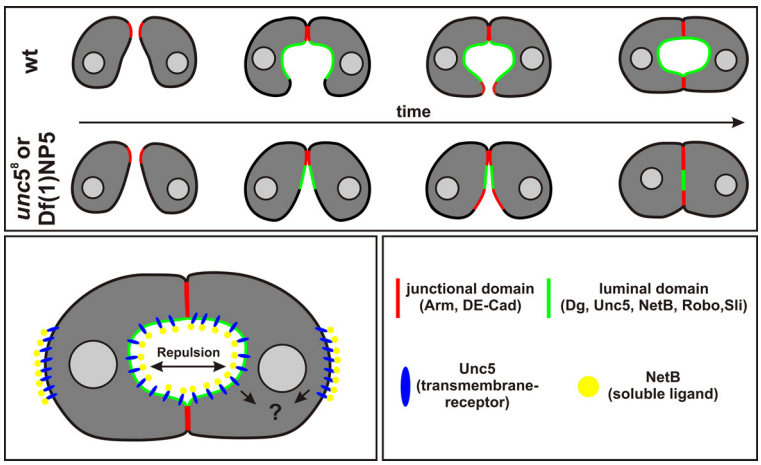

Fig. 6 Cardiac lumen formation in *Drosophila* embryos. During migration towards the dorsal midline the cardiomyocytes (CBs) adopt a triangular shape and display a dorsal future contact zone (in red; upper panel). During assembly at the dorsal junction, the CBs undergo further cell shape changes and an additional specific membrane domain is defined: the L-domain (in green; upper panel) expressing receptors like Unc5, Robo and there ligands NetB and Sli. Afterwards, a second contact region, the ventral J-domain, is specified by the same expression profile as the dorsal J-domain. (in red; upper panel). At the end of heart tube formation a perfect lumen is formed when the two cardiomyocytes attach at there ventral J-domains to each other. In *unc5*^{8} mutant embryos the formation of the distinct membrane domains (in red and green) between the cardiomyocytes is not altered but changes in cell shape do not occur (mid panel). The cardiomyocytes attach to each other along there entire luminal side, without enclosing a luminal space. No lumen is formed in *unc5*^{8} mutants.

The distribution of the transmembrane receptor Unc5 in the cardiomyocytes of Drosophila can be localized to the luminal membrane domain as well as to the abluminal side of the cells facing the adjacent pericardial cells. The corresponding ligand of Unc5 seems to be NetrinB. The soluble ligand accumulates at the same regions as the Unc5 receptor, the L-domain and the abluminal side of the cardiomyocyte.

We propose Unc5/Netrin to act independent of Slit and Robo on the establishment of a luminal space between the cardiomyocytes because Slit and Robo distribution is wild typic in

unc5 mutant embryos (Fig. 2+4). It is known from the literature that a loss of components of the Slit/Robo pathway, for example Robo itself, leads to an altered localization of Slit in the cardiomyocytes (Santiago-Martínez et al., 2008). In contrast, the loss of Unc5/Netrin function does not affect the localization of any tested protein involved in lumen formation.

Our findings provide an independent proof for the lumen formation model proposed by Medioni et al. (2008) and Santiago-Martínez et al. (2008). This model postulates that cell shape changes and repulsive activities at the prospective luminal membrane area, resulting in bending of the ventral side of cardiomyocytes are the driving forces for lumen formation. The extended dorsal J-domain in cardiomyocytes of *unc5* mutant embryos, as well as the presence of adjacent luminal membrane compartments, exhibiting the characteristic matrix proteins of the cardiac luminal wall, argues strongly for this model. An alternative mechanism would be that cardiomyocytes first align throughout their entire luminal side and afterwards luminal space appears. This model is neither supported by the previous observations of Medioni et al. (2008) and Santiago-Martínez et al. (2008) nor by our findings presented herein. In summary, our data suggests the existence of a second repulsively active system present at the L-domain of cardiac cells expanding the list of key components known to be crucial for heart tubulogenesis.

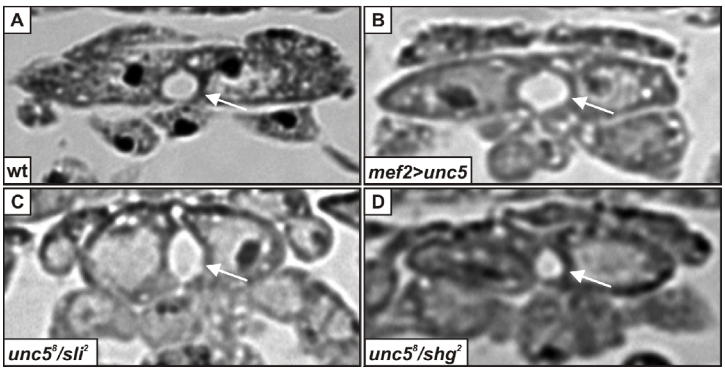

Supplemental Fig. S1 (A-D) Semi-thin cross sections of wild type hearts display a clear luminal space between the cardiomyocytes. Overexpression of Unc5 in all cardiomyocytes has no effect on lumen formation (B). Transheterozygote embryos lacking one copy of *unc5* and one copy of *slit* (C) or *shg* (D), respectively, exhibit a wild typic heart lumen.

Acknowledgements

We thank G. J. Bashaw, R. Bodmer, C. Rauskolb, H. Nguyen, M. Mlodzik, J. Royet and W.M. Deng for generous gifts of *Drosophila* stocks or antibodies, Kerstin Etzold for excellent technical assistance and Christine Lehmacher for help with the semi-thin cross sections. Part of this work was supported by grants from the DFG (SFB 431: Membrane proteins – Functional dynamics and coupling to cellular networks).

References

Azpiazu, N., Frasch, M., 1993. *tinman* and *bagpipe*: two homeo box genes that determine cell fates in the dorsal mesoderm of *Drosophila*. Genes & Development. 7**,** 1325-1340.

Baer, M. M., Chanut-Delalande, H., Affolter, M., 2009. Cellular and molecular mechanisms underlying the formation of biological tubes. Current Topics in Developmental Biology. 89**,** 137-162.

Bashaw, G. J., Goodman, C. S., 1999. Chimeric axon guidance receptors: the cytoplasmic domains of Slit and Netrin receptors specify attraction versus repulsion. Cell. 97**,** 917-926.

Bier, E., Bodmer, R., 2004. *Drosophila*, an emerging model for cardiac disease. Gene. 342**,** 1-11.

Bodmer, R., 1993. The gene *tinman* is required for specification of the heart and visceral muscles in *Drosophila*. Development. 118**,** 719-729.

Bour, B. A., O'Brien, M. A., Lockwood, W. L., Goldstein, E. S., Bodmer, R., Taghert, P. H., Abmayr, S. M., Nguyen, H. T., 1995. *Drosophila* MEF2, a transcription factor that is essential for myogenesis. Genes & Development. 9**,** 730-741.

Brand, A. H., Perrimon, N., 1993. Targeted gene expression as a means of altering cell fates and generating dominant phenotypes. Development. 118**,** 401-415.

Brankatschk, M., Dickson, B. J., 2006. Netrins guide *Drosophila* commissural axons at short range. Nature Neuroscience. 9**,** 188-194.

Bryant, D. M., Mostov, K. E., 2008. From cells to organs: building polarized tissue. Nature Reviews Molecular Cell Biology. 9**,** 887-901.

Bryantsev, A. L., Cripps, R. M., 2009. Cardiac gene regulatory networks in *Drosophila*. Biochimica et Biophysica Acta. 1789**,** 343-353.

Colavita, A., Culotti, J. G., 1998. Suppressors of ectopic UNC-5 growth cone steering identify eight genes involved in axon guidance in *Caenorhabditis elegans*. Developmental Biology. 194**,** 72-85.

Cripps, R. M., Olson, E. N., 2002. Control of cardiac development by an evolutionarily conserved transcriptional network. Developmental Biology. 246**,** 14-28.

Deng, W. M., Schneider, M., Frock, R., Castillejo-Lopez, C., Gaman, E. A., Baumgartner, S., Ruohola-Baker, H., 2003. Dystroglycan is required for polarizing the epithelial cells and the oocyte in *Drosophila*. Development. 130**,** 173-184.

Duan, H., Skeath, J. B., Nguyen, H. T., 2001. *Drosophila* Lame duck, a novel member of the Gli superfamily, acts as a key regulator of myogenesis by controlling fusion-competent myoblast development. Development. 128**,** 4489-4500.

Englund, C., Steneberg, P., Falileeva, L., Xylourgidis, N., Samakovlis, C., 2002. Attractive and repulsive functions of Slit are mediated by different receptors in the *Drosophila* trachea. Development. 129**,** 4941-4951.

Fremion, F., Astier, M., Zaffran, S., Guillen, A., Homburger, V., Sémériva, M., 1999. The heterotrimeric protein Go is required for the formation of heart epithelium in *Drosophila*. Journal of Cell Biology. 145**,** 1063-1076.

Gajewski, K., Choi, C. Y., Kim, Y., Schulz, R. A., 2000. Genetically distinct cardial cells within the *Drosophila* heart. Genesis. 28**,** 36-43.

Geisbrecht, B. V., Dowd, K. A., Barfield, R. W., Longo, P. A., Leahy, D. J., 2003. Netrin binds discrete subdomains of DCC and UNC5 and mediates interactions between DCC and heparin. Journal of Biological Chemistry. 278**,** 32561-32568.

Gong, Q., Rangarajan, R., Seeger, M., Gaul, U., 1999. The Netrin receptor Frazzled is required in the target for establishment of retinal projections in the *Drosophila* visual system. Development. 126**,** 1451-1456.

Haag, T. A., Haag, N. P., Lekven, A. C., Hartenstein, V., 1999. The role of cell adhesion molecules in *Drosophila* heart morphogenesis: *faint sausage*, *shotgun*/*D*E-cadherin, and *laminin A* are required for discrete stages in heart development. Developmental Biology. 208**,** 56-69.

Harris, R., Sabatelli, L. M., Seeger, M. A., 1996. Guidance cues at the *Drosophila* CNS midline: identification and characterization of two *Drosophila* Netrin/UNC-6 homologs. Neuron. 17**,** 217-228.

Jin, S. W., Beis, D., Mitchell, T., Chen, J. N., Stainier, D. Y., 2005. Cellular and molecular analyses of vascular tube and lumen formation in zebrafish. Development. 132**,** 5199-5209.

Keleman, K., Dickson, B. J., 2001. Short- and long-range repulsion by the *Drosophila* Unc5 netrin receptor. Neuron. 32**,** 605-617.

Kesper, D. A., Stute, C., Buttgereit, D., Kreisköther, N., Vishnu, S., Fischbach, K. F., Renkawitz-Pohl, R., 2007. Myoblast fusion in *Drosophila melanogaster* is mediated through a fusion-restricted myogenic-adhesive structure (FuRMAS). Developmental Dynamics. 236**,** 404-415.

Kruger, R. P., Lee, J., Li, W., Guan, K. L., 2004. Mapping Netrin receptor binding reveals domains of Unc5 regulating its tyrosine phosphorylation. The Journal of Neuroscience. 24**,** 10826-10834.

Labrador, J. P., O'Keefe, D., Yoshikawa, S., McKinnon, R. D., Thomas, J. B., Bashaw, G. J., 2005. The homeobox transcription factor Even-skipped regulates netrin-receptor expression to control dorsal motor-axon projections in *Drosophila*. Current Biology. 15**,** 1413-1419.

Lehmacher, C., Tögel, M., Pass, G., Paululat, A., 2009. The *Drosophila* wing hearts consist of syncytial muscle cells that resemble adult somatic muscles. Arthropod Structure & Development. 38**,** 111-23.

Leiss, D., Hinz, U., Gasch, A., Mertz, R., Renkawitz-Pohl, R., 1988. ß3-*tubulin* expression characterizes the differentiating mesodermal germ layer during *Drosophila* embryogenesis. Development. 104**,** 525-531.

Lilly, B., Galewsky, S., Firulli, A. B., Schulz, R. A., Olson, E. N., 1994. D-MEF2: a MADS box transcription factor expressed in differentiating mesoderm and muscle cell lineages during *Drosophila* embryogenesis. Proceedings of the National Academy of Sciences (USA). 91**,** 5662-5666.

Liu, D., Hou, J., Hu, X., Wang, X., Xiao, Y., Mou, Y., De Leon, H., 2006. Neuronal chemorepellent Slit2 inhibits vascular smooth muscle cell migration by suppressing small GTPase Rac1 activation. Circulation Research. 98**,** 480-489.

Liu, Z., Patel, K., Schmidt, H., Andrews, W., Pini, A., Sundaresan, V., 2004. Extracellular Ig domains 1 and 2 of Robo are important for ligand (Slit) binding. Molecular and Cellular Neuroscience. 26**,** 232-240.

Lo, P. C., Frasch, M., 2001. A role for the COUP-TF-related gene *seven-up* in the diversification of cardioblast identities in the dorsal vessel of *Drosophila*. Mechanisms of Development. 104**,** 49-60.

Lundstrom, A., Gallio, M., Englund, C., Steneberg, P., Hemphala, J., Aspenstrom, P., Keleman, K., Falileeva, L., Dickson, B. J., Samakovlis, C., 2004. Vilse, a conserved Rac/Cdc42 GAP mediating Robo repulsion in tracheal cells and axons. Genes & Development. 18**,** 2161-2171.

MacMullin, A., Jacobs, J. R., 2006. Slit coordinates cardiac morphogenesis in *Drosophila*. Developmental Biology. 293**,** 154-164.

Medioni, C., Astier, M., Zmojdzian, M., Jagla, K., Sémériva, M., 2008. Genetic control of cell morphogenesis during *Drosophila melanogaster* cardiac tube formation. Journal of Cell Biology. 182**,** 249-261.

Medioni, C., Sénatore, S., Salmand, P. A., Lalevée, N., Perrin, L., Sémériva, M., 2009. The fabulous destiny of the *Drosophila* heart. Current Opinion in Genetics & Development. 19**,** 518-525.

Miller, K. G., Field, C. M., Alberts, B. M., 1989. Actin-binding proteins from *Drosophila* embryos: a complex network of interacting proteins detected by F-actin affinity chromatography. Journal of Cell Biology. 109**,** 2963-75.

Mitchell, K. J., Doyle, J. L., Serafini, T., Kennedy, T. E., Tessier-Lavigne, M., Goodman, C. S., Dickson, B. J., 1996. Genetic analysis of *Netrin* genes in Drosophila: Netrins guide CNS commissural axons and peripheral motor axons. Neuron. 17**,** 203-215.

Mlodzik, M., Hiromi, Y., Weber, U., Goodman, C. S., Rubin, G. M., 1990. The *Drosophila seven-up* gene, a member of the steroid receptor gene superfamily, controls photoreceptor cell fates. Cell. 60**,** 211-224.

Molina, M. R., Cripps, R. M., 2001. Ostia, the inflow tracts of the *Drosophila* heart, develop from a genetically distinct subset of cardial cells. Mechanisms of Development. 109**,** 51-59.

Monier, B., Tevy, M. F., Perrin, L., Capovilla, M., Sémériva, M., 2007. Downstream of homeotic genes: In the heart of Hox function. Fly. 1**,** 59-67.

Ocorr, K., Akasaka, T., Bodmer, R., 2007. Age-related cardiac disease model of *Drosophila*. Mechanisms of Ageing and Development. 128**,** 112-116.

Qian, L., Liu, J., Bodmer, R., 2005. Slit and Robo control cardiac cell polarity and morphogenesis. Current Biology. 15**,** 2271-2278.

Rauskolb, C., Smith, K. M., Peifer, M., Wieschaus, E., 1995. extradenticle determines segmental identities throughout *Drosophila* development. Development. 121**,** 3663-73.

Reim, I., Frasch, M., 2005. The Dorsocross T-box genes are key components of the regulatory network controlling early cardiogenesis in *Drosophila*. Development. 132**,** 4911-4925.

Rugendorff, A., Younossi-Hartenstein, A., Hartenstein, V., 1994. Embryonic origin and differentiation of the *Drosophila* heart. Roux's Archives of Developmental Biology. 203**,** 266-280.

Santiago-Martinez, E., Soplop, N. H., Kramer, S. G., 2006. Lateral positioning at the dorsal midline: Slit and Roundabout receptors guide *Drosophila* heart cell migration. Proceedings of the National Academy of Sciences (USA). 103**,** 12441-12446.

Santiago-Martínez, E., Soplop, N. H., Patel, R., Kramer, S. G., 2008. Repulsion by Slit and Roundabout prevents Shotgun/E-cadherin-mediated cell adhesion during *Drosophila* heart tube lumen formation. Journal of Cell Biology. 182**,** 241-248.

Sellin, J., Albrecht, S., Kölsch, V., Paululat, A., 2006. Dynamics of heart differentiation, visualized utilizing heart enhancer elements of the *Drosophila melanogaster* bHLH transcription factor Hand. Gene Expression Patterns. 6**,** 360-375.

Sellin, J., Drechsler, M., Nguyen, H. T., Paululat, A., 2009. Antagonistic function of Lmd and Zfh1 fine tunes cell fate decisions in the Twi and Tin positive mesoderm of *Drosophila melanogaster*. Developmental Biology. 326**,** 444-455.

Simpson, J. H., Bland, K. S., Fetter, R. D., Goodman, C. S., 2000. Short-range and long-range guidance by Slit and its Robo receptors: a combinatorial code of Robo receptors controls lateral position. Cell. 103**,** 1019-1032.

Taghli-Lamallem, O., Bodmer, R., Chamberlain, J. S., Cammarato, A., 2008. Genetics and pathogenic mechanisms of cardiomyopathies in the *Drosophila* model. Drug Discovery Today: Disease Models. 5**,** 125-134.

Tao, Y., Schulz, R. A., 2007. Heart development in *Drosophila*. Seminars in Cell & Developmental Biology. 18**,** 3-15.

Taylor, A. S., Braude, P. R., 1995. Evaluation of a simple method for measuring the cellular DNA content of mouse oocytes and embryos, human fibroblasts and parthenogenetically activated human oocytes using a computerised image analysis system (Seescan). Zygote. 3**,** 85-94.

Taylor, M. V., Beatty, K. E., Hunter, H. K., Baylies, M. K., 1995. *Drosophila* MEF2 is regulated by *twist* and is expressed in both the primordia and differentiated cells of the embryonic somatic, visceral and heart musculature. Mechanisms of Development. 50**,** 29-41.

Tepass, U., Hartenstein, V., 1994. The development of cellular junctions in the *Drosophila* embryo. Developmental Biology. 161**,** 563-596.

Tögel, M., Pass, G., Paululat, A., 2008. The *Drosophila* wing hearts originate from pericardial cells and are essential for wing maturation. Developmental Biology. 318**,** 29-37.

Volohonsky, G., Edenfeld, G., Klämbt, C., Volk, T., 2007. Muscle-dependent maturation of tendon cells is induced by post-transcriptional regulation of stripeA. Development. 134**,** 347-356.

von Hilchen, C. M., Hein, I., Technau, G. M., Altenhein, B., 2010. Netrins guide migration of distinct glial cells in the *Drosophila* embryo. Development. 137**,** 1251-62.

Ward, E. J., Coulter, D. E., 2000. *odd-skipped* is expressed in multiple tissues during *Drosophila* embryogenesis. Mechanisms of Development. 96**,** 233-236.

Wayburn, B., Volk, T., 2009. LRT, a tendon-specific leucine-rich repeat protein, promotes muscle-tendon targeting through its interaction with Robo. Development. 136**,** 3607-3615.

Wolf, M. J., Amrein, H., Izatt, J. A., Choma, M. A., Reedy, M. C., Rockman, H. A., 2006. *Drosophila* as a model for the identification of genes causing adult human heart disease. Proceedings of the National Academy of Sciences (USA). 103**,** 1394-1399.

Wolf, M. J., Rockman, H. A., 2008. *Drosophila melanogaster* as a model system for the genetics of postnatal cardiac function. Drug Discovery Today: Disease Models. 5**,** 117-123.

Yarnitzky, T., Volk, T., 1995. Laminin is required for heart, somatic muscles, and gut development in the *Drosophila* embryo. Developmental Biology. 169**,** 609-618.

Zaffran, S., Frasch, M., 2002. Early signals in cardiac development. Circulation Research. 91**,** 457-469.

Zettervall, C. J., Anderl, I., Williams, M. J., Palmer, R., Kurucz, E., Ando, I., Hultmark, D., 2004. A directed screen for genes involved in *Drosophila* blood cell activation. Proceedings of the National Academy of Sciences (USA). 101**,** 14192-14197.

4. Resümee

4.1. Erstellung des *hand*C-GFP Reporters

(Sellin et al. 2006)

Drosophila melanogaster hat sich in den letzten Jahren zu einem intensiv analysierten Modellsystem entwickelt. Die sehr gute genetische Manipulierbarkeit und die Vielzahl an etablierten Untersuchungsmethoden bieten ideale Voraussetzungen zur Analyse komplexer Regulationsmechanismen. Der einfache Aufbau des Herzens als röhrenförmiges Organ ist ein weiteres Kriterium für die Auswahl von *Drosophila* als Modell zur Analyse der Organogenese des Herzens. Die Kardiogenese kann in distinkte Entwicklungsphasen unterteilt werden: Spezifizierung des kardialen Mesoderms, Determinierung der bilateral-symmetrischen Herzanlagen, Differenzierung der Kardioblasten und Bildung des Herzrohres. Während dieser Entwicklungsphasen unterliegen die Anlagen des Herzens und die daraus entstehenden Herzvorläuferzellen komplexen morphologischen Veränderungen. Um diese dynamischen Prozesse im Detail analysieren zu können bietet *Drosophila* das Potential, mit Hilfe von Reportergenkonstrukten Lebendzellmarker in den Organismus stabil zu integrieren, um so individuelle Strukturen und/oder Abläufe der Organogenese im lebenden Tier zu verfolgen.

Um die Entwicklung des Herzens vom Embryo bis zum adulten Tier detektieren zu können, wurde eine herzspezifische GFP-Reporterlinie generiert (Sellin et al., 2006, vorliegende Arbeit). Hand ist ein hoch konservierter bHLH Transkriptionsfaktor, der innerhalb der höheren Vertebraten (Maus und Mensch) als zwei paralog entstandene Gene (*ehand/Hand1* und *dhand/Hand2*) vorkommt und dort sowohl in den Herzvorläuferzellen als auch im sich differenzierenden Herz exprimiert ist (Firulli, 2003; Srivastava and Olson, 1997). Mutationen, die die *hand* Gene betreffen führen zu schweren Entwicklungsdefekten im Herz. Bei Tieren, die eine Null-Mutation im *dhand* Gen tragen unterbleibt die Bildung des gesamten rechten Herzventrikels (Srivastava and Olson, 1997). In *Drosophila* wird *hand* durch ein einziges Gen repräsentiert und zeigt eine Expression in allen Herzzellen. Damit ist Hand der bislang einzige Faktor, der in allen Herzzellen vorkommt (Kölsch and Paululat, 2002). Kürzlich konnte gezeigt werden, dass das Fehlen von Hand die Entwicklung der Lymphdrüse, die postembryonale Herzfunktion sowie Remodellierungsprozesse im Darm während der Metamorphose beeinträchtigt (Han et al., 2006; Lo et al., 2007). Trotz der prominenten Expression von *hand* in allen Herzzellen scheint Hand jedoch nicht essentiell während der

embryonalen Kardiogenese zu sein (Lo et al., 2007). Ein Fehlen von Hand führt zu keiner signifikanten Veränderung des embryonalen Herzens, das Herzrohr bildet sich wildtypisch aus (Lo et al., 2007).

Mit Hilfe des von uns etablierten *hand*C-GFP Reporters ist es möglich, von der Embryonalentwicklung beginnend, die Organogenese des Herzens zu verfolgen (Sellin et al., 2006, vorliegende Arbeit). Dabei spiegelt der *hand*C-GFP Reporter das endogene Expressionsmuster von *hand* während der Embryogenese wieder (Sellin et al., 2006). Die Detektion von GFP-Fluoreszenz im lebenden Tier bietet somit die Möglichkeit die dynamischen Prozesse der putativ passiven Progenitoren-Migration zur dorsalen Mittellinie und des Herzschlusses *in vivo* zu untersuchen (Albrecht et al., 2010 in revision; Sellin et al., 2006, vorliegende Arbeit). Durch die Aktivität des *hand*C-GFP Reporters über die embryonalen Stadien hinaus können auch postembryonale, morphologische Umbauprozesse im Detail studiert werden (Sellin et al., 2006, vorliegende Arbeit). Eine simultane Analyse aller Herzzellen während der postembryonalen Herzentwicklung im lebenden Tier war zuvor in dieser Form nicht möglich, da bislang nur einzelne Herzzellen markiert werden konnten oder in späten Stadien die Reporteraktivität fehlte (Ponzielli et al., 2002; Wang et al., 2005). Die nicht invasive Detektionsmöglichkeit des *hand*C-GFP Reporters bietet außerdem die Möglichkeit in Screeningansätzen eine große Anzahl an Tieren effizient auf Herzphänotypen zu analysieren, wie bereits von dem Labor um E. Olson gezeigt werden konnte. Mit Hilfe eines unabhängig etablierten *hand*-GFP Reporters wurde von ihnen ein Screen auf embryonale Herzphänotypen durchgeführt (Han and Olson, 2005; Yi et al., 2006). Um Gene zu identifizieren, die während der postembryonalen Herzentwicklung benötigt werden, können Analysen postembryonal letaler Mutanten-Kollektionen, wie zum Beispiel die „Zuker Kollektion“, genutzt werden (Koundakjian et al., 2004; Herzscreen der AG Paululat, unpubliziert). Der etablierte Reporter bietet damit neue Analysemöglichkeiten der diversen, dynamischen Entwicklungsprozesse während der Organogenese des *Drosophila* Herzens.

4.2 Einfluss von Kuzbanian/ADAM10 auf die Kardiogenese

(Albrecht et al. 2006)

Die Regulation des Notch/Delta-Signalwegs ist für einen korrekten Ablauf der Determinierungs- und Differenzierungsprozesse während der Kardiogenese von *Drosophila melanogaster* essentiell. Hartenstein und Kollegen konnten in den 1990er Jahren zeigen, dass es bei dem Verlust von Notch-Aktivität während bestimmten Zeiträumen der Embryogenese zu Veränderungen der Herzzellzahl kommt (Hartenstein et al., 1992). Diese Beobachtung

konnte während der vorliegenden Doktorarbeit bestätigt werden. Die Analyse von Mutanten aus zwei Komplementationsgruppen erbrachten die Beschreibung von 5 beziehungsweise 3 neuen Allelen von *kuzbanian/ADAM10* und *mastermind*. Eine Mutation dieser im Notch/Delta-Signalweg agierenden Faktoren führen zu einer deutlichen Hyperplasie des Herzens. Die Anzahl der Kardioblasten ist stark erhöht während die Perikardzellen in ihrer Zahl reduziert sind.

Die ADAM Metalloprotease Kuzbanian und das Vertebraten Homolog ADAM10 gehören zur Gruppe der membranständigen Proteasen, die durch ihre proteolytische Aktivität vorwiegend membrangebundene Proteine prozessieren und so zur Freisetzung der löslichen Ektodomänen ihrer Zielproteine führen (Sheddasen). Eine prominente Funktion von ADAM10 in Vertebraten ist die Prozessierung des Amyloid-Precursor-Proteins (APP) als α-Sekretase im nicht-amyloidogenen Signalweg. Diese Spaltung verhindert die Entstehung des Alzheimer auslösenden Amyloid-ß-Peptides. Kürzlich konnte gezeigt werden, dass ADAM10 neben der Funktion als α-Sekretase auch im amyloidogenen Signalweg fungiert, in dem es mit dem γ-Sekretasekomplex um die Spaltung des APP konkurriert (Kuhn et al., 2010).

In der vorliegenden Arbeit konnte gezeigt werden, dass Kuzbanian/ADAM10 während zwei grundlegenden Prozessen der Kardiogenese eine Rolle spielt. Fehlt Kuzbanian, kommt es zu einer Fehlregulation der lateralen Inhibition. Die Determinierung der genauen Anzahl an Progenitoren aus den Kompetenzfeldern des kardialen Mesoderms ist beeinträchtigt und führt zu einer Hyperplasie der Herzzellvorläufern. Des Weiteren ist die Differenzierung der Progenitoren in kardiale und perikardiale Zellen mittels asymmetrischer Zellteilung ebenfalls von Kuzbanian/ADAM10 abhängig. In *kuzbanian* Mutanten wird die Linie der Perikardzellen zu Gunsten der Kardioblasten verschoben, so dass sich die Anzahl der differenzierten Kardioblasten auf Kosten der Perikardzellen stark erhöht. Auch für Mutanten von *mastermind*, kann ein ähnlicher Phänotyp festgestellt werde. Mastermind, interagiert als Kofaktor mit der intrazellulären Domäne von Notch und dem DNA-Bindeprotein Supressor of Hairless um so Gentranskription zu regulieren (Kidd et al., 1998; Wu et al., 2000). Zusammengefasst sprechen diese Ergebnisse für eine Aktivität von Kuzbanian und Mastermind während den Notch/Delta abhängigen Selektionsprozessen der Kardiogenese. Mehrere Studien weisen bereits auf eine zweiphasige Aktivität des Notch/Delta-Signalweges während der Organogenese des Herzens hin (Han and Bodmer, 2003; Hartenstein et al., 1992; Popichenko and Paululat, 2004; Ward and Skeath, 2000). Weiterhin ist bekannt, dass Kuzbanian/ADAM10 in einer Vielzahl von Geweben sowohl in *Drosophila* als auch in

Vertebraten die Prozessierung der extrazellulären Domäne des Notch-Transmembranrezeptors ausführt (Alfandari et al., 2009; Klein, 2002; Lieber et al., 2002; van Tetering et al., 2009).
Mäuse, die eine Mutation in *ADAM10* tragen, weisen starke Defekte während der Kardiogenese auf (Zhang et al., 2010), und geben so Hinweise auf eine speziesübergreifende Funktion von Kuzbanian/ADAM10 während den Notch/Delta abhängigen Determinierungs- und Differenzierungsprozessen in der Kardiogenese. Neuere Untersuchungen in *Drosophila* konnten weitere Prozesse identifizieren, die durch Kuzbanian/ADAM10 reguliert werden und während der Organogenese des Herzens relevant sind. Die korrekte stereotype Anordnung der Herzzellen an der dorsalen Mittellinie ist eine weitere essentielle Voraussetzung für die Funktionalität des *Drosophila* Herzens. In *kuzbanian/ADAM10* Mutanten konnte eine Beeinträchtigung der Herzzellmorphologie und Fehler der Kardiomyozyten-Anordnung beobachtet werden (Albrecht et al., 2006, vorliegende Arbeit). Die Positionierung der Herzzellen liegt einer bis jetzt nur wenig untersuchten Interaktion von Adhäsionsmoleküle sowie dem Kontakt zur extrazellulären Matrix (*engl. extracellular matrix* (ECM)) zu Grunde. Studien in Vertebraten haben gezeigt, dass ADAM10 ebenfalls für die Regulation von Zell-Zelladhäsions Prozessen benötigt wird, in dem es N-Cadherin und E-Cadherin prozessiert (Maretzky et al., 2005; Reiss et al., 2005). Auch die dynamische Modulierung der Herzzell-ECM-Verbindung während des Herzwachstums scheint in Vertebraten von der $ß_1$-Integrin Prozessierung durch Metalloproteasen der ADAM Familie und weiteren Matrix-Metalloproteasen abhängig zu sein (Goldsmith et al., 2003; Manso et al., 2006).
Die Sheddase-Aktivität von Kuzbanian/ADAM10 erstreckt sich ebenfalls auf so genannte Zielfindungsmoleküle. Kürzlich konnten Coleman und Kollegen zeigen, dass in *Drosophila* Kuzbanian/ADAM10 die extrazelluläre Domäne des Transmembranrezeptor Roundabout (Robo) proteolytisch spaltet. Durch diese Prozessierung wird die repulsive Funktion von Robo im Nervensystem aktiviert (Coleman et al., 2010). Des Weiteren scheint Kuzbanian/ADAM10 in *Drosophila* für die Slit anhängige Rekrutierung von Son of sevenless (Sos), einem Guanin-Austausch-Faktor (GEF) essentiell zu sein, der die Zytoskelettreorganisation über Rho/Rac G-Proteine reguliert (Yang and Bashaw, 2006). Auch für die Prozessierung des Robo-Liganden Slit selbst durch Kuzbanian/ADAM10 gibt es Indizien aus *Drosophila*. Die Positionierung der lateral auswachsenden Axone scheint von einer Spaltung des Liganden abzuhängen (Coleman et al., 2010; Schimmelpfeng et al., 2001). Die proteolytische Aktivität von ADAM10 erstreckt sich auch in Vertebraten auf Faktoren, die während der neuronalen Repulsion agieren. ADAM10 wirkt als Sheddase auf die Ephrin-Rezeptor Liganden Ephrin2 und Ephrin5 und gewährleistet so die Aktivierung der Ephrin-

Kinase-Domäne, die zu dem Rückzug der Axone führt (zusammengefasst in Alfandari et al. (2009); Halloran and Wolman (2006)).
Eine direkte Übertragung dieser Daten auf eine Rolle von Kuzbanian/ADAM10 während der Kardiogenese in *Drosophila* ist zwar zu diesem Zeitpunkt nicht möglich, bietet aber Ansatzpunkte für weitere Analysen. Für eine Vielzahl von Faktoren, die in der Zelldifferenzierung und in Adhäsionsprozessen während der Entwicklung des Nervensystems eine Rolle spielen, konnte bereits eine essentielle Bedeutung während der Kardiogenese von *Drosophila* nachgewiesen werden (Hartenstein et al., 1992; MacMullin and Jacobs, 2006; Qian et al., 2005; Santiago-Martinez et al., 2006).

4.3 Herzlumenbildung ist abhängig von Uncoordinated 5 & Netrin B

(Albrecht et al. 2010, in revision)

Um den Zusammenschluss der kontralateralen Kardiomyozyten an der dorsalen Mittellinie zu einem Herzzohr zu ermöglich, muss die runde Zellform der Kardioblasten zu einer Halbmondform modifiziert werden. Der exakte Kontakt zwischen den Kardiomyozyten bedingt weiterhin die Ausbildung von drei distinkten Membrandomänen zwischen den Kardiomyozyten (Medioni et al., 2008 und vorliegende Arbeit). An den dorsalen und ventralen Kontaktbereichen der Kardiomyozyten bilden sich Adhäsionsdomänen (auch J-Domänen) aus, die Zell-Zell-Verbindungen (*engl. adherens junctions*) beherbergen. Die das Lumen umschließende luminale Domäne (L-Domäne) weist neben typischen ECM-Bestandteilen auch die Zielfindungsmoleküle Slit und Robo auf (zusammengefasst in Medioni et al. (2009)). In der vorliegenden Arbeit konnte gezeigt werden, dass das Rezeptor/Liganden-Paar Uncoordinated 5 (Unc5) und Netrin B (NetB) an der L-Domäne lokalisiert sind. Unc5 und NetB repräsentieren wie Robo und Slit Zielfindungsmoleküle, welche als Motoraxon-Repellanten im Nervensystem von *Drosophila* fungieren (Harris et al., 1996; Keleman and Dickson, 2001). Während der Kardiogenese sind Unc5 und NetB essentiell für die Ausbildung eines Herzlumens. Die zentrale Aufgabe des Herzen, das Pumpen der Hämolymphe durch den Tierkörper, ist in *unc5* Mutanten nicht mehr gewährleistet. Trotz der peristaltischen Kontraktion der Kardiomyozyten ist kein Hämolymphsfluß zu beobachten. Die Kardiomyozyten bilden kein Herzrohr aus. In *unc5* Mutanten lagern sich die Kardiomyozyten entlang ihrer gesamten apikalen Membranseite aneinander ohne dass ein luminaler Raum entsteht. Dieser Phänotyp kann auch bei einem Fehlen des korrespondierenden Unc5-Liganden NetrinB beobachtet werden. Aufgrund des Verlustes von Unc5 oder NetrinB vollziehen die Kardioblasten keine Änderung der Zellmorphologie sondern verbleiben in

einer runden Zellform. Diese Beobachtung impliziert eine Funktion von Unc5 und NetB als Repellanten der apikalen Membranseite der Kardiomyozyten. Die Ausbildung der distinkten Membrankompartimente entlang der apikalen Zellmembran ist allerdings durch den Unc5/NetrinB Signalweg nicht beeinträchtigt. Sowohl die beiden J- als auch die L-Domäne werden in *unc5* Mutanten korrekt determiniert (Albrecht et al., 2010 in revision, vorliegende Arbeit). Das Sicherstellen der Distanz zwischen den luminalen Membrandomänen und somit die dynamische Modellierung der Zellform scheint eine der Hauptaufgaben des Unc5/NetrinB Signalweges während der Kardiogenese bei *Drosophila* zu sein. Eine direkte Wirkung des Unc5/NetrinB Signalweges auf Regulatoren des Zytoskeletts ist jedoch bisher nicht bekannt. Allerdings könnte eine ähnliche Interaktion zwischen repulsiver Signalgebung und der Aktivierung von Actinfilamentverlängerung vorliegen, wie zum Beispiel zwischen dem Robo/Slit Signalweg und dem Zytoskelettadaptorprotein Enabled/VASP, welches direkt an die zytoplasmatische Domäne des Robo-Rezeptors bindet (zusammengefasst in O'Donnell et al. (2009)).

Während in *Drosophila* die Interaktion von Netrinen und Unc5 zu einem repulsiv wirkenden Signal führt, bedingt die Bindung von Netrinen und dem Transmembranrezeptor Frazzled eine anziehenden Wirkung auf die auswachsenden Axonen im Nervensystem (Kolodziej et al., 1996; Labrador et al., 2005). Frazzled repräsentiert das *Drosophila* Homolog des Immunglobulin-Rezeptors Deleted in Colorectal Carcinoma (DCC). Neben der intensiv analysierten Funktion von Frazzled als Zielfindungsmolekül konnten Hiramoto und Kollegen zeigen, dass Frazzled während der Entwicklung von Photorezeptoraxonen eine zellautonome Aufgabe übernimmt, indem er NetrinB bindet und für andere Rezeptoren präsentiert (Hiramoto et al., 2000). Der in *frazzled* Mutanten zu beobachtende Herzphänotyp (unpublizierte Daten) bietet einen Hinweis auf eine eventuelle Rolle von Frazzled während der Kardiogenese. Mutationen, die das Gen *frazzled* betreffen, resultieren in einer veränderten Anordnung der Kardiomyozyten, ähnlich der Verschiebungen der Kardiomyozyten in *unc5* Mutanten. Bislang gibt es keine eindeutigen Daten zur Expression von Frazzled im Herz von *Drosophila* (unpublizierte Daten); auch Analysen zur direkten Interaktion von Frazzled und Unc5 in *Drosophila* liegen bis jetzt noch nicht vor. Studien an murinen Nervenzellen haben allerdings gezeigt, dass eine direkte Interaktion von Unc5 und DCC zur Endozytose von Unc5 führt. Die repulsive Signalgebung (Netrin&Unc5) wird damit unterbrochen und in eine anziehende Signalgebung umwandelt (Netrin&DCC) (O'Donnell et al., 2009; Williams et al., 2003).

Diese Daten aus Vertebraten zeigen die Möglichkeit eines generellen Zusammenspieles von Unc5, Netrin und Frazzled. Eine solche, noch hypothetische Interaktion könnte auch die Verbindung zwischen der unterbleibenden Zellformänderung in *unc5* Mutanten und der Modulierung des Zytoskeletts herstellen. Verschiedene Gruppen konnten zeigen, dass Frazzled direkt mit Regulatoren der Actinfilamentpolymerisierung interagiert und auch die Aktivität von Myosin II steuert (Dorsten et al., 2007; Forsthoefel et al., 2005). Dennoch ist ein direktes Zusammenspiel von Unc5, Netrin und Frazzled bislang rein hypothetisch und bedarf weiterer intensiver Analysen der beteiligten Komponenten.
Die Vielzahl an Proteininteraktionen, zum Beispiel während der Entstehung eines funktionellen Organs, bedingt eine koordinierte Regulation der einzelnen Komponenten. Eine Steuerungsmöglichkeit für die Aktivität von Zielfindungsmolekülen ist, wie bereits beschrieben, die proteolytische Aktivierung /Reprimierung durch Proteasen. Untersuchungen in Vertebratenzellen haben gezeigt, dass Metalloproteaseinhibitoren die Regulation des *frazzled* Homologs DCC beeinflussen können und eine Akkumulation von DCC an der Membranoberfläche auslösen. Die Autoren postulieren, dass die Regulation von DCC abhängiger Signalgebung über die Prozessierung des DCC-Rezeptores durch Metalloproteasen gesteuert wird (Galko and Tessier-Lavigne, 2000). Diese Daten bieten einen Anhaltspunkt für einen Prozess, der auch in der Organogenese des *Drosophila* Herzens eine Rolle spielen könnte. Eine Steuerung der Rezeptoraktivität durch proteolytische Prozessierung ist auch während der Kardiogenese denkbar. Das beobachtete Auftreten mehrfacher Herzlumen in *kuzbanian* mutanten *Drosophila* Embryonen könnte als Ausgangspunkt für weitere Analysen einer putativen Beziehung zwischen Kuzbanian/ADAM10, Frazzled und Unc5 genutzt werden (Albrecht et al., 2006, vorliegende Arbeit). Die beschriebene proteolytische Aktivierung von Robo durch Kuzanian/ADAM10 ist zur vollständigen Erklärung des *kuzbanian* Phänotyps im Herz nicht ausreichen, da durch eine Mutation im Gen *robo* eine Herzlumenbildung unterbleibt, *kuz* Mutanten aber mehrere Lumen aufweisen (Albrecht et al., 2006; Coleman et al., 2010; Santiago-Martinez et al., 2008).

Diese vorliegende Dissertation beschäftigt sich mit der Regulation der klar strukturierten, dynamischen Prozesse während der Kardiogenese von *Drosophila melanogaster*. Die Analyse der Rolle von Uncoordinated 5 und Kuzbanian während der Organogenese des Herzens zeigt eine komplexe Verflechtung grundlegender Regulationsmechanismen auf, die für die Bildung eines funktionellen Herzens essentiell sind. Da nur Teile der beteiligten speziesübergreifenden

und hoch konservierten Signalwege bis heute untersucht sind, bedarf die Aufklärung des gesamten regulatorischen Netzwerks noch weiterer, detaillierter Analysen.

Referenzen

Albrecht, S., Altenhein, B., and Paululat, A. (2010 in revision). The transmembrane receptor Uncoordinated 5 (Unc5) is essential for heart lumen formation in *Drosophila melanogaster*.

Albrecht, S., Wang, S., Holz, A., Bergter, A., and Paululat, A. (2006). The ADAM metalloprotease Kuzbanian is crucial for proper heart formation in *Drosophila melanogaster*. *Mech Dev* **123,** 372-87.

Alfandari, D., McCusker, C., and Cousin, H. (2009). ADAM function in embryogenesis. *Semin Cell Dev Biol* **20,** 153-63.

Coleman, H. A., Labrador, J. P., Chance, R. K., and Bashaw, G. J. (2010). The Adam family metalloprotease Kuzbanian regulates the cleavage of the Roundabout receptor to control axon repulsion at the midline. *Development* **137,** 2417-26.

Dorsten, J. N., Kolodziej, P. A., and Vanberkum, M. F. (2007). Frazzled regulation of myosin II activity in the *Drosophila* embryonic CNS. *Dev Biol* **308,** 120-32.

Firulli, A. B. (2003). A HANDful of questions: the molecular biology of the heart and neural crest derivatives (HAND)-subclass of basic helix-loop-helix transcription factors. *Gene* **312,** 27-40.

Forsthoefel, D. J., Liebl, E. C., Kolodziej, P. A., and Seeger, M. A. (2005). The Abelson tyrosine kinase, the Trio GEF and Enabled interact with the Netrin receptor Frazzled in Drosophila. *Development* **132,** 1983-94.

Galko, M. J., and Tessier-Lavigne, M. (2000). Function of an axonal chemoattractant modulated by metalloprotease activity. *Science* **289,** 1365-7.

Goldsmith, E. C., Carver, W., McFadden, A., Goldsmith, J. G., Price, R. L., Sussman, M., Lorell, B. H., Cooper, G., and Borg, T. K. (2003). Integrin shedding as a mechanism of cellular adaptation during cardiac growth. *Am J Physiol Heart Circ Physiol* **284,** H2227-34.

Halloran, M. C., and Wolman, M. A. (2006). Repulsion or adhesion: receptors make the call. *Curr Opin Cell Biol* **18,** 533-40.

Han, Z., and Bodmer, R. (2003). Myogenic cells fates are antagonized by Notch only in asymmetric lineages of the *Drosophila* heart, with or without cell division. *Development* **130,** 3039-51.

Han, Z., and Olson, E. N. (2005). Hand is a direct target of Tinman and GATA factors during *Drosophila* cardiogenesis and hematopoiesis. *Development* **132,** 3525-36.

Han, Z., Yi, P., Li, X., and Olson, E. N. (2006). Hand, an evolutionarily conserved bHLH transcription factor required for *Drosophila* cardiogenesis and hematopoiesis. *Development* **133,** 1175-82.

Harris, R., Sabatelli, L. M., and Seeger, M. A. (1996). Guidance cues at the *Drosophila* CNS midline: identification and characterization of two *Drosophila* Netrin/UNC-6 homologs. *Neuron* **17,** 217-28.

Hartenstein, A. Y., Rugendorff, A., Tepass, U., and Hartenstein, V. (1992). The function of the neurogenic genes during epithelial development in the Drosophila embryo. *Development* **116,** 1203-20.

Hiramoto, M., Hiromi, Y., Giniger, E., and Hotta, Y. (2000). The *Drosophila* Netrin receptor Frazzled guides axons by controlling Netrin distribution. *Nature* **406,** 886-9.

Keleman, K., and Dickson, B. J. (2001). Short- and long-range repulsion by the *Drosophila* Unc5 netrin receptor. *Neuron* **32,** 605-17.

Kidd, S., Lieber, T., and Young, M. W. (1998). Ligand-induced cleavage and regulation of nuclear entry of Notch in *Drosophila melanogaster* embryos. *Genes Dev* **12,** 3728-40.

Klein, T. (2002). kuzbanian is required cell autonomously during Notch signalling in the *Drosophila* wing. *Dev Genes Evol* **212,** 251-5.

Kolodziej, P. A., Timpe, L. C., Mitchell, K. J., Fried, S. R., Goodman, C. S., Jan, L. Y., and Jan, Y. N. (1996). *frazzled* encodes a *Drosophila* member of the DCC immunoglobulin subfamily and is required for CNS and motor axon guidance. *Cell* **87,** 197-204.

Kölsch, V., and Paululat, A. (2002). The highly conserved cardiogenic bHLH factor Hand is specifically expressed in circular visceral muscle progenitor cells and in all cell types of the dorsal vessel during *Drosophila* embryogenesis. *Dev Genes Evol* **212,** 473-85.

Koundakjian, E. J., Cowan, D. M., Hardy, R. W., and Becker, A. H. (2004). The Zuker collection: a resource for the analysis of autosomal gene function in *Drosophila melanogaster*. *Genetics* **167,** 203-6.

Kuhn, P. H., Wang, H., Dislich, B., Colombo, A., Zeitschel, U., Ellwart, J. W., Kremmer, E., Rossner, S., and Lichtenthaler, S. F. (2010). ADAM10 is the physiologically relevant, constitutive alpha-secretase of the amyloid precursor protein in primary neurons. *Embo J* **29,** 3020-32.

Labrador, J. P., O'Keefe, D., Yoshikawa, S., McKinnon, R. D., Thomas, J. B., and Bashaw, G. J. (2005). The homeobox transcription factor even-skipped regulates netrin-receptor expression to control dorsal motor-axon projections in *Drosophila*. *Curr Biol* **15,** 1413-9.

Lieber, T., Kidd, S., and Young, M. W. (2002). Kuzbanian-mediated cleavage of *Drosophila* Notch. *Genes Dev* **16,** 209-21.

Lo, P. C., Zaffran, S., Senatore, S., and Frasch, M. (2007). The *Drosophila* Hand gene is required for remodeling of the developing adult heart and midgut during metamorphosis. *Dev Biol* **311,** 287-96.

MacMullin, A., and Jacobs, J. R. (2006). Slit coordinates cardiac morphogenesis in *Drosophila*. *Dev Biol* **293,** 154-64.

Manso, A. M., Elsherif, L., Kang, S. M., and Ross, R. S. (2006). Integrins, membrane-type matrix metalloproteinases and ADAMs: potential implications for cardiac remodeling. *Cardiovasc Res* **69,** 574-84.

Maretzky, T., Reiss, K., Ludwig, A., Buchholz, J., Scholz, F., Proksch, E., de Strooper, B., Hartmann, D., and Saftig, P. (2005). ADAM10 mediates E-cadherin shedding and regulates epithelial cell-cell adhesion, migration, and beta-catenin translocation. *Proc Natl Acad Sci U S A* **102,** 9182-7.

Medioni, C., Astier, M., Zmojdzian, M., Jagla, K., and Semeriva, M. (2008). Genetic control of cell morphogenesis during *Drosophila melanogaster* cardiac tube formation. *J Cell Biol* **182,** 249-61.

Medioni, C., Senatore, S., Salmand, P. A., Lalevee, N., Perrin, L., and Semeriva, M. (2009). The fabulous destiny of the *Drosophila* heart. *Curr Opin Genet Dev* **19,** 518-25.

O'Donnell, M., Chance, R. K., and Bashaw, G. J. (2009). Axon growth and guidance: receptor regulation and signal transduction. *Annu Rev Neurosci* **32,** 383-412.

Ponzielli, R., Astier, M., Chartier, A., Gallet, A., Therond, P., and Semeriva, M. (2002). Heart tube patterning in *Drosophila* requires integration of axial and segmental information provided by the Bithorax Complex genes and hedgehog signaling. *Development* **129,** 4509-21.

Popichenko, D., and Paululat, A. (2004). Cell fate decisions in the *Drosophila* dorsal vessel depend on the multiadapter protein inscuteable. *Genesis* **40,** 218-22.

Qian, L., Liu, J., and Bodmer, R. (2005). Slit and Robo control cardiac cell polarity and morphogenesis. *Curr Biol* **15,** 2271-8.

Reiss, K., Maretzky, T., Ludwig, A., Tousseyn, T., de Strooper, B., Hartmann, D., and Saftig, P. (2005). ADAM10 cleavage of N-cadherin and regulation of cell-cell adhesion and beta-catenin nuclear signalling. *Embo J* **24,** 742-52.

Santiago-Martinez, E., Soplop, N. H., and Kramer, S. G. (2006). Lateral positioning at the dorsal midline: Slit and Roundabout receptors guide *Drosophila* heart cell migration. *Proc Natl Acad Sci U S A* **103,** 12441-6.

Santiago-Martinez, E., Soplop, N. H., Patel, R., and Kramer, S. G. (2008). Repulsion by Slit and Roundabout prevents Shotgun/E-cadherin-mediated cell adhesion during *Drosophila* heart tube lumen formation. *J Cell Biol* **182,** 241-8.

Schimmelpfeng, K., Gogel, S., and Klambt, C. (2001). The function of *leak* and *kuzbanian* during growth cone and cell migration. *Mech Dev* **106,** 25-36.

Sellin, J., Albrecht, S., Kolsch, V., and Paululat, A. (2006). Dynamics of heart differentiation, visualized utilizing heart enhancer elements of the *Drosophila melanogaster* bHLH transcription factor Hand. *Gene Expr Patterns* **6,** 360-75.

Srivastava, D., and Olson, E. N. (1997). Knowing in your heart what's right. *Trends Cell Biol* **7,** 447-53.

van Tetering, G., van Diest, P., Verlaan, I., van der Wall, E., Kopan, R., and Vooijs, M. (2009). Metalloprotease ADAM10 is required for Notch1 site 2 cleavage. *J Biol Chem* **284,** 31018-27.

Wang, J., Tao, Y., Reim, I., Gajewski, K., Frasch, M., and Schulz, R. A. (2005). Expression, regulation, and requirement of the toll transmembrane protein during dorsal vessel formation in *Drosophila melanogaster*. *Mol Cell Biol* **25,** 4200-10.

Ward, E. J., and Skeath, J. B. (2000). Characterization of a novel subset of cardiac cells and their progenitors in the *Drosophila* embryo. *Development* **127,** 4959-69.

Williams, M. E., Wu, S. C., McKenna, W. L., and Hinck, L. (2003). Surface expression of the netrin receptor UNC5H1 is regulated through a protein kinase C-interacting protein/protein kinase-dependent mechanism. *J Neurosci* **23,** 11279-88.

Wu, L., Aster, J. C., Blacklow, S. C., Lake, R., Artavanis-Tsakonas, S., and Griffin, J. D. (2000). MAML1, a human homologue of *Drosophila mastermind*, is a transcriptional co-activator for NOTCH receptors. *Nat Genet* **26,** 484-9.

Yang, L., and Bashaw, G. J. (2006). Son of sevenless directly links the Robo receptor to Rac activation to control axon repulsion at the midline. *Neuron* **52,** 595-607.

Yi, P., Han, Z., Li, X., and Olson, E. N. (2006). The Mevalonate Pathway Controls Heart Formation in *Drosophila* by Isoprenylation of Gγ1. *Science* **313,** 1301-3.

Zhang, C., Tian, L., Chi, C., Wu, X., Yang, X., Han, M., Xu, T., Zhuang, Y., and Deng, K. (2010). Adam10 is essential for early embryonic cardiovascular development. *Dev Dyn*.

5. Publikationsliste

Artikel:

Sellin, J., Albrecht, S., Kölsch, V. and Paululat, A. (2006).
Dynamics of heart differentiation, visualized utilizing heart enhancer elements of the *Drosophila melanogaster* bHLH transcription factor Hand.
Gene Expression Patterns 6, 360-75.

Albrecht, S., Wang, S., Holz, A., Bergter, A. and Paululat, A. (2006).
The ADAM metalloprotease Kuzbanian is crucial for proper heart formation in *Drosophila melanogaster*.
Mechanisms of Development 123, 372-87.

Albrecht, S., Altenhein, B. and Paululat, A. (2011).
The transmembrane receptor Uncoordinated 5 (Unc5) is essential for heart lumen formation in *Drosophila melanogaster*.
Developmental Biology 350, 89-100

Tagungsbeiträge:

2005: 46th Annual Drosophila Research Conference, San Diego (USA); Posterbeitrag
Albrecht S. and Paululat A.
"The screening of 700 Drosophila lines from an EMS mutagenesis collection revealed several heart phenotypes"

2005: 16. Jahrestagung der Gesellschaft für Entwicklungsbiologie, Münster; Posterbeitrag
Albrecht S. and Paululat A.
"New Drosophila melanogaster mutants affecting heart differentiation"

2006: 99. Jahrestagung der Deutschen Zoologischen Gesellschaft, Münster; Posterbeitrag
Albrecht S. Sellin J. and Paululat A.
"*Drosophila* heart differentiation in *kuzbanian* mutants studied by a *hand*-GFP reporter line"

2006: 12th Regional Drosophila Meeting, Wien (Österreich); Vortrag
Albrecht S. and Paululat A.
"The ADAM metalloprotease Kuzbanian is crucial for proper heart formation in *Drosophila melanogaster"*

2006: SFB-Symposium (SFB 431), Osnabrück; Posterbeiträge
Albrecht S. Wang S. and Paululat A.
„Functions of the membrane spanning metalloprotease Kuzbanian during Drosophila heart differentiation"

Albrecht S. and Paululat A.

"Cell recognition, adhesion and alignment during Drosophila heart differentiation is mediated by the membrane receptor-ligand pair Frazzled and Netrin."

2007: 17. Jahrestagung der Gesellschaft für Entwicklungsbiologie, Marburg; Posterbeitrag
Albrecht S., Wang S., Braksiek M. and Paululat A.

"A phenotypic screen for heart pattern defects induced by randomized EMS mutagenesis in *Drosophila melanogaster*"

2008: SFB 431 PhD-Symposium, Osnabrück; Vortrag und Posterbeitrag
Albrecht S. and Paululat A.

„Correct heart assembly in Drosophila depends on pathfinding molecules"
Albrecht S. and Paululat A.

2008: 14th Regional Drosophila Meeting, München; Posterbeitrag
Albrecht S. and Paululat A.

„Correct heart assembly in Drosophila depends on pathfinding molecules "

2009: 18. Jahrestagung der Gesellschaft für Entwicklungsbiologie, Hannover; Posterbeitrag
Albrecht S. and Paululat A.

„Heart assembly in *Drosophila* depends on pathfinding molecules"

6. Danksagung

Herrn Prof. Dr. Achim Paululat möchte ich sehr herzlich für die Möglichkeit danken, in seiner Arbeitsgruppe zu promovieren, für die Bereitstellung des Themas und für die geduldige Diskussionsbereitschaft und Unterstützung während der gesamten Zeit meiner Promotion. Bedanken möchte ich mich auch für die Möglichkeit, Erfahrungen auf den Gebieten der Laborорganisation und Verwaltung sammeln zu können. Weiterhin möchte ich mich ausdrücklich für die Bereitstellung einer Finanzierung während der Zeit meiner Promotion bedanken – die in meinen Augen nicht als selbstverständlich angesehen werden kann.

Herrn Prof. Dr. Brandt danke ich für bereitwillige Übernahme das Zweitgutachten meiner Arbeit.

Ich danke Herrn Prof. Dr. Heinisch und Herrn Dr. Schmitz für ihre Bereitschaft, meiner Prüfungskommission anzugehören.

Bei der gesamten Arbeitsgruppe Zoologie möchte ich mich herzlich für die tolle Arbeitsatmosphäre bedanken. Auch wenn die Anfänge hauptsächlich durch Um- und Aufräumarbeiten geprägt waren, haben wir doch alle zusammen eine – wie ich finde – tolle Arbeitsgruppe aufgebaut. Besonders danken möchte ich Martina Biedermann, Mechthild Krabusch und Lydia Reckers für ihre große Hilfsbereitschaft bei allen möglichen und auch unmöglichen Angelegenheiten. Kerstin Etzhold gilt mein Dank für die Erstellung der TEM Schnitte – die Bilder sind super geworden!

Julia Sellin und Annette Bergter möchte ich für eine schöne Zeit gerade zu Beginn meiner Promotion in Osnabrück danken. Unsere Zusammenarbeit und unser Zusammenhalt im Labor und auch die Zeit „außerhalb des Labors“ möchte ich nicht missen. Trotz oder gerade wegen unserer unterschiedlichen Charaktere waren wir ein sehr gutes Team.

Markus, Bettina und Ariane möchte ich für unsere vielen schönen und witzigen Momente danken. Es ist sehr schön wenn man die Möglichkeit hat mit Freunden zusammenzuarbeiten
@ Markus: Vielen Dank für die kontinuierliche Versorgung mit spannender Lektüre aus London.

Meiner besten Freundin Christina möchte ich einfach für „Alles“ danken. Sie ist immer für mich da und ich bin sehr froh und stolz sie als Freundin zu haben.

Ein ganz besonderes Dankeschön geht an meinen Freund Maik. Ich kann mich sehr glücklich schätzen, dass ich in ihm einen hilfsbereiten und kritischen Kollegen, einen wunderbaren Freund und Lebenspartner habe. DANKE!

Meinen Eltern, Chris & Kerstin möchte ich an dieser Stelle für die bedingungslose Unterstützung und das entgegengebrachte Verständnis Danke sagen. Sie sind immer für mich da und haben nie am mir gezweifelt. Ohne sie hätte ich es nicht geschafft!
Ich hab Euch sehr lieb!!

7. Lebenslauf

Persönliche Daten

Name	Albrecht
Vorname	Stefanie
Geburtsdatum	13. Mai 1977
Geburtsort	Herborn

Akademische und berufliche Ausbildung

2004 – 2010	Promotion am Lehrstuhl für Zoologie/Entwicklungsbiologie der Universität Osnabrück mit dem Thema: „Analyse der Funktion von Kuzbanian und Uncoordinated 5 während der Herzzelldeterminierung und Herzlumenbildung von *Drosophila melanogaster*“
1998 – 2004	Diplomstudium der Biologie an der Universität Marburg Schwerpunkte: Entwicklungsbiologie, Genetik, Virologie Abschluss: Diplom Biologin
1996 – 1998	Ausbildung zur Staatlich geprüften Biologisch-technischen Assistentin an der Rheinischen Akademie e.V., Köln
1993 – 1996	Johanneum Gymnasium, Herborn Abschluss: Allgemeine Hochschulreife

8. Erklärung über die Eigenständigkeit der erbrachten wissenschaftlichen Leistung

Ich erkläre hiermit, dass ich die vorliegende Arbeit ohne unzulässige Hilfe Dritter und ohne Benutzung anderer als der angegebenen Hilfsmittel angefertigt habe. Die aus anderen Quellen direkt oder indirekt übernommenen Daten und Konzepte sind unter Angabe der Quelle gekennzeichnet.

Bei der Auswahl und Auswertung folgenden Materials haben mir die nachstehend aufgeführten Personen in der jeweils beschriebenen Weise ~~entgeltlich~~ / unentgeltlich geholfen.

1. Julia Sellin - Erstellung des *hand*C-GFP Reporters, Durchführung und Auswertung der Studien zur larvalen und pupalen Entwicklung von *Drosophila melanogaster* sowie der Untersuchung zur Regulation von *hand.*

2. Verena Kölsch – Erhebung der *in situ* Daten zu *hand*

3. Shuoshuo Wang - Lokalisation der Punktmutation in *kuzbanian* $^{R1-4}$

4. Dr. Anne Holz – Vorselektion der EMS-Kollektion

5. Annette Bergter – Erstellung der Semidünnschnitte von wildtyp und *kuzbanian* $^{F2-16}$ Embryonen

6. Dr. Benjamin Altenhein – Bereitstellung der Antikörper gegen Unc5 und NetrinB

Alle oben aufgeführten Personen sind als Koautoren auf den entsprechenden Publikationen geführt.

Weitere Personen waren an der inhaltlichen materiellen Erstellung der vorliegenden Arbeit nicht beteiligt. Insbesondere habe ich hierfür nicht die entgeltliche Hilfe von Vermittlungs- bzw. Beratungsdiensten (Promotionsberater oder andere Personen) in Anspruch genommen. Niemand hat von mir unmittelbar oder mittelbar geldwerte Leistungen für Arbeiten erhalten, die im Zusammenhang mit dem Inhalt der vorgelegten Dissertation stehen.

Die Arbeit wurde bisher weder im In- noch im Ausland in gleicher oder ähnlicher Form einer anderen Prüfungsbehörde vorgelegt.

---------- ----------

(Ort. Datum) (Stefanie Albrecht)